Influence of Nanoclay on Interlaminar Fracture Characterization of GFRP, and Intralaminar Fracture Characterization of SIMS & Glass Mat Reinforced Thermoplastics Materials

By:
Mulugeta H. Woldemariam

Supervisor: Giovanni Belingardi (Professor)
Co-supervisor I: Daniel T. Redda (Associate Professor)
Co-supervisor II: Ermias G. Koricho (Assistance Professor)

A Dissertation Submitted to School of Mechanical and Industrial Engineering Presented in Fulfillment of the Requirements for the Degree of Doctor of Philosophy (PhD) in Mechanical Engineering (Applied Mechanics)

Addis Ababa Institute of Technology (AAiT)
Addis Ababa University
Addis Ababa, Ethiopia

June, 2020, Addis Ababa, Ethiopia

ADDIS ABABA UNIVERSITY
ADDIS ABABA INSTITUTE OF TECHNOLOGY (AAiT)
SCHOOL OF MECHANICAL AND INDUSTRIAL ENGINEERING
APPLIED MECHANICS STREAM
ADDIS ABABA, ETHIOPIA

Influence of Nanoclay on Interlaminar Fracture Characterization of GFRP, and Intralaminar Fracture Characterization of SIMS & Glass Mat Reinforced Thermoplastics Materials

Mulugeta H. Woldemariam	----------	----------
	Signature	Date
Professor Giovanni Belingardi	----------	----------
Supervisor	Signature	Date
Dr. Daniel T. Redda	----------	----------
Co-supervisor-I	Signature	Date
Dr. Ermias G. Koricho	----------	----------
Co-Supervisor-II	Signature	Date

ADDIS ABABA UNIVERSITY
ADDIS ABABA INSTITUTE OF TECHNOLOGY (AAiT)
SCHOOL OF MECHANICAL AND INDUSTRIAL ENGINEERING
APPLIED MECHANICS STREAM
ADDIS ABABA, ETHIOPIA

Influence of Nanoclay on Interlaminar Fracture Characterization of GFRP, and Intralaminar Fracture Characterization of SIMS & Glass Mat Reinforced Thermoplastics Materials

By
Mulugeta H. Woldemariam

Approved by Board of Examiners:

Dr. Yilma Tadesse	----------	----------
Dean, School of Mechanical and Industrial Engineering	Signature	Date
Professor Giovanni Belingardi	----------	----------
Supervisor	Signature	Date
Dr. Daniel T. Redda	----------	----------
Co-supervisor -I	Signature	Date
Dr. Ermias G. Koricho	----------	----------
Co-Supervisor-II	Signature	Date
Professor Eyasu Woldesenbet	----------	----------
Internal Examiner	Signature	Date
Dr. Addis A. Kidane	----------	----------
External Examiner	Signature	Date
Mr. Araya Abera (PhD candidate)	----------	----------
(Chair of Mechanical Design Stream)	Signature	Date

Endorsed By:

Dr. Yilma Tadesse	----------	----------
(School Dean of Mechanical and Industrial Engineering)	Signature	Date
Dr. Ermias Tesfaye	----------	----------
(Associate Director of Post Graduate Program)	Signature	Date

DECLARATION

I declare that "**Influence of Nanoclay on Interlaminar Fracture Characterization of GFRP, and Intralaminar Fracture Characterization of SIMS & Glass Mat Reinforced Thermoplastics Materials**" is original work of my own, has not been presented for a degree of any other university, and all the sources that I have used or quoted have been indicated and acknowledged by means of referencing. It is submitted in partial fulfillment of the requirements for the degree of Doctor of Philosophy in Mechanical Engineering, Mechanical Design Engineering (Applied Mechanics Stream) at Addis Ababa University.

Mulugeta H. Woldemariam	----------	----------
	Signature	Date

This is to certify that the above declaration made by the candidate is correct to the best of my knowledge.

Professor Giovanni Belingardi	----------	----------
Supervisor	Signature	Date
Dr. Daniel T. Redda	----------	----------
Co-supervisor-I	Signature	Date
Dr. Ermias G. Koricho	----------	----------
Co-Supervisor -II	Signature	Date

Authors

Mulugeta H. Woldemariam
PhD Student at School of Mechanical & Industrial Engineering, Addis Ababa Institute of Technology, Addis Ababa University, Addis Ababa, Ethiopia
E-mail: mulugeta.habtemariam@aait.edu.et

ProfessorGiovannie Belingardi
Professor of Mechanical Engineering at, Department of Mechanical & Aerospace Engineering(DIMEAS),Politecnico di Torino, Turin, Italy
E-mail: giovanni.belingardi@polito.it
Dr. Daniel T. Redda
Associate Professor of Mechanical Engineering at School of Mechanical & Industrial Engineering, Addis Ababa Institute of Technology, Addis Ababa University, Addis Ababa, Ethiopia
E-mail: tdaniel412@yahoo.com
Dr. Ermias G. Koricho
Assistance Professor of Mechanical Engineering at Allen E. Paulson College of Engineering &information Technology, Georgia Southern University, USA
E-mail: ekoricho@georgiasouthern.edu

Acknowledgements

First, I would like to express my heartfelt appreciation and gratitude to my supervisor Professor Giovanni Belingardi, professor of mechanical engineering at Politecnico di Torino, Turin Italy, for his invaluable guidance, tireless support, unreserved efforts, continual encouragement, and understanding in the overall activities of the dissertation. Equally, I appreciate the role of my first co-supervisor Dr. Daniel T. Redda, associate professor of mechanical engineering at Addis Ababa Institute of Technology, for his continuous follow-up, valuable suggestion on how I proceed and what I would have to follow from the beginning to carry out my Ph.D. study. The role of my second co-supervisor Dr. Ermias G. Koricho, assistance professor of mechanical engineering at Allen E. Paulson College of Engineering & Information Technology, Georgia Southern University, USA, was vital for his continuous guidance and his instigation to direct me towards experimental research-based dissertation was memorable. Dr. Ermias G. Koricho also supplied some of the materials and he requires my extensive approbation. The directions that I acquired from Dr. Alem Tekalign were essential to my experimental research activities during my stay for experimental work at Politecnico di Torino, Turin, Italy. The practical experimental work/activities might have been difficult without his unstinting support. His continuous effort helped me to accomplish this work.

I am thankful to Araya Abera, chair of Mechanical Design under the School of Mechanical and Industrial Engineering for his continual encouragement and support during all activities of my work. The official support of the School and all deans of the School of Mechanical and Industrial Engineering were very important. Thus, I would like to express my appreciation to Dr. Yilma Tadesse, dean of School of Mechanical and Industrial Engineering, and to the former dean of the School Getasew Tadesse. Dr. Yilma Tadesse facilitated all the activities that were required to present my dissertation with the time of COVID 19 situation. My gratefulness also extended to all other staff of the School of Mechanical and Industrial Engineering.

Finally, yet importantly I am quite indebted to Addis Ababa Institute of Technology (AAiT) and the School of Mechanical and Industrial Engineering. Equally, I thank the Politecnico di Torino, Department of Mechanical and Aerospace Engineering (DIMEAS). DIMEAS of Politecnico di Torino provided me the full resources to conduct the experiments and all related and available research materials. Additionally, I want to extend my gratitude to the research group of Professor

Belingardi and special thanks to the mechanical laboratory of DIMEAS, the manager, and the staff of the laboratory.

Abstract

The needs of lightweight and customizable structural materials instigate researchers to conduct rigorous materials characterization, with particular attention toward failure mechanisms and safety standards, and to study the materials' development. Furthermore, the currently available structural and semi-structural composite materials made up of fiber-reinforced plastic, that are presently considered to keep the environmental regulations, require multidimensional examination and analysis because of its heterogeneous nature a non-isotropic behavior. Consequently, this research aims to improve the knowledge on specific lightweight material and to contribute the confidence that toward their use in spite of its poor nature and suspicious to fail, focusing on some fundamental material properties, such as interlaminar and intralaminar behaviors. The research started from failure characteristics and mechanisms, followed by the analysis of the modifications adopted to enhance its structural properties in advanced level, and finally report the adopted experimental characterization procedures and discuss the main findings.

The first part of the study has been focused on composite materials with special targets of enhancement and the structural behavior of these materials was experimentally characterized. The material was manufactured with a plain-woven S-glass fiber-reinforce plastic. The material modification was obtained by adding nanoparticles to the matrix; therefore a nano-modified composite was developed by the appropriate combination of epoxy and nanoclay family particles, Cloisite 20B. Thus, the fundamental experimental work included the effect of nanoclay, Cloisite 20B inclusion on the mechanical behavior of a woven type glass fiber reinforced plastic (GFRP) composite. Specifically, the study examined the effect of nanoclay, added with various weight percentages, on the tensile, compressive strengths, and modulus of elasticity of GFRP in both weft and warp directions. Results showed that depending on the warp and weft directions, the inclusion of nanoclay, Cloisite 20B, altered the mechanical behavior of GFRP. The advanced investigations focus on the interlaminar characteristics of the material. In this work, the effect of meticulous nanoclay, Cloisite 20B, inclusion on the interlaminar fracture toughness glass fiber reinforced plastic composite was investigated using careful experimental procedure. Afterwards the study moved to the fracture mechanics behavior, with particular reference to the mode-I interlaminar behavior. Tests were conducted based on a double cantilever beam (DCB) specimen using the specific American Society of Testing Materials standard (ASTM D5528). Results

showed that the inclusion of nanoclays improved the interlaminar fracture toughness of the GFRP composite in the range of 12.65% and 54.07% relative to pristine, with progressive percentage increment of the nanoclays weight percentage content (from 0.5 to 2%). Therefore, the dissemination of this experimental research results contributes to overlook a better understanding of nanoclay fillers and their contribution to mechanical behaviors; this can lead to a better design of novel structural composites. Moreover, it guides how Cloisite fillers contribute to improve the delamination resistance with this special composite material having a better retardant flame propagation property that can be relevant for some structures.

The second part dealt with lightweight materials that are intended for the vehicle /automotive industry. The intralaminar behavior of the two types of materials, which were supplied by two international companies, was investigated. The fundamental behavior, impact, and special structural application studies of these two types of innovative materials were examined, once again with particular attention toward the impact response and the fracture nature of these materials. The first material type is semi impregnated micro sandwich structure (SIMS) and it is manufactured with two specific reinforcing fibers (carbon and glass). The other material belongs to the glass mat thermoplastic (GMT) family that has also two types: the conventional GMT and the GMT modified by adding unidirectional fibers (GMT-UD) to stiff the structure. For those materials, the intralaminar fracture and the nature of the crack behavior were experimentally investigated using compact tension specimen test. The intralaminar fracture toughness of each material was determined along with crack propagation behavior. As a result, the output of this research fills the gaps and it can contribute to having a full picture of the GMT and SIMS materials.

Keywords: Nanoclay, Cloisite 20B, nanoparticles, structural performance enhancement, fracture toughness, interlaminar, intralaminar, compact tension, DCB, SIMS, GMT, S-glass, composite materials

Table of Contents

List of Tables

List of Figures

List of Abbreviations and Acronyms

e_1	*strain in the direction 1*
e_2	*strain in the direction 2*
B_y	*percent bending*
s_{ut}	*ultimate tensile strength*
s_{ti}	*tensile stress at each data point*
F_{ut}	*maximum tensile load at failure*
F_{ti}	*tensile load at each data point*
A_t	*specimen gage area*
s_{uc}	*ultimate compressive strength*
s_{ci}	*ultimate compressive strength*
F_{uc}	*maximum compressive load at failure*
F_{ci}	*compressive load at each data point*
P	*load*
δ	*load point displacement*
B	*specimen width*
a	*delamination/growing crack/ length*
a_o	*initial delamination/crack/ length*
Δ	*rotational factor during DCB test*
G_I	*energy release rate of mode I*
G_{IC}	*fracture toughness of mode I(energy release rate)*
G_{IIC}	*fracture toughness of mode II(energy release rate)*
h	*height of specimen*
n	*slope of the method of compliance calibration*
A_1	*slope of the method of modified compliance calibration*
C	*compliance*
F	*bending factors of DCB moment of arms*
t	*thickness of the specimen*
P_c	*the measured critical load that causes fracture*
t	*the thickness of the specimen*
w	*the effective length of the specimen/ dimension*
E_1	*the Young's modulus in the direction 1*
E_2	*the Young's modulus in the direction 2*
G_{12}	*the shear modulus*
ν_{12}	*the Poisson's ratio*

P_Q	*maximum effective load*
K_I	*stress intensity factor of mode I*
K_{IC}	*fracture toughness of mode I (stress intensity factor)*
J_{IC}	*J integral of mode I*
J_{IIC}	*J integral of mode II*
SIMS	*semi impregnated micro sandwich*
G-SIMS	*Glass fiber semi impregnated micro sandwich*
C-SIMS	*Carbon fiber semi impregnated micro sandwich*
GMT	*glass mat-reinforced thermoplastic*
GMT-UD	*glass mat-reinforced thermoplastic with unidirectional fiber*
FEA	*finite element analysis*
FEM	*finite element method*
SLB	*single leg bending*
DCB	*double cantilever beam*
GFRP	*glass fiber reinforced plastics*
NL	*nonlinearity*
VIS	*visual observation*
MBT	*modified beam theory*
CC	*compliance calibration*
MCC	*modified compliance calibration*
ASTM	*American Society of Testing Materials*
GT	*giga ton*
MG	*mega ton*
KT	*kilo ton*

Chapter 1: Background and Justification of the Research

The chapter introduces the basic concepts, history, application, and, in particular, failure/damage mechanics of composite materials. The interlaminar and intralaminar behaviors of composite materials are briefly addressed. In the same way, the previous achievements, failure mechanisms, and used methodology are briefly reported. Based on the current material development, challenging applications and research needs, the state of the art is shortly presented paying attention towards purpose, objectives, methodology, and approaches of the research.

1.1. Introduction

Composite materials are those materials containing more than one constituent material, each with specific structural properties. Though composite materials have been used during primordial times, the modern composite material formation was used in the 1930s when glass fibers reinforced plastic had been brought to structures [1]. Boats and aircraft were built out of these glass composites, commonly called fiberglass. Since the 1970s, the application of composites has widely increased due to the development of new fibers such as carbon, boron, and aramids and new composite systems with matrices made of metals and ceramics.

The main benefit of composite materials that researchers and engineers initiate to incline the new technology is the potential for a high ratio of stiffness to weight [2, 3, 4]. Due to their great potential in weight saving and specific strength, laminated structures made of plies of a fiber-reinforced polymer have become more and more important over the past years [2, 5]. In recent years, they are successfully used in many applications where high stiffness, high strength, and low weight are required, such as spacecraft, aircraft, ship hulls, automobiles, wind turbine blades, sports' equipment, electronic devices, naval construction, civil engineering, and many other consumer products[2, 5, 6 - 9]. Even if widely utilized, their full potential is not yet exploited [5].

Unlike conventional materials, composite materials fail in complex ways. The heterogeneous properties of composite materials make the behavior more complicated. Various types of damage, fragile strength, cracks and failure modes, such as (buckling-driven) delamination and delamination due to low-velocity impact could be developed in composite structures [2, 4 - 6, 10,

11]. Often, damages are developed from manufacturing-induced flaws [10]. More precise and more reliable modes are required to handle progressive damage and to predict the behavior of laminated composite components. The failure behavior of composites has been currently studied that are used for typical engineering applications that contain advanced fiber or laminated composites, such as glass, carbon, boron, graphite, and Kevlar reinforced plastics.

Even though composite materials have great advantages in strength to weight ratio and customization of structures, their heterogeneous behavior have greatly affected their application [11]. However, progressive improvements have been obtained to improve their applicability and minimize their drawbacks. Otherwise, catastrophic failure would happen. To analyze the failure of composite materials, the basic concepts of mechanics can lead to actual behavior [12]. When a laminated composite panel is loaded, stresses are magnified a lot by the presence of inclusions or features like notches and holes. Unlike observed in the isotropic crystalline materials, there are various types of failure modes in composites as mentioned earlier. This is due to the heterogeneous nature of composites. Therefore, it would be better to contemplate the strength, stiffness, typical cracks, and the delamination while putting the causes aside [4].

The structure of a composite laminate, the plane defined by a constituent lamina corresponds to the plane of laminate. Similarly, loads and stresses are in plane only if they are applicable in that plane. For in-plane tension loading, there are various failure events possible to occur. The first damage is generally the matrix failure, in particular at the locations where a stress concentration feature is located. One of those matrix failure modes is the matrix tensile cracking, especially in 90° plies (in transverse loading direction). The other failure mode is the matrix shear cracking between fibers [13], especially in off-axis 45° plies. On the other hand, one can distinguish 45° and 90° plies from the texture and corresponding oriented cracks relating to the mentioned failure modes [14]. Although the resemblance of the delamination is a crack, the delamination phenomenon cannot be treated as easily as for the in-plane cracks. However the initiation process is difficult to model, once well-defined cracks have formed, fracture mechanics methods are applicable [15]. In order to be able to model and understand the evolution of damage in a composite materials' structure, the relevant fracture mechanics properties of each material and the interfaces between the materials must be characterized.

Cracks in composite material structure and delamination can be investigated using fracture mechanics theory for instance, the in-plane cracks are analyzed in terms of stresses and

intralaminar approaches. On the other hand, the stresses are fully out-of-plane for the delamination cracks that would result in the surface between laminas [4]. Therefore, delamination analysis literally depends on the so-called interlaminar stresses. Because of the behavior of weak adhesion in out of the plane direction, delaminations are more critical than in-plane cracks. Such behaviors make the delamination a treacherous phenomenon. The main reason for this conflict is the typical lack of any reinforcement in through-thickness direction. In some rare cases, stitches are added to reinforce the laminate in through-thickness direction. Unlikely if the loading is tension, delamination are not largely influenced compared to compression. Thus, all the characteristics make the delamination insidious.

Delamination can be characterized using the finite element method or/and experimental methods. Finite Element methods generally depend on the way of performing the calculation of the strain energy release rate [16]. On the contrary, it is possible to calculate directly SIF (stress intensity factor) or other factors by directly using Finite Element Analysis (FEA). However, such direct finite element method (FEM) applications require unique designed crack-tip elements, especially unavoidable for complicated geometries [17, 18].

The interface between the layers of a composite structure is of special interest because when this type of structure is subjected to certain types of external loading, the failure process (delamination) takes on a unique character. Interface delamination is traditionally simulated using fracture mechanics methods as earlier mentioned. Fracture along an interface between phases plays a major role in limiting the toughness and the ductility of the multi-phase materials, such as matrix-matrix composites and laminated composite structure. This has motivated considerable research on the failure of the interfaces however; the experimental investigation has become of crucial importance.

In the case of finite element analysis, currently, most of the published papers dealt with mode I and mode II delamination of composite materials however many have been done using different methods. Li et al. [19, 20] developed energy-based semi-empirical, analytical, and numerical models to quantify the results of cohesive finite element method (CFEM) predictions. They studied fracture toughness of two-phase ceramic composites as a function of statistically defined morphological attributes of microstructure, constituent properties, and interfacial bonding characteristics to provide an analytical relation between the fracture toughness and microstructure. The authors quantified the fracture toughness by an assessment of the

contributions of different fracture mechanisms including matrix fracture, interfacial debonding, and particle cracking to the overall energy release rate. This helps in the selection of materials and the design of new materials with customized properties. Albedah et al [21] established an analytical model for the stress intensity factor for a repaired crack emanating from central holes. The model also highlights the difference in the value of SIF for small and long cracks. The use of this model can be very useful for the repairing of aircraft structures. Likewise, Chen et al.[5] investigated the failure mechanism of fiber composite T-piece specimens under mixed-mode loading conditions by simulation of multi-delamination using a modified cohesive model with a coupled damage scale and added thermal effects. The other research that was done by Wimmer et al [2], discussed the numerical treatment of delamination in laminated composite components. The work used the first ply failure criterion to predict delamination initiation, while delamination propagation was analyzed using linear elastic fracture mechanics. Moreover, the researchers stated the combination of an initiation criterion and a propagation criterion that allows for a conservative estimation of the size and the location of the critical initial delamination, the delamination load, and the load-carrying capacity of the structure.

The other method of investigation is experimental approach. Jiet et al [17] conducted an experimental study, based on the global and local analysis of the results of fracture tests, in order to investigate the effect of adhesive thickness on the interfacial energy release rate, interfacial strength, and shapes of the interfacial traction–separation laws under the mixed I/II mode loading condition. The measured interface laws based on the single-leg bending (SLB) specimens reflect the equivalent and lumped interfacial fracture behaviors, which include the cohesive fracture, damage, and plasticity. Their global test results indicated that the J integrals: J_{IC}, J_{IIC}, and J_C increase as the adhesive thickness increases. The principle of dealing with delamination is similar to the adhesive joint characterization. For similar adhesive joints, Suzuki et al [22] constructed a simplified formula to predict the toughness. In this study, the prediction of the effect of the microstructures on the composite/adhesive interface toughness, crack growth analysis of the interface with microstructures was performed using the finite element method and a cohesive zone model.

As mentioned earlier, the failure of composite materials is mainly due to the failure of the bond between fiber and matrix. Further, matrix cracking and fiber rapture are additional damage modes in composite materials. Both damages lead to delamination (interlaminar) and

intralaminar fracture. The debonding and matrix cracking could be improved by means of some modification interventions. Stitching and nanomaterial additions could be the main, more effective interventions in the enhancement of the behavior of materials.

Based on the above review and in particular on the mentioned papers, it comes clear that the following points need to have additional consideration and investigation. Because of the above immediate research ideas, the complexity of the failure mechanism and the increments of the demand of composite material structures instigate the manufacturers and consumers to have a reliable, durable, efficient and minimum maintenance cost including prevention of catastrophic failures. The previously mentioned indicators have been striking the interest of scientists and engineers to fulfill the stipulations from various design points of view.

1.2. Statement of the problem

The challenge of humanity nowadays and in the future is to overcome economic challenges of escalation of the price of fuel or energy due to scarcity of non-renewable natural sources and environmental pollution. One of the existing solutions that scientists and engineers' belief to overcome the problem are by the exploiting of structures those having lightweight and substantial properties of materials. The solution that engineers and scientists developed is composite materials.

Whether countries are developed or undeveloped, the global problems obligate every society or country to march in the same line. The car that is being manufactured, the fire engines that are used, the power generation plant that is being built, the sports; equipment that the society needs, electric equipment that people have started using will be changed partially either in a short period of time or completely in the future by composite materials. All those materials shall be known in detail with respect to their mechanical properties, manufacturing methods, failure criterion, and synthesis of the materials in comparison with convectional/ homogeneous materials. Unless in-depth study has been conducted on the failure of composite materials, the consequences of failures will become more and more devastating as the technology becomes more and more sophisticated. Equally, structures must be improved through time as the history of technology has taught us. Thus, customization of materials and properties enhancement shall be considered.

One of the causes of failure of composite materials, as aforementioned under the section of background, is the weakness of the interfacial strength in the out of the plane direction, which is known as interlaminar failure. Equivocally composite materials are susceptible to intralaminar damage due to impact load, which introduces crack propagation in the in-plane direction. Failure of materials due to fracture/crack, as a whole, is more catastrophic unlike other failure characteristics in the application of debonair technologies. Since a large number of mechanical properties of composite materials with specific constituents and at glance case, detail and deep study should be taken to avoid risks and to be economical that the world demands.

Thus, all the aforementioned problems need to have a solution accordingly. Consequently, the weakness of the interfacial failure requires the enhancement and the improved interfacial behaviors need characterization using strength and fracture approaches. Likewise, the intralaminar conditions of the material need to be investigated, similarly the fractography and crack growing behavior have a need of summarization.

1.3. Objectives of the research

1.3.1. General objectives

The wide-ranging purpose of the research is to examine the effects of nanoclay on strength, modulus of elasticity, fracture characteristics of glass fiber reinforced plastic and investigating the intralaminar fracture behavior of the novel semi impregnated micro sandwich structure and the intralaminar fracture characteristics of two manufacturing types of GMT based composite materials

1.3.2. Specific objectives

The explicit intentions of the research include:

- Observing the influence of a particular type of nanoclay, Cloisite 20B, considering different concentrations of nanoclay, on the strength, modulus of elasticity, and Poisson's ratios of the material
- Investigation of the interlaminar fracture toughness of the pristine and modified composite materials in out of the plane direction
- Examining the crack growing resistance curve of the pristine and modified material after the addition of specific concentrations of the nanoparticles

- Determining the intralaminar fracture toughness and investigating the crack growing behavior of SIMS and GMT

1.4. Significance of the study

Structures have to be designed to match safety targets in order to minimize the possible loss of life and to conserve resources. Besides, structural behavior must contribute considerably to have green environment and to preserve the globe safely. Additionally, engineers have to know the material behavior in detail before a design has been developed. Thus, this research is significant as it focuses on failure modes, specifically the strength and fracture behavior of composite materials. This will help researchers in initiating and developing wider researches to improve appropriately structural materials taking into account the output of this research as reference and benchmark. In the same way, it has a great contribution to the awareness about the composite material and structure for the community and helps the composite material manufacturers to produce and improve their design in an efficient and advanced way to have contemporary equipments and structures.

Therefore, the significance of the research is dual, in which the front is facilitating the innovative researchers in the area to have a deeper understanding of possible strategies for enhancing and investigating the strength and fracture characteristics of composite material. And equally important in initiating the people participation in advanced and enhanced composite materials production to substitute structures and components that have been made up of using conventional materials for future structural components.

1.5. Research procedures and methodology

The overall framework for the research method has two important circumstances. The first performed activity includes literature review, experimental setting design, material synthesis, and development of specimens. The second performed activity includes the conduction of the experimental tests that are followed by the determination of the traditional mechanical properties and analysis of the interlaminar and intralaminar fracture behavior by proper characterization procedure. The research methodology has been organized accordingly. More importantly, the research will carry out:

- Data collection, information anthology or literature review
- Experimental setting design

- Development of GFRP plates to determine the mechanical properties of materials and fracture behavior according to specific nonmaterial specifications
- Preparation of specimens and fixtures according to ASTM D 3039/D 3039M – 00, ASTM D 3410/D 3410M – 03, ASTM D5528 – 01 and Modified ASTM E399 – 09
- Conducting experimental tests according to specific ASTMs standards
- Manipulation, interpretation, and justification of results

The detailed illustration and the methodology adopted to perform those tasks and procedures will be briefly deployed in the following sections.

1.5.1. Literature review

Literature review focus on principal theory, enhancement, production, damages, mechanical properties, and fracture characterization of composite materials. In the same way, the literature review includes the description of experimental techniques to determine mechanical properties and the fracture toughness and behavior of composite material.

1.5.2. Experimental setting and design

In addition to the theoretical part of the research, it also includes defining the detailed solution of the stated problem. Initially, the effect of weakness of the material and the previous measure are discussed. Thus, appropriate material synthesis with specific enhancement concentration has been defined and the sizes of the plates have been designed. Following manufacturing design, the types of equipment required to conduct the experimental test have been defined and identified.

1.5.3. Development of GFRP plates

The manufacturing process has been undertaken to obtain good nano distributive and dispersive mixing. Initially, epoxy was mixed with the desired concentration of nanoclay and the resulting compound was sonicated. The resulting mixture became cool. Then the solutions mixed thoroughly, degassed before applied on each ply using hand layup process and other manufacturing processes according to the material types. Finally, the materials became ready for specimen preparation and testing.

1.5.4. Preparation of specimens and fixtures

Specimens required for material characterization specifically for tensile and compressive tests have been prepared according to ASTM D 3039M – 00 and ASTM D 3410M – 03 standards respectively from the GFRP plates. Similarly, double cantilever beam (DCB) specimens that are required for interlaminar fracture behavior have been produced. The specimen size and the test

procedure follow ASTM D5528 – 01 standard. Since, the DCB specimens require fixtures, all the fixtures, and the experiment setting have been designed and organized according to the mentioned standard.

The intralaminar fracture behavior characterizations have been planned to be conducted using SIMS and GMT materials. These specimens need special dimensions and fixtures/clevis. Thus, the specimens have been developed using Modified ASTM E399 – 09.

1.5.5. Conducting experimental tests according to specific ASTMs standards

Each type of test has been organized to conduct using a universal testing machine (Instron 8801) according to specific ASTM standards. For material characterization, data acquisition equipment has been prepared while the camera has been prearranged for all types of fracture behavior characterization.

1.5.6. Manipulation, interpretation, and justification of results

Equipments and simple software have been used to elaborate the acquired results and to construct the output diagrams. The standards and literature have been used to interpret and justify results.

1.6. Scope of the study

The research does not consider the nanoclay type effect and the sonication influence though it focuses on the specific nanoclay type and single sonication procedure for the enhanced GFRP material. Similarly, the study has dealt with specific fiber matrix composition. For SIMS materials it is limited to two types of fibers, which include glass fiber semi impregnated micro sandwich (G-SIMS) and carbon fiber semi impregnated micro sandwich (C-SIMS), while the GMT includes traditional GMT and unidirectional reinforced GMT materials. GFRP, SIMS, and GMT have been considered. All tests have been conducted according to their specific standards and followed static condition (quasi-static).

1.7. Organization of the research

This doctoral research thesis consists of six chapters under part I & part II and is organized in the following manner. The first chapter gives an overview of the research problem, expected solution objective, methodology, significance, and scope. The second chapter discusses the entire detail background and related works of literature on the damages, advantage of composite materials, manufacturing, application, and enhancement of composite materials. It also discusses the type

of nanoparticles and the appropriate loadings for both strength and fracture toughness improvement. Chapter three dealt about the manufacture of specimens and test procedure of the mechanics of GFRP. It discusses the effects of nanoclay loadings over strength and modulus of elasticity for both tensile and compressive behaviors. Chapter four explains the influence of Cloisite 20B on the interlaminar mode I fracture toughness and the resistance curves. Correspondingly, chapter five examines the intralaminar mode I fracture toughness and crack growing behavior for SIMS and GMT. Each chapter includes the whole results' discussion and justification. Finally, chapter six concludes the general findings of the research and it gives recommendations and future research directions.

1.8. Reference of chapter one

[1] Kaw AK, Mechanics of composite materials, 2nd edition, Taylor & Francis Group, LLC 2006

[2] Wimmer G, Schuecker C, Pettermann HE. Numerical simulation of delamination in laminated composite components – A combination of a strength criterion and fracture mechanics. Compos Part B 2009; 40: 158–165

[3] Burton WS, Comput AKN, Assessment of continuum models for sandwich panel honeycomb cores, Methods Appl. Mech. Engrg. 145 (1997) 341-360

[4] Peng L, Xu J, Zhang J, Zhao L, Mixed mode delamination growth of multidirectional composite laminates under fatigue loading, Engineering Fracture Mechanics 96 (2012) 676–686

[5] Chen J, Fox D, Numerical investigation into multi-delamination failure of composite T-piece specimens under mixed mode loading using a modified cohesive model, Composite Structures 94 (2012) 2010–2016

[6] Maillet I, Michel L, Ric G, Fressinet M, Gourinat Y, A new test methodology based on structural resonance for mode I fatigue delamination growth in an unidirectional composite, Composite Structures 97 (2013) 353–362

[7] Shokrieh MM, Heidari-Rarani M, Rahimi S, Influence of curved delamination front on toughness of multidirectional DCB specimens, Composite Structures 94 (2012) 1359–1365

[8] Wetzel B, Rosso P, Haupert F, Friedrich K, Epoxy nanocomposites – fracture and toughening mechanisms, Engineering fracture mechanics 73 (2006) 2375–2398

[9] Hamitouche L, Tarfaoui M, Vautrin A, An interface debonding law subject to viscous regularization for avoiding instability: Application to the delamination problems, Engineering Fracture Mechanics 75 (2008) 3084–3100

[10] Short GJ, Guild FJ, Pavier MJ, The effect of delamination geometry on the compressive failure of composite laminates, Composites Science and Technology 61(2001) 2075–2086

[11] Taraghi I, Fereidoon A, Taheri-Behrooz F, Low-velocity impact response of woven Kevlar/epoxy laminated composites reinforced with multi-walled carbon nanotubes at ambient and low temperatures, Materials and design 53 (2014) 152–158

[12] Lin KY, Composite Materials: Materials, Manufacturing, Analysis, Design and Repair, 2014

[13] Li Y, Zhou M, Prediction of fracture toughness of ceramic composites as function of microstructure: I Numerical simulations, Journal of the mechanics and physics of solids 61 (2013) 472–488

[14] Morais JJL, Moura MFSF_, Pereira FAM, Xavier J, Dourado N, Dias MIR,Azevedo JMT, The double cantilever beam test applied to mode I fracture characterization of cortical bone tissue, Journal of mechanical behaviour of biomedical materials (2010)446 - 453

[15] Adrian G, Orifici C , Krueger R, Benchmark assessment of automated delamination propagation capabilities in finite element codes for static loading, Finite Elements in Analysis and Design 54 (2012) 28–36

[16] Ji G , Ouyang Z , Li G, On the interfacial constitutive laws of mixed mode fracture with various adhesive thicknesses, Mechanics of materials 47 (2012) 24–32

[17] Ji G, Ouyang Z,Li G, Fabrication and study on mechanical properties and fracture behavior of nanometric Al2O3 particle-reinforced A356 composites focusing on the parameters of vortex method, Composites: Part B 47 (2013) 1–7

[18] Sundararaman V, Davidson BD, An unsymmetrical double cantilever beam test for interfacial fracture toughness determination, lnl. J. Solid. Structures Vol. 34. No. 7, pp. 799 817, 1997

[19] Morais AB, Mode I cohesive zone model for delamination in composite beams, Engineering Fracture Mechanics 109 (2013) 236–245

[20] Li Y, Zhou M, Prediction of fractures toughness of ceramic composites as function of microstructure: II: Analytical model, Journal of the mechanics and physics of solids 61 (2013) 489–503

[21] Albedah A, Benyahia F, Dinar H, Bouiadjra BB, Analytical formulation of the stress intensity factor for crack emanating from central holes and repaired with bonded composite patch in aircraft structures, Composites: Part B 45 (2013) 852–857

[22] Suzuki T, Matsuzaki R, Todoroki A, Mizutani Y, Crack growth analysis of a composite/adhesive interface toughened by in-mold surface preparation, International Journal of Adhesion & Adhesives 42 (2013) 36–43

Chapter 2: Basics and Literature Review

This chapter reviews the evolution of materials, the basics of lightweight materials and the manufacturing process of composite materials. The constituents of composite materials (i.e. the different types of fibers and matrices) are introduced. The knowledge of intended applications of composite materials is crucial to determine the appropriate type of constituents and manufacturing methods so that the major application areas are included in the review. Furthermore, since to prolong and improve the lifetime of the materials is the main target of this research, the basics on damage/failure of the composite materials are incorporated. The interlaminar and intralaminar behaviors are considered. The nanoparticles that are used in enhancement processes for various types of composite materials and applications, and the related affection mechanisms are summarized.

2.1. Background of composite materials

Selecting appropriate materials should have to be considered according to their application, mechanical properties, physical properties, electrical properties, thermal properties, chemical properties, coloring, process, cost, availability, environmental compatibility, and human interaction with the material [1]. Mechanical properties of materials are one of the determining factors in the design process of structural parts of mechanical components and systems. Materials have evolved various stages as indicated in Figure 2.1 (a, b &c). Material evolutions have progressed along with human knowledge and effort.

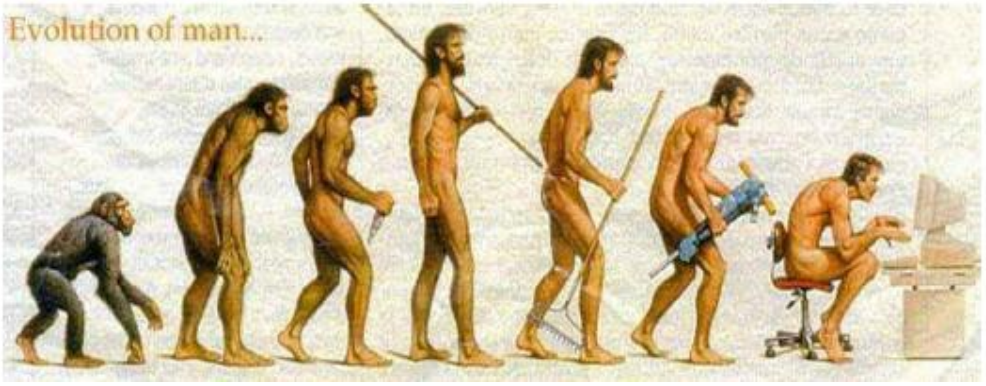

(a)

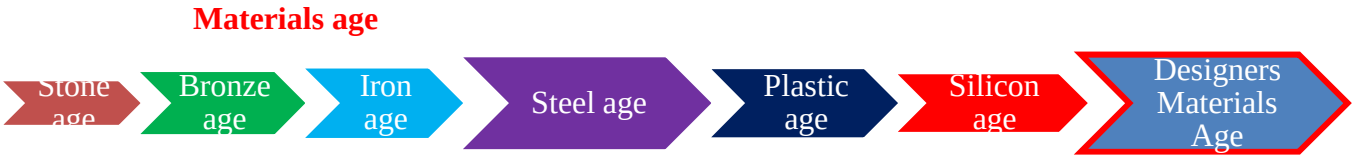

(b)

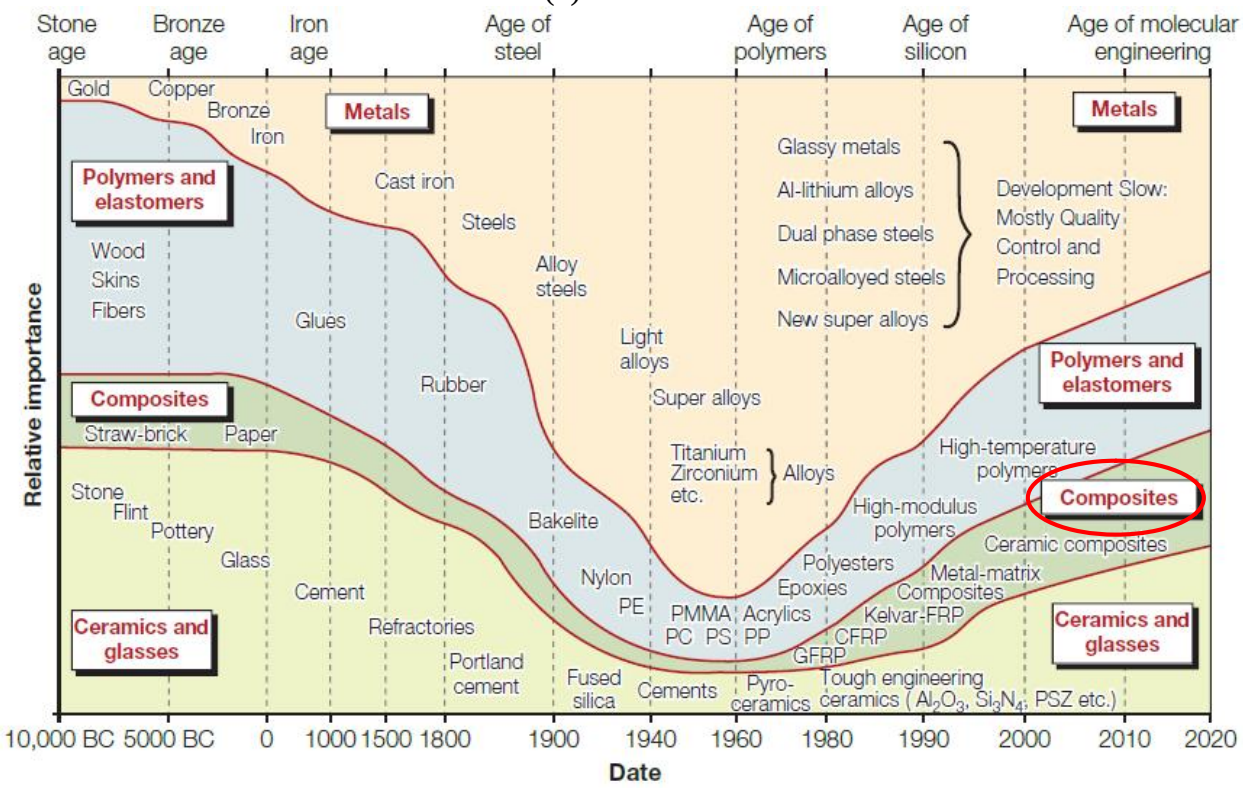

(c)

Figure 2.1 Evolutions of materials (a) Evolution of human being and modernization with knowledge, (b) materials age(c) The evolution of engineering materials with time [2]

Globally, steel is still used in a large percentage. According to the study undertaken by JeC group, in 2016, the world consumes 1.578 GT next to concrete, which is about 4GT. The new materials, glass fiber, and carbon fiber are approaching 4.7MT and 41kT respectively [3].

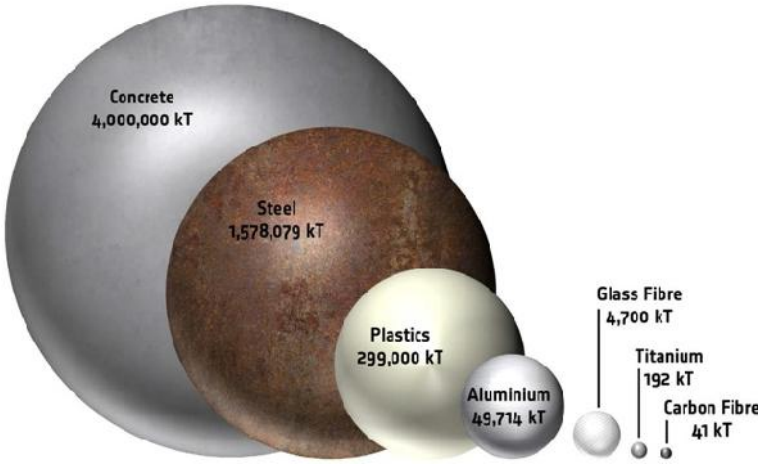

Figure 2.2 Materials used globally (2016)[3]

Material scientists often involve themselves in understanding the influence of materials processing on its structure, and thus its material properties and performance called the materials paradigm [4]. Two of the material properties fracture behavior and mechanical properties that include mass, strength, stiffness. Composite materials are one of the structural, semi-structural and non-structural materials, which are generally lighter than metals and have almost comparable strength, so these materials can replace metals in many applications; however, they lack the toughness of metals. So nowadays, the studies of composite materials have extensively used to substitute conventional materials. The study includes all its characteristics, manufacturing, properties, customization, enhancement, etc.

These relatively new materials are those materials containing more than one bonded material, each with different structural properties. Thus, the current contemplation of composite material is a structural material that consists of two or more distinct materials with a distinct, macroscopic interface that achieves the best properties not possessed by any constituent acting alone and is not soluble in each other [5]. A typical composite has two parts: a strong, stiff material, commonly referred to as the fiber, that provides the strength and rigidity, which is embedded in a second material, called the matrix, which serves to bind and protect these fibers.

People have been used composite materials since they started living in a hut. Registered human efforts to exploit composite materials date back to the primeval times when Israelites using bricks made of clay and reinforced with straw. The individual constituents, clay, and straw could not serve the function by themselves but did when putting together [6]. Even nowadays African people have been constructing their house wall using wood and mud-hay composite in rural and small towns in some parts of the continent. The hay is used to reinforce the mud as the Israelis

did before B.C. In the 20th century, modern composites were used in the 1930s when glass fibers reinforced resins. Boats and aircraft were built out of these glass composites, commonly called fiberglass. Since the 1970s, the application of composites has widely increased due to the development of new fibers such as carbon, boron, and aramids and new composite systems with matrices made of metals and ceramics. Now times the use of composite materials has been escalating from marine structures to spacecraft components in large mechanical parts and electronics.

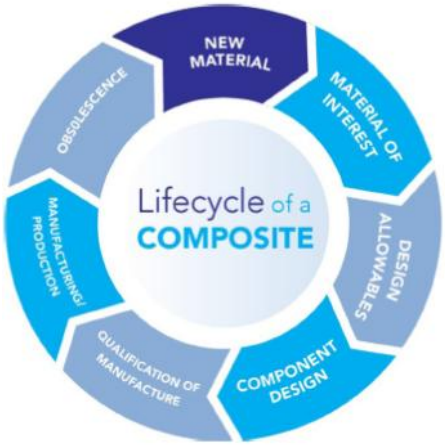

Figure 2.3 Typical lifecycle of a composite [7]

Composite materials are multidisciplinary and they have their own life cycle as shown in figure 2.3[7]. It involves material sciences, structural mechanics, mechanical design, manufacturing, and business and economics. Similarly, the scope of composite materials consists of various specializations [5].

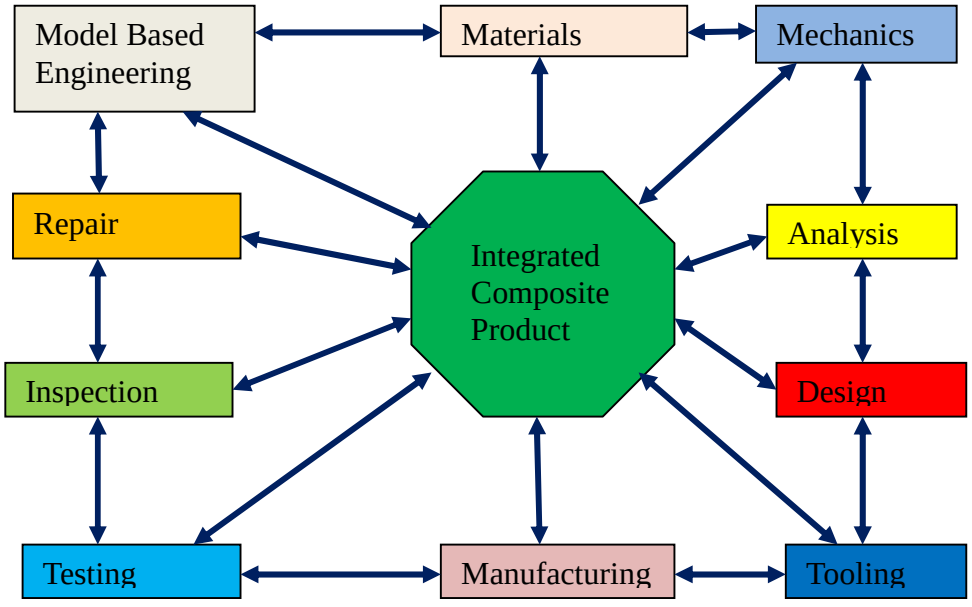

Figure 2.4 Requirement to obtain integrated composite product [5]

Figure 4 shows how an integrated composite product requires various activities in which to achieve a well prepared structural part. Materials, mechanics, analysis, manufacturing, and testing are some of the above important disciplines that are more related to design/ mechanics. The work followed by this general description will target on the specific properties of some of the particular composite materials. The basic combinations of composite materials are shown in figure 2.5.

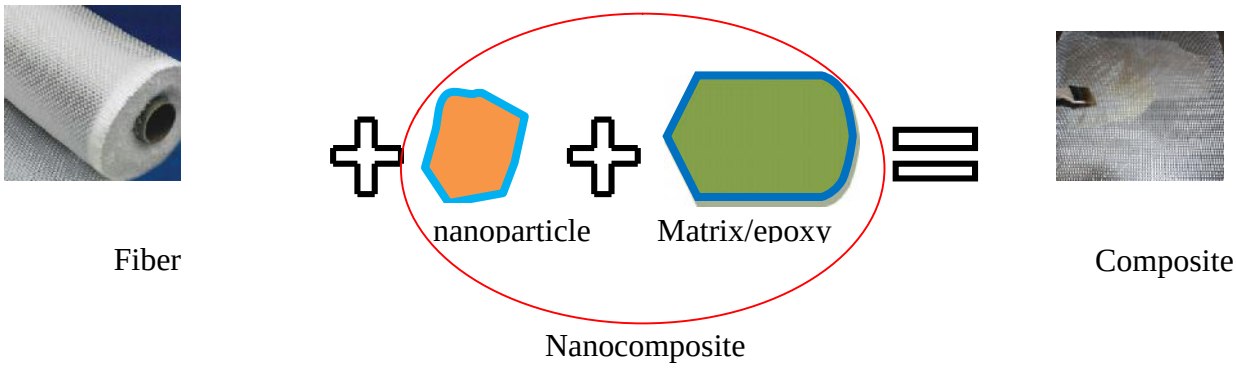

Figure 2.5 Composition of composite materials

2.1.1. Advantage of composite materials

As earlier mentioned, from the very beginning, starting from 1950, scientists had been investigating renewable materials. Meanwhile, they were thinking about formable structures and, in the late 70's, they became worried about the energy consumption of airplanes and vehicles. There were two main reasons, escalation of the fuel price with its non-renewability and growth of the environmental pollution. The former reason instigated airplane-manufacturing companies to deal with the weight of the structures. Commonly they used to build with aluminum at largest amount while titanium and steel were used in a considerable percentage. Thus, the companies had focused on researching lightweight materials with a comparable modulus of elasticity and strength as shown in figures 2.6 and 2.7. Finally, they also considered the number of components and assemblies to construct the aircraft structure. However, the manufacturing cost of this material became a headache.

Later on, the increments of the demand for composite material structures initiate the manufacturers and consumers to have a reliable, durable, efficient, and minimum maintenance cost structure able to prevent the consequences of catastrophic failure. The aforementioned

interests have been striking the interest of scientists and engineers to fulfill the stipulations from various design points of view.

Thus, the main advantage of composite materials can be considered because of their potential due to a high stiffness to weight ratio [8-10].

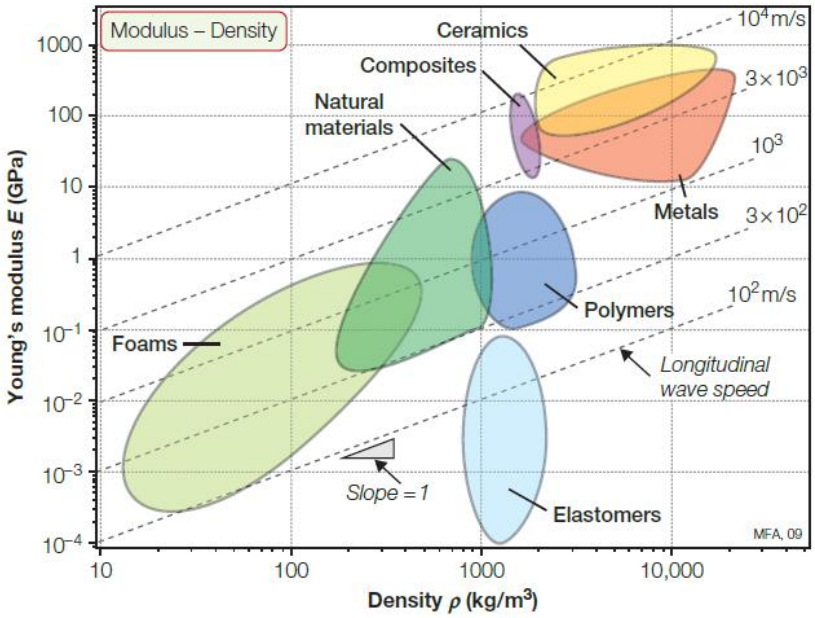

Figure 2.6 The idea of a material property chart: Young's modulus plotted against the density [2]

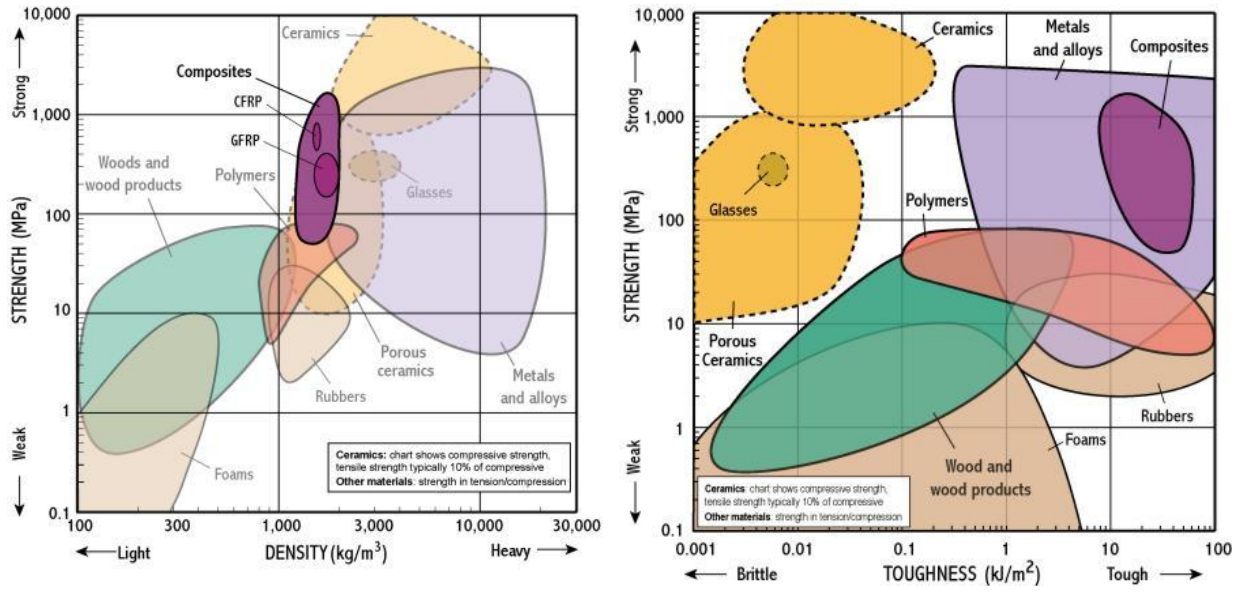

Figure 2.7 Ashby maps for strength to weight (a) and strength toughness (b) comparisons of materials

2.1.2. Fibers and matrix

As described earlier, composite materials are a combination of two or more materials, which can give the best property instead of the constituents. It could also contain nanoparticles to enhance the combined property at an advanced level. The bonding between fibers and matrix is created during the manufacturing phase of the composite material. This has a fundamental influence on the mechanical properties of the composite material. The enhancement process must be done before combining the fiber and matrix as shown in figure 2.5. The pre-process of matrix creates nanocomposite if nano enhancement is required. Composite materials have to be evaluated with specific properties to optimize and customize the appropriate behavior (figure 2.8).

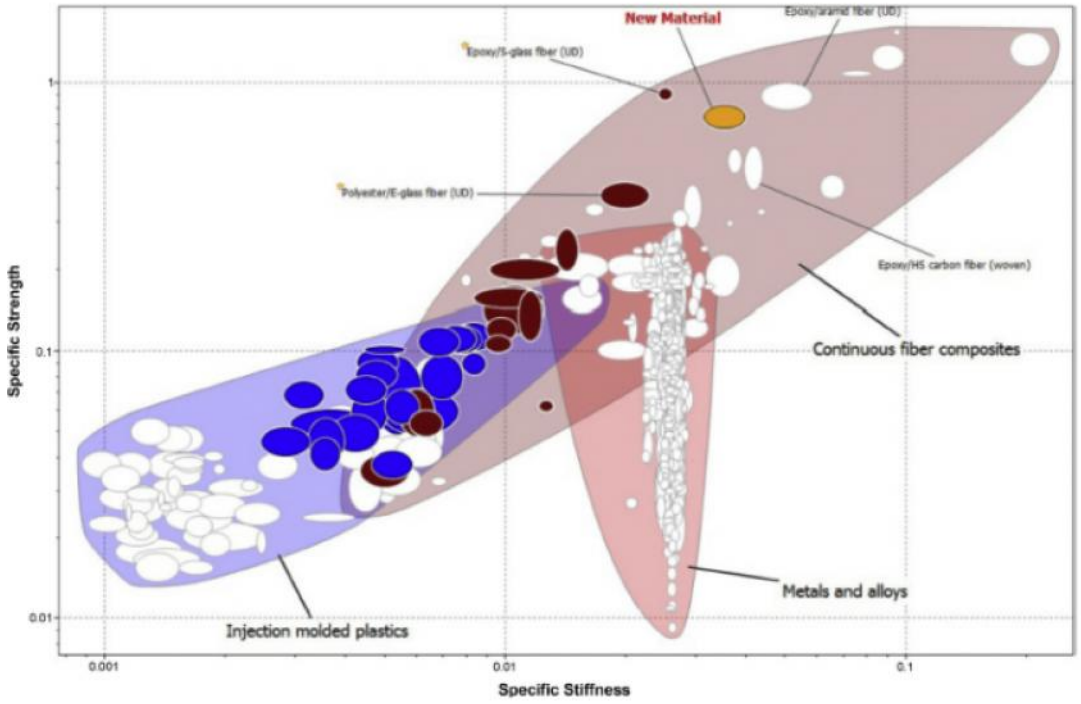

Figure 2.8 Materials property chart comparing a new composite to existing materials [7]

2.1.3. Type of fiber

Fibers consist of thousands of filaments, each filament having a diameter of between 4 and 15 micrometers/ microns, allowing them to be producible using textile machines. The most used fibers in the composite material production are the glass fibers, the carbon (or graphite) fibers, and natural fibers. However, boron fibers, which are very light and expensive, and the Kevlar (aramid polymer) fibers are also, even if rarely, used [11].

Glass fibers are characterized by a high strength (SR = 3500-4600 MPa), nearly the double of the most resistant steels, and a high value of the elastic modulus (E = 72 – 85 GPa, that is close to

the aluminum values), relatively low cost and low thermal and electrical conductivity. There are three different types of glass fibers: E, S and R types: type E is constituted essentially of silica (SiO2), alumina (Al2O3) and calcium carbonate (CaCO3), at the beginning it was used in the electric industry (E means its original electric use). The type S is constituted essentially of silica (SiO2), alumina (Al2O3) and magnesia (MgO), it is characterized by higher strength (S stays for strength). The final glass type R is rarer and is characterized by strength higher than the previous ones. Although the fiber diameter can vary in a quite range of values, the most used diameter is equal to about 12 micrometers. The other fiber properties are summarized in Table 2.1.

Table 2.1 Types of fibers and properties [12]

Material	**Diameter (μm)**	**Density ρ(g/cm^3)**	**Tensile Modulus(E) (GPa)**	**Tensile Strength (σ)(GPa)**	**Specific Modulus (E/ρ)**	**Specific Strength**	**Melting Point (°C)**	**% Elongation at Break**	**Relative Cost**
E-glass	7	2.54	70	3.45	27	1.35	1540+	4.8	Low
S-glass	15	2.5	86	4.50	34.5	1.8	1540+	5.7	Moderate
Graphite, high modulus	7.5	1.9	400	1.8	200	0.9	>3500	1.5	High
Graphite, high strength	7.5	1.7	240	2.6	140	1.5	>3500	0.8	High
Boron	130	2.6	400	3.5	155	1.3	2300	-	High
Kevlar	12	1.45	80	2.8	55.5	1.9	500(D)	3.5	Moderate
Bulk materials	12	1.45	130	2.8	89.5	1.9	500(D)	2.5	Moderate
Steel		7.8	208	0.34-2.1	27	0.04-0.027	1480	5-25	<low
Aluminum alloys		2.7	69	0.14-0.62	26	0.05-0.023	600	8-16	Low

2.1.4. Type of matrix

The matrix material is continuous phases, which transfer stress to the other constituents and protect the other phases from environmental influence. Matrices can be categorized into three groups that include metal matrix composite materials (MMC), inorganic non-metallic matrix composite materials (i.e. ceramic matrix composite, CMC) and polymer matrix composites (PMC). The properties of composites are a function of the properties of the constituent phases, their relative amounts, and the geometry of the dispersed phase. Metal matrices enhance the yield stress, tensile strength and creep resistance while the ceramic matrix increases the fracture toughness of the multiphase materials. Polymer matrix composite is the most common type of

matrix, which improves the modulus of elasticity, yield stress, tensile strength, and creep resistance.

The polymer matrix system can be a thermoplastic, thermoset, or elastomer. A thermoplastic polymer softens when heated above the glass transition temperature (Tg) and thus can be molded into a particular shape upon cooling. This process is repeatable, which makes thermoplastic materials processable and recyclable. Thermosetting materials become permanently hard through cross-linking when heated above Tg. Thus, thermosetting polymers cannot be molded by softening. Instead, they must be fabricated during the cross-linking process. Elastomer resins are lightly cross-linked polymer systems and have properties that lie between thermosets and thermoplastics.

2.1.5. Type of composite materials

There are many ways to classify composite materials. For example, in accordance with the reinforcing principle, there are diffusion-enhanced composite materials, particle-enhanced composite materials, and fiber-reinforced composite materials. Based on the different application requirements, there are structural and functional composite materials. Functional composite materials, in accordance with its function, can also be divided into electrical functional composite materials, thermal functional composite materials, optical functional composite materials, and so on. According to different preparation processes, it is classified as laminated composite materials, winding structural composites, pultrusion composite materials, textile structural composite materials and so on. In addition to this, the composite materials are grouped according to fiber orientation and structures as indicated in figures 2. 9, 2.10, and 2.11.

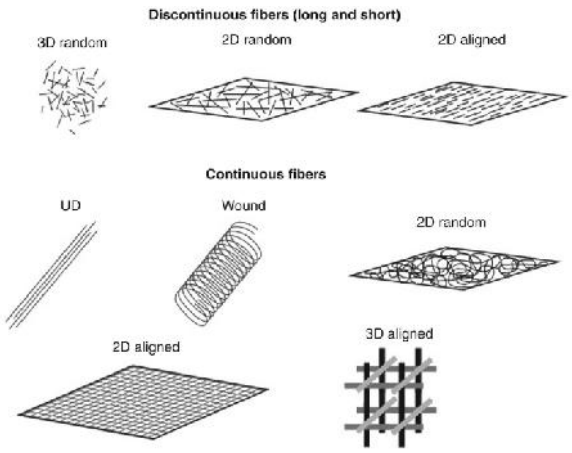

Figure 2.9 Fiber architecture diagrams [13]

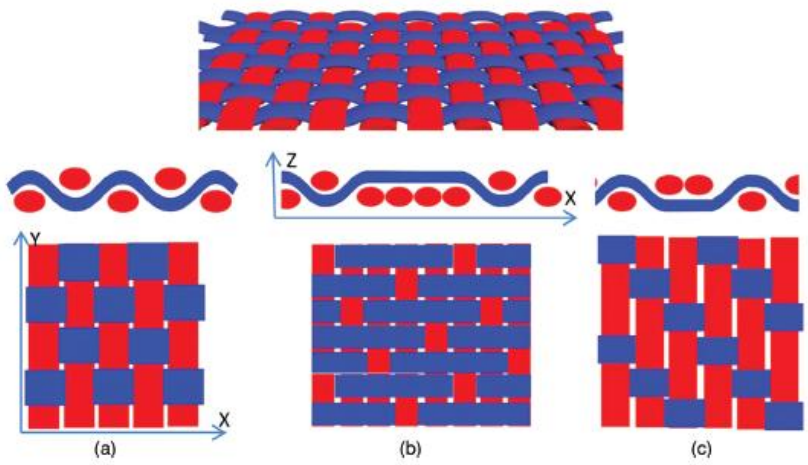

Figure 2.10 2D woven composites: (a) 2D plain weave composite, (b) five harness satin weave composite, (c) 2D twill weave composite [14]

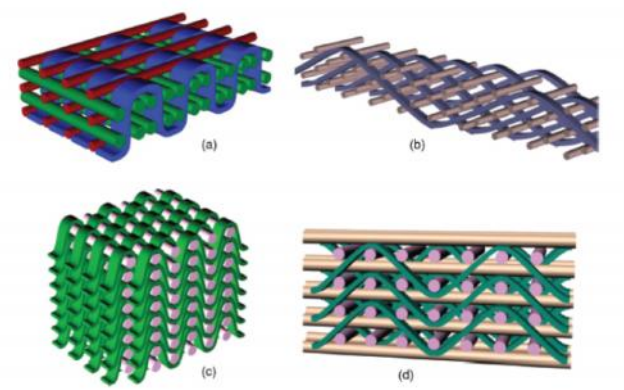

Figure 2.11 Different architectures of 3D woven composites: (a) 3D orthogonal woven composite,(b) 3D through-thickness angle interlock woven composite, (c) 3D layer to layer angle interlock woven composite, (d) 3D layer to layer angle interlock woven composite[14]

2.1.6. Manufacturing

One of the material costs in the production and composite materials is expensive manufacturing methods, unlike conventional materials. Nowadays composite manufacturing becomes automated. The good examples are additive manufacturing methods such as automated tape layup (ATL), automated fiber placement (AFP), filament winding (FW) [15]. The manufacturing types and processes may depend on the materials, which are required to be produced. FW is to create axisymmetric as well as some non-axisymmetric parts (i.e. pipe bends) by winding continuous prepreg sheets, rovings, and monofilaments around a rotating mandrel before curing while pultrusion to produce low cost, constant cross-section parts. Besides infusion is used to produce large parts with one smooth surface and RTM (Resin Transfer Molding) to produce

medium/large parts with two smooth surfaces. The other manufacturing method is SMC (Sheet molding compound) which is usually used to produce short cycle time parts whereas prepregging is commonly used to produce high-performance parts. Hand (or wet) lay-up is another development process that the most basic and lowest cost thermoset composite processing method. Correspondingly, compression molding is the oldest manufacturing technique, which avoids voids and where the material is compressed between two steel dies [15-18].

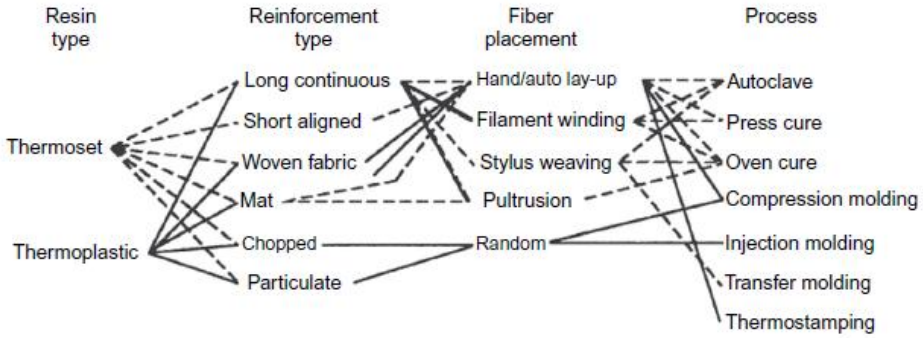

Figure 2.12 Composite constituent materials and manufacturing options [17]

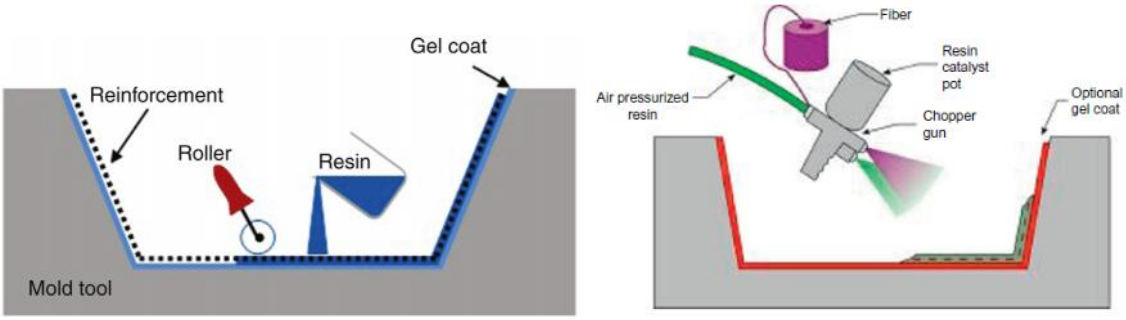

(a) (b)

Figure 2.13Manufacturing process (a) Schematic illustration of Hand lay-up diagram [15] and (b) schematic illustration of the spray lay-up technique [16]

The composite material development passes all necessary steps starting from fiber production to composite production. The detail processes are indicated in figure 2.14.

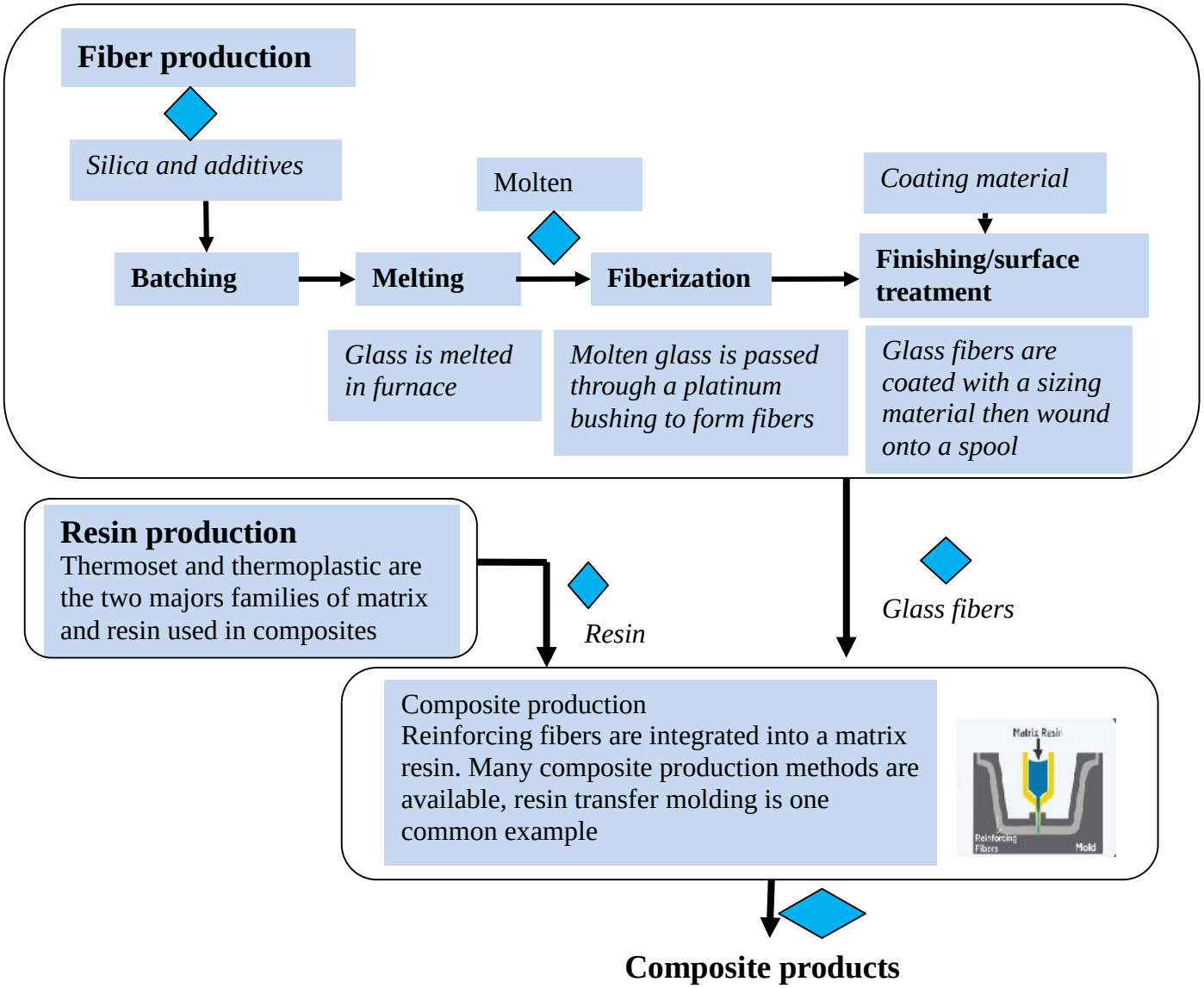

Figure 2.14 composite material production processes [19]

2.1.7. Summary

Materials are improved from time to time and composite materials are the current new technology materials that are more preferable because of their customizable behavior besides their specific properties. Moreover, the development of these materials requires a detail study including constituent properties and the final material development/ manufacturing. To obtain the best material property and apposite customization, the study should follow the type of application.

2.2. Application of Composite Materials

Composite materials have been playing an ever-increasing role in composite structures for automotive, aerospace, wind turbine, spacecraft, sports goods, marine, medical equipment, electronic devices, naval construction, civil engineering, and many other consumer products applications. This is due to their high specific strength and stiffness or high stiffness and strength with low weight, better fatigue behavior, good corrosion resistance, thermal expansions, low creep and good elevated temperature for substituting conventional materials such as steel, aluminum, and other alloy materials [9, 20]. Due to their great potential in weight-saving, laminated structures made of plies of a fiber-reinforced polymer have become more and more important over the past years [8, 21].

The applications of composite materials have been growing through time. In the USA, the fiber-reinforced composite materials market was forecasted for different application segments as shown in Fig. 15. (a) The market grew by 6.3% to reach a value of $ 8.2 billion in 2014 from the previous years and it will be expected to grow 6.6% by 2020 [22]. The percentage of volume reported as shown in figure 2.15(b) and aerospace and defense take the largest share. Similarly, according to Naqvi et al. [22] for carbon fiber, composite materials the industry demand curve was forecasted up to 2070 as indicated in fig. 16.

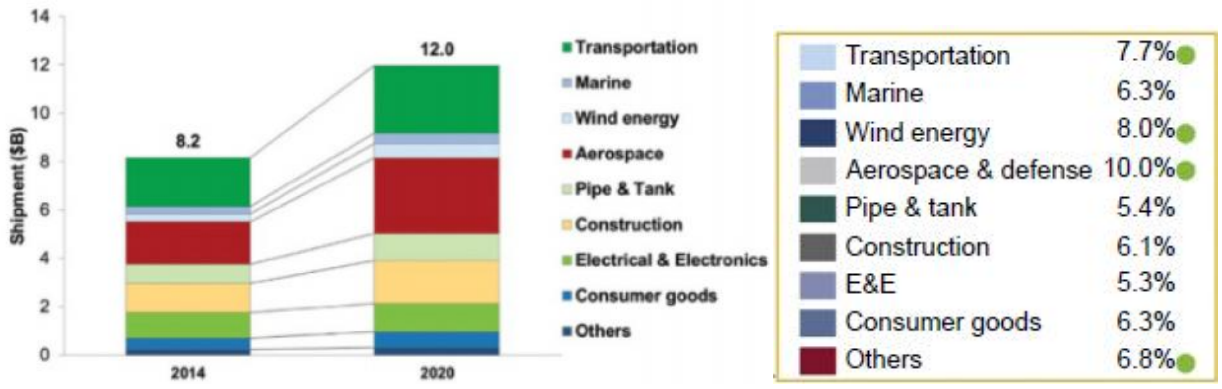

(a) (b)

Figure 2.15 Composite materials market share (a) USA Composite materials market forecast by application [22], (b) percentage of volume usage [23]

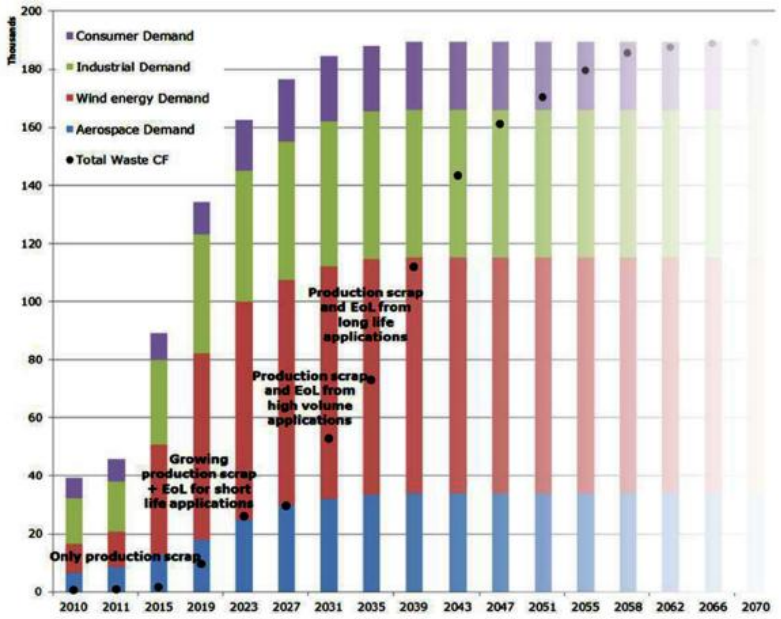

Figure 2.16 Carbon fiber demand in bar and waste in black dot for high value industry [22]

Furthermore, glass fiber reinforced plastic (GFRP) material productions are escalating from time to time and the market grew by 2% foe each year from 2012 to 2017 in Europe. For instance, the 2017 European glass fiber reinforced plastic has a large application in the area of transport [24].

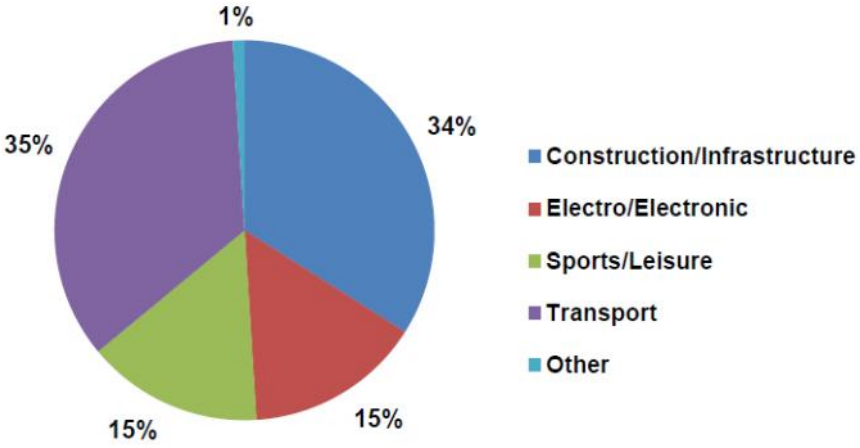

Figure 2.17: GRP production in Europe by application industry (year: 2017) [24]

2.2.1. Aircraft

Aircraft as a part of aerospace structures require low weight and high mechanical performances in order to save fuel and to be economical as well as to keep the globe safe. Currently, the appropriate materials to fit with this need are composite materials [5]. Boeing airplane, 787 Dreamliner attains to use composite materials up to 50% while Airbus, A380 approaches to use

Al 2524 and Fiber Laminates (GLARE), 22% [25]. A350 of Airbus used composite materials up to 38% [26].

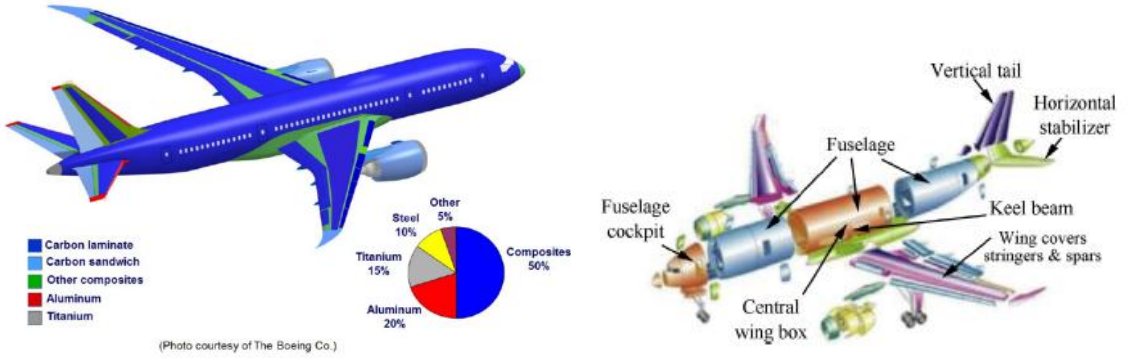

(a) (b)

Figure 2.18 Application of composite materials for (a) Boeing 787 airplane by percentage [5] (b) large-size carbon fiber reinforced plastic composite components used in Airbus 350 [27]

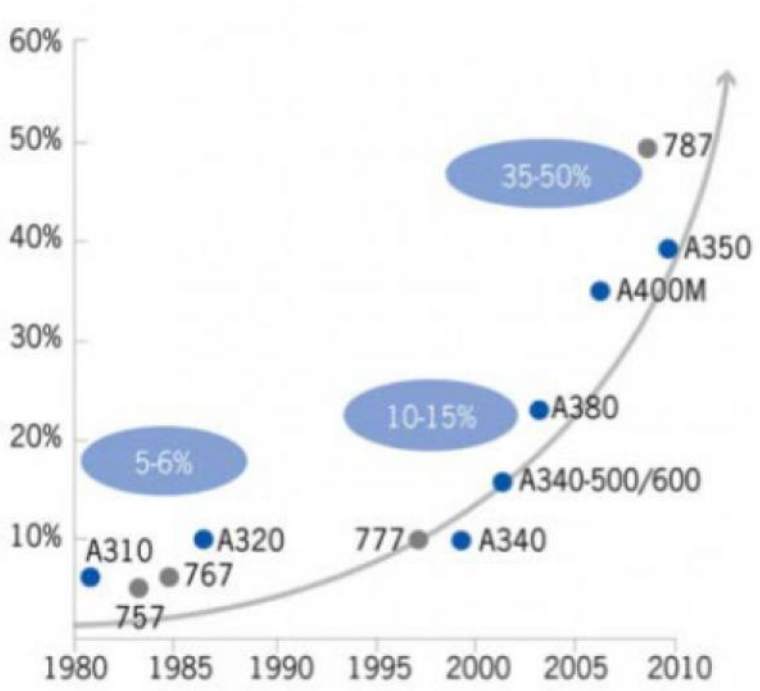

Figure 2.19 An illustration of increasing composite content, by weight, in Boeing and Airbus aircraft [26]

2.2.2. Automotive

The world automotive industry income is about 2 trillion US dollars. In 2014 the production of materials used in vehicle manufacturing were Steel 1,300,000,000, Aluminum 36,000,000, Glass fibers 3,000,000, Natural fibers 1,600,000 and Carbon fibers 58,000 tons [28]. Nevertheless, the demand for lightweight solution and high-performance requirements in automotive industry the composite material components such as glass fiber, carbon fiber, and

natural fibers will be governing the future global market [29]. The demand that is shown in figure 2.20 confirms the history of composite usage and the forecast in the very near future, up to 2021[23].

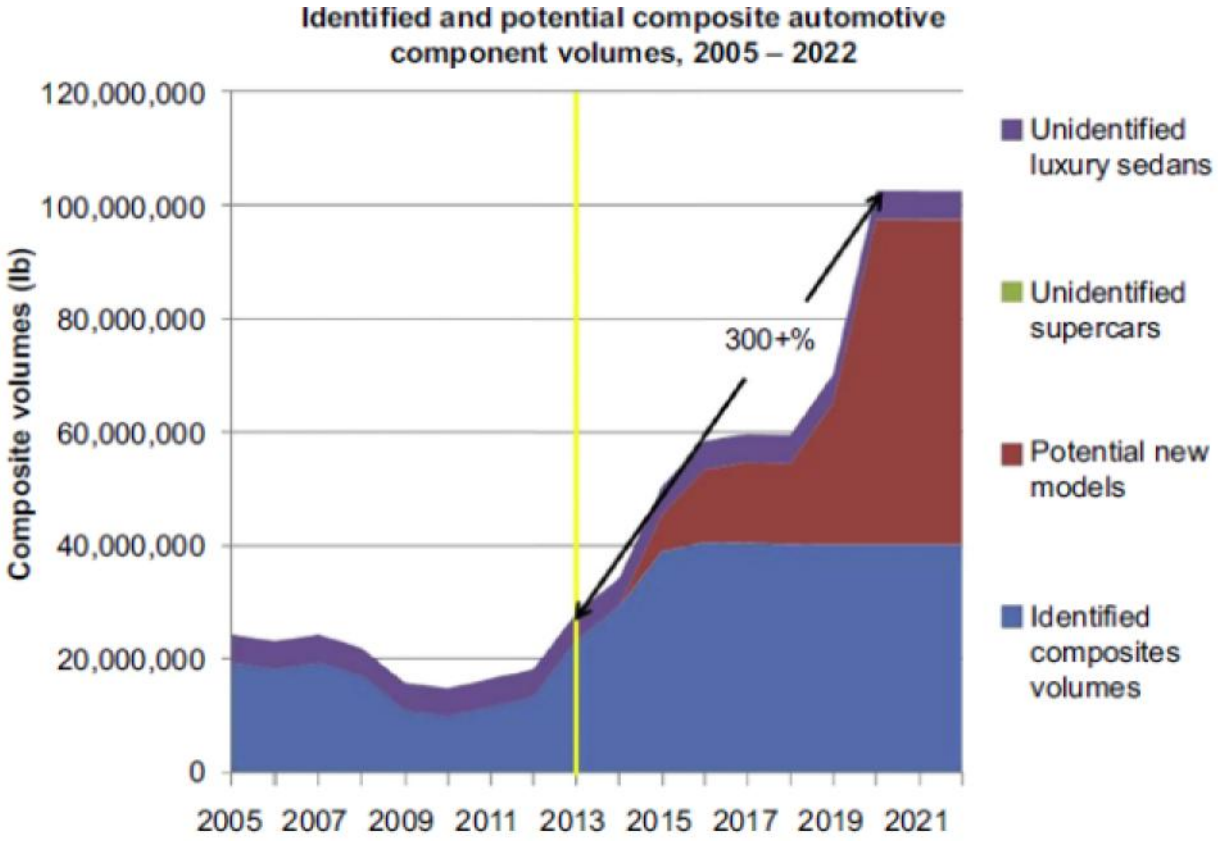

Figure 2.20 Automotive composites usage forecast [23]

2.2.3. Energy

Energy demand is increasing from time to time, for instance, the market was growing 22% each year starting from 2001 to 2007 [30]. Furthermore, wind power could supply global electricity by 12% and 20% in the year 2020 and 2030 respectively [31]. The world seeks renewable energy and one of the renewable energy is wind turbines. However, the wind turbines are being manufactured from small scale to large-scale turbines, harvesting from large-scale turbines leads to the global market. Large-scale wind turbine results in heavyweight, which causes less efficiency. Thus, suitable materials, like composite materials become more advantageous because of its low density, longer life, higher performance, ease of processing, and fatigue resistance [32].

2.2.4. Marine and defense

Naval structures are susceptible to corrosions and rots but steel and aluminum have sensitive behavior to corrosion. Composites are advantageous because of high specific properties unlike conventional materials and they are user friendly to form large structures and complex seamless parts [33]. Besides, marine vehicles are floating machines and they entail lightweight materials to be made. Because of this the composite materials usage in naval structure expected to grow annually by 5.6% from 2011 to 2018 [34].

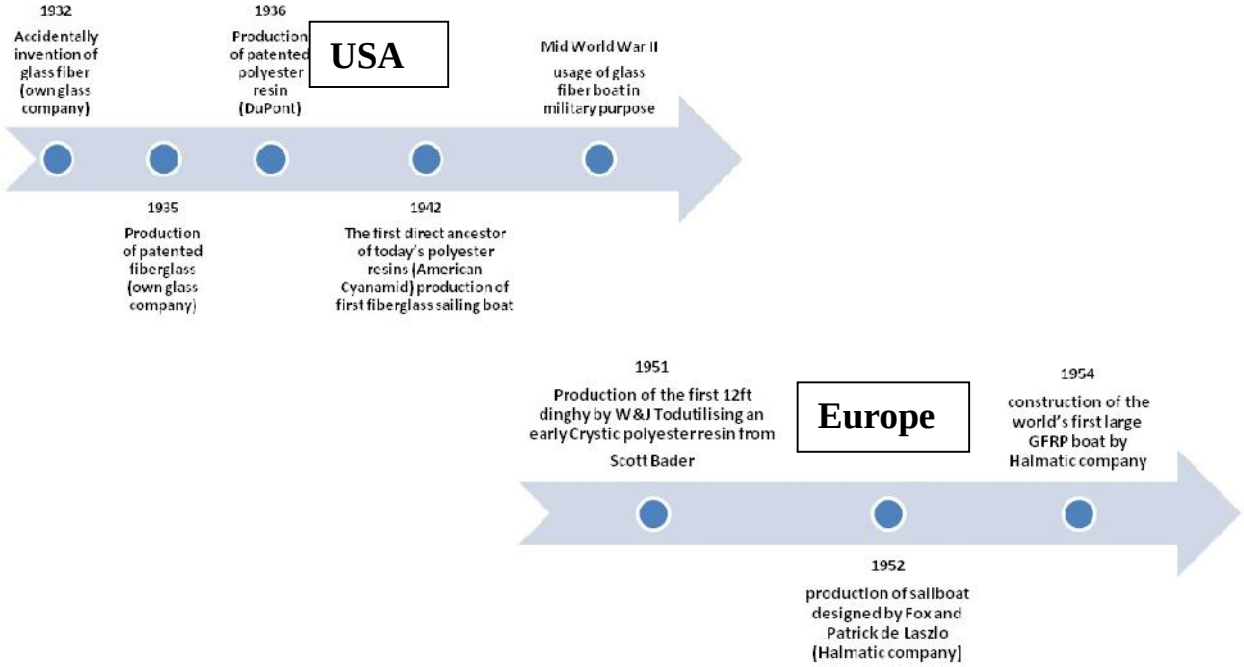

(a)

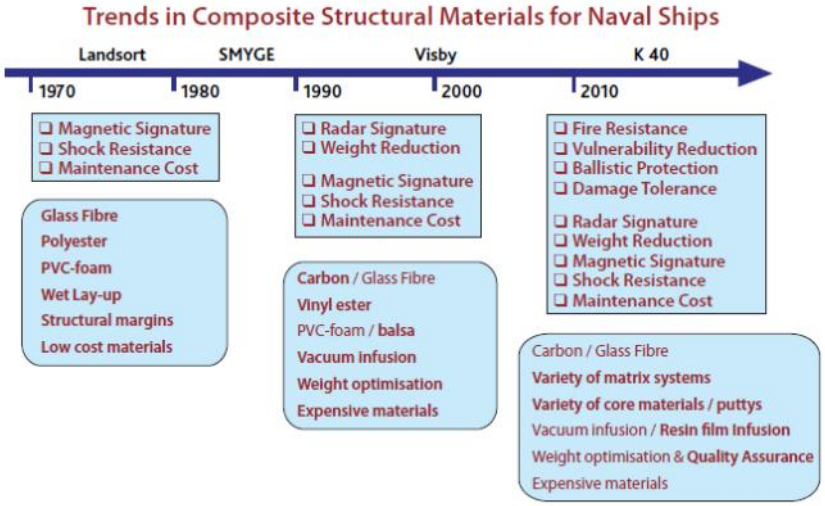

(b)

Figure 2.21 Trends of naval structures (a) Short history of polymer composites in marine use (b) naval use of composites [34]

Ballistic materials are important in defense engineering likewise the structures should be lightweight to save fuel [35]. The reason is that these materials are exposed to an explosion, blast loading, bullet, fire retardant, etc. in other words the structure has to be good enough in impact resistance. According to Owens-Corning [36], technical information using composite materials in defense structures can archive remarkable economic advantages. For instance, it is possible to save 60% of the cost; moreover, it is possible to attain 40% and 50% weight savings when replacing aluminum and steel respectively.

Figure 2.22 Defense vehicles made of s shield strand [36]

2.2.5. Sport goods

Like other types of equipment, sports goods are being made using composite materials. The bicycle, ski sticks, golf club, skeleton of tennis rackets, hockey sticks, fishing poles, etc. are some of the areas that composite materials have been used significantly for the past decades. Glass, carbon, Kevlar, boron fibers, etc. composites are used to obtain good impact, abrasion, bending resistance along with lightness behavior. Strength, springiness, and stiffness behavior, which depend on reinforcing fiber make composite materials preferable in some types of sports goods.

2.2.6. Summary

One of benefits of composite material is the property of customization according to the desired application and load types. The applications from sports equipment to space structures make the composite materials more attractive and instigative. However, the specific structural application

requires specific composite design methodology, general damage of constituents and the combined structure get the big picture to be common.

2.3. Damage and Failure of Composite Materials

Mechanical structures are designed to fulfill the intended objective within a certain period or design life of the structure. However, structural health may be affected by various factors. Manufacturing defects, impurities, voids, wet regions, unexpected external loads, environmental conditions, and degradation are some of the factors that lead to damage/ failure. Z pinning and stitching can cause damages to fibers and degrades the in-plane properties of the laminate.

Before final failure happens, damages of the materials may occur at micro-scale, meso-scale and macro-scale. For composite, its heterogeneous nature makes the damage condition multifarious. Unlike heterogeneous materials, failure of monolithic materials, in particular, metals are yielding and fracture. Therefore, the fields of analyses to treat these failure modes are plasticity and fracture mechanics [37]. Whereas the large difference between constituent properties in composite materials, the presence of interfaces as well as directionality of reinforcement that induces anisotropy in overall properties, are reasons for the complexities observed in geometrical features of micro-level failure (micro cracks). Furthermore, the presences of interfaces between fibers/ matrix, nanoparticles/matrix and between plies in a laminate that provide stress transfer are susceptible to multiple cracking [38]. In many structural applications, composite materials are exposed to high energy, high-velocity dynamic loadings producing multi-axial dynamic states of stress. Under these conditions, composites exhibit nonlinear and rate-dependent behavior that sophisticates the mechanism-based failure types [39].

Figure 2.23 Damage of flight 103 (Boeing 747)

2.3.1. Mechanisms and mode of failures

Damage could occur in composite materials in the form of matrix cracking, fiber kinking, fiber breakage and fiber pullout, pure delamination between plies, delamination between plies with fiber-bridge, and joint delamination. In addition, in the case of the addition of nano-particles to modify the matrix properties, there could be occurred debonding damage between nanoparticle and matrix. When the bonding force is stronger, failure may be nano particle cracking. The nanoparticle cracking may be affected by the shape of the particle in addition to the bonding strength between matrix and nanoparticle. The interface exists anywhere two materials are joined together. Within these distinctive failure mechanisms, delamination is a major failure mechanism in composite structures [40]. The main modes of failure for layered materials are (buckling-driven) delamination and failure of adhesive joints [21]. Due to this, the interface between the layers of a composite structure is of special interest. Because when this type of structure is subjected to certain types of external loading, the failure process (delamination) takes on a unique character.

Delaminations in layered composite materials are areas of de-bonding between adjacent plies and may result from manufacturing imperfections, weak interfacial strength between plies, the weak joining force between laminates, compression loading/ buckling, and bending loading or from low-velocity impact damage whilst in service [41]. Figure 2.24 shows how the delamination can occur when the compression load is applied in a laminate that has layers. It has local and global modes of delamination conditions.

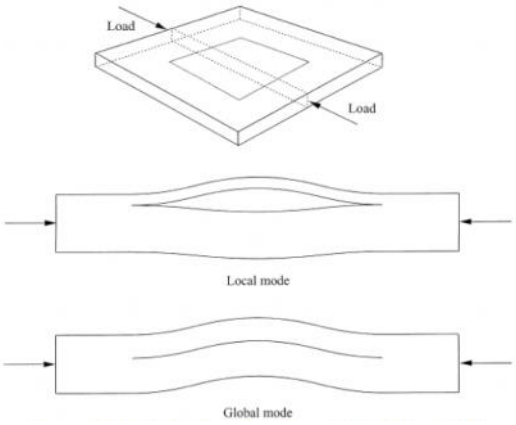

Figure 2.24 Delamination due to buckling [41]

In the same way, the model in Figure 2.25 demonstrates the failure area of a specific wind turbine blade that was experimented and modeled by the Denmark Technical University Research Center [42]. The diagram clearly shows the processes involved in the failure of a specific wind turbine blade that includes several types of damages in the load-carrying structural members of the blade such as the skins and the main spar [31,42].

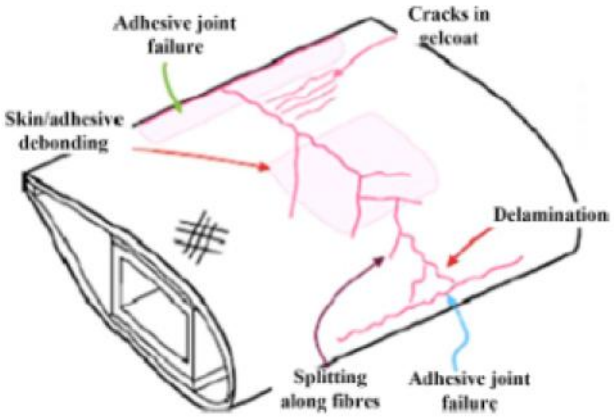

(a)

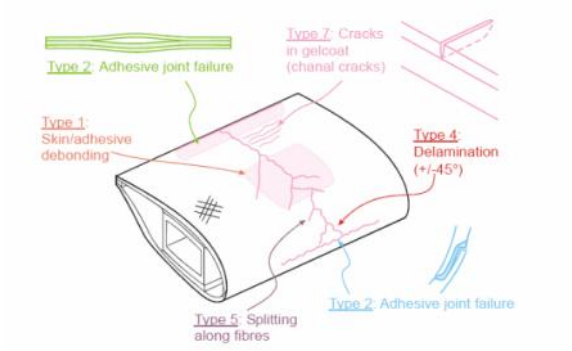

(b)

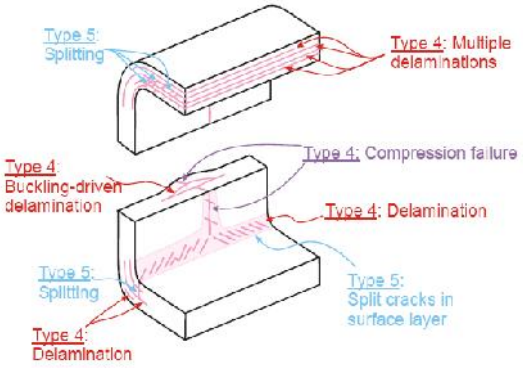

(c)

Figure 2.25 Delamination of composite materials (a) Types of damage that may be sustained by a wind turbine blade [31], (b) Failure modes of a wind turbine blade [31, 42]

Failures mechanisms due to delamination depend on the type of loading that is applied to the composite layered structure. The type of load generates peeling, shearing, or tearing effects for the growth of the cracks that are inside the structure [43]; mixed modes have to be considered.

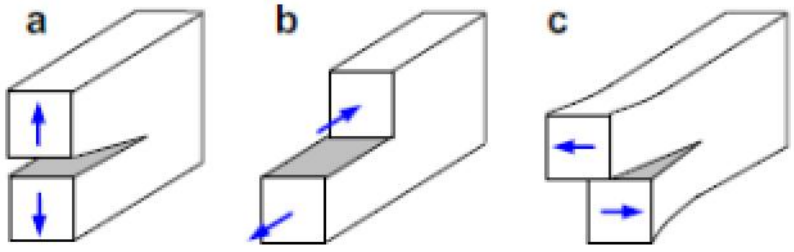

Figure 2.26 Crack growth modes (a) peeling, (b) shearing and (c) tearing [43]

The other important type of failure in composite materials is the damage between fiber and matrix or between matrix and particles. The interface plays a significant role in stress transfer between fiber and matrix as shown in Figure 2.27 (a). For instance, if the fibers are weakly held by the matrix, the composite starts to form a matrix crack at relatively low stress. On the other hand, if the fibers are strongly bonded to the matrix, the matrix cracking is delayed and the composite fails catastrophically because of fiber breakage when the matrix cracks.

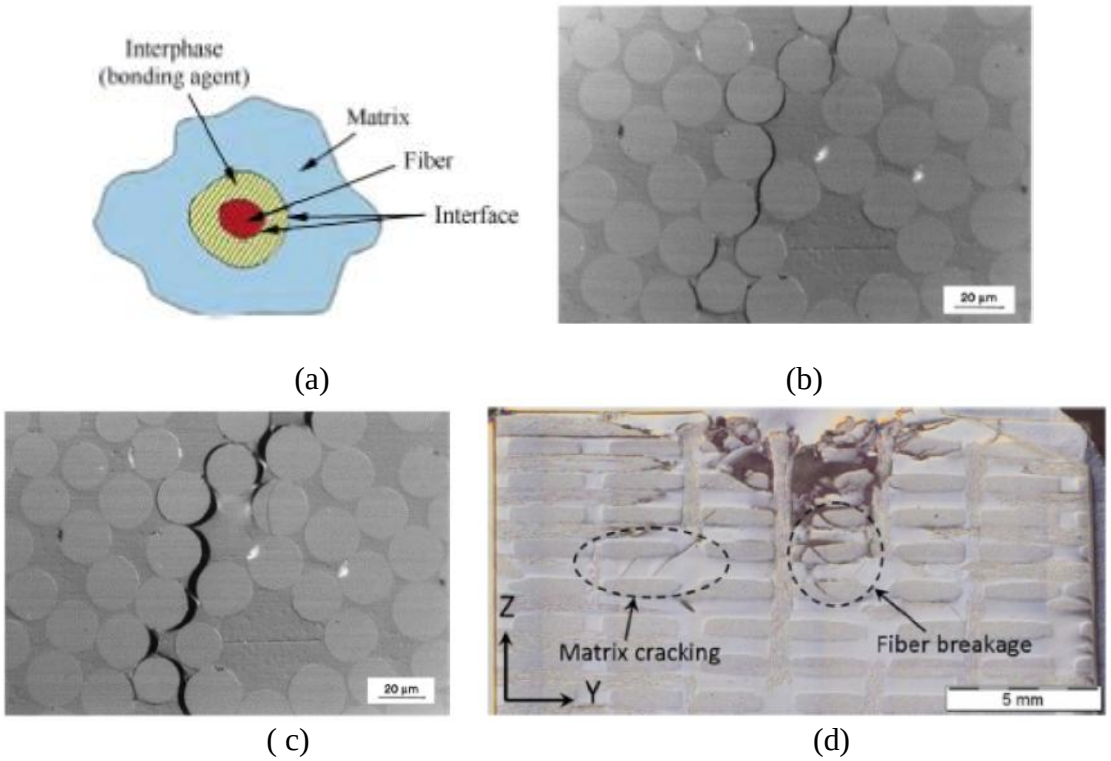

Figure 2.27 (a) Schematic illustration of composite material structure [27], (b) Fibre–matrix debonds [37],(c) matrix crack formed by coalescence of debonds [37], (d) Cross-section along y—z plane showing low-depth indentation damage consisting of matrix cracking and fiber breakage [49]

Similarly, particle to matrix damage is one type of failure mechanism. The particle-matrix failure may also include the damage of particles as shown in Figure 2.28.

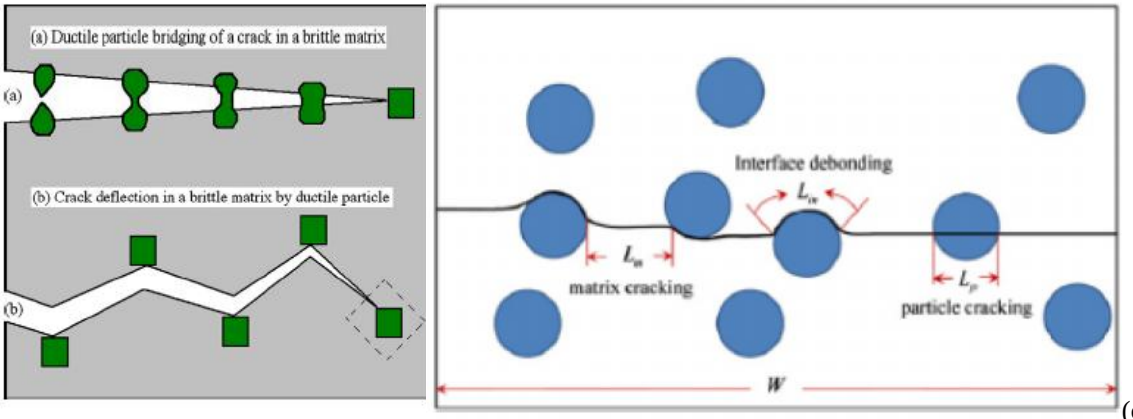

(c)

Figure 2.28 Schematic illustrations of particles: (a) ductile particle bridging [44]; (b) crack deflection by ductile particle [44]; (c) crack path modeling [45] of particles in composite materials

2.3.2. Matrix failure

Matrix failure in laminated composites is a complex phenomenon, in which matrix cracks initiate typically at defects or fiber-matrix interfaces, accumulate throughout the laminate, and coalesce leading to failure across a critical fracture plane [46]. As shown in Figure 2.28(c), either damage occurs in matrix, fiber and particles alone or a combination of the three constituents. As described earlier, the matrix is the weakest part of the three constituents and damage mainly begins with this weak part. After the damage grows at the interface between the fiber and the matrix or between the particle and the matrix, it leads to the catastrophic failure when the applied load increases. For specific material of carbon and glass fiber-polymer composites, damage starts as fiber-matrix interfacial cracks and cracks within the polymer-rich regions and fibrous tows [47] and longitudinal compressive failure quasi-isotropic 2D woven fiber architectures create interfacial debonding [48]. Figure 2.29 clearly shows how the damage initiation takes place in the wet region and propagates to the dry region.

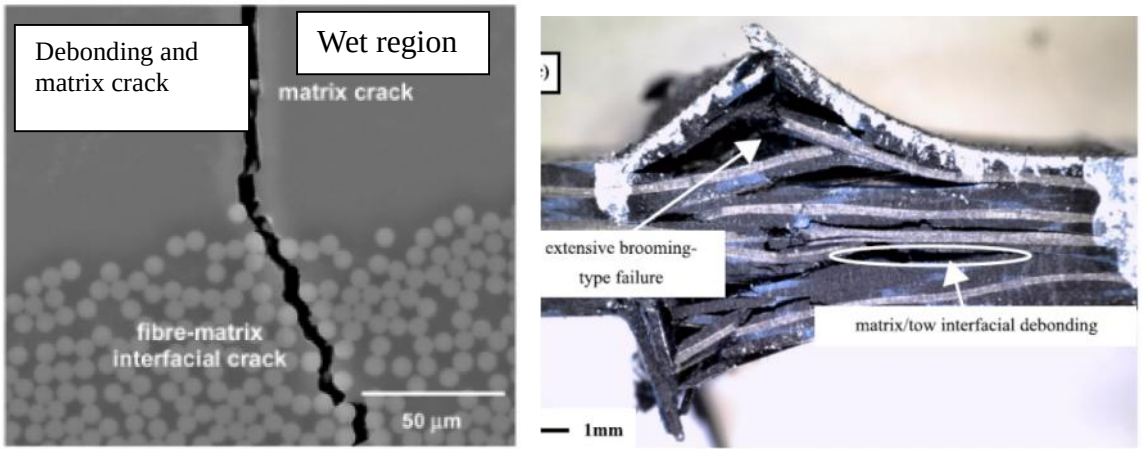

(a) (b)

Figure 2.29 Fibre-matrix interfacial debonding and matrix cracking a) [47], b) [48]

2.3.3. Fiber failure

The reinforcing fiber is stronger than the matrix and thus the damage is affected at first the matrix but then the damage may grow to affect also the fibers [11]. This is also due to fiber imperfections or defects (Figure 2.30). Fiber damage of fiber-reinforced composite materials leads to catastrophic failure since the fiber is the main loading components in unidirectional fiber composite structure. The fiber damage may start from matrix/fiber debonding due to weak interfacial strength or weak interfacial toughness. The debonding does not always follow the interfacial line but the stress can be transferred to the fiber and this causes the fiber rupture. Figure 2.31 shows the damage of fiber due to the compression load [37]. Compression load creates fiber kinking and micro buckling under the micro-scale alike to the separation of plies for the macro level. The micro buckling deformation represented as extensional and shears modes.

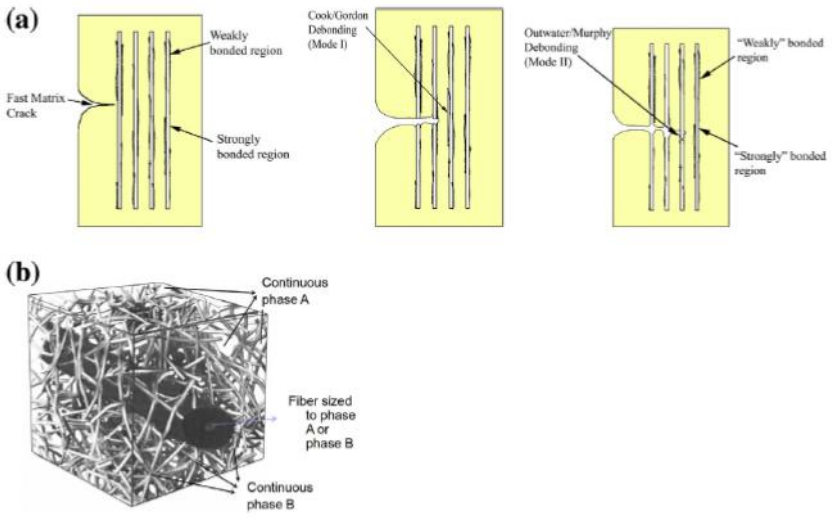

Figure 2.30 Bonding between fiber and matrix (a) Effects of intermittent bonding in UD fiber reinforced composites and (b) intermittent bonding achieved by matrix structuring [11]

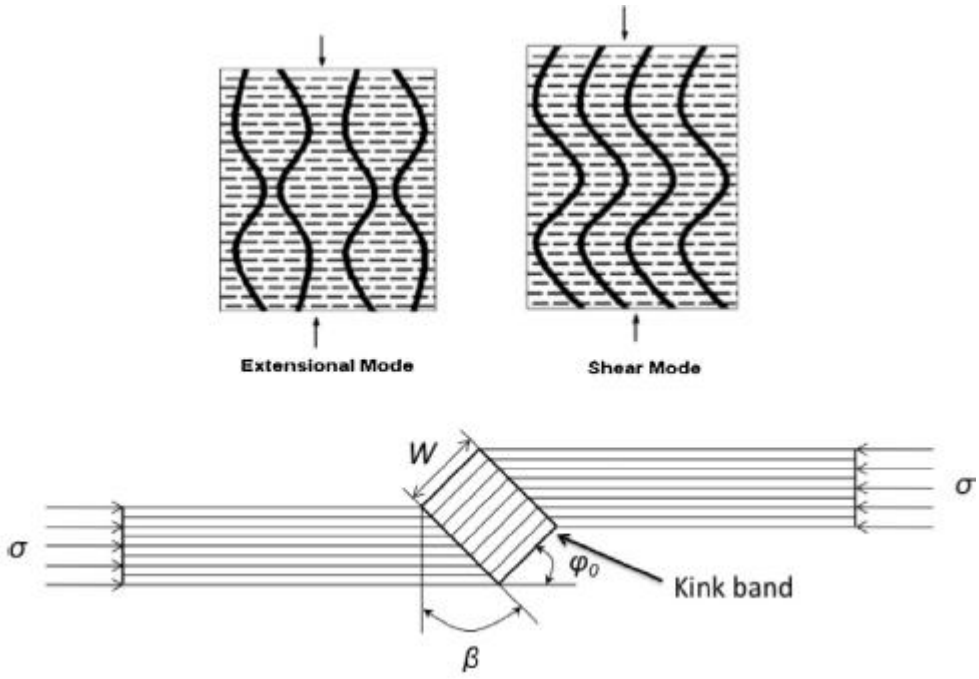

Figure 2.31 Failure modes in unidirectional composite under axial compression [37]

When loads create bending action due to tension (flexural) or pure tensile, fiber pullout or fiber rupture comes about. Figure 2.32 describes the fiber rupture and matrix cracking at the same time.

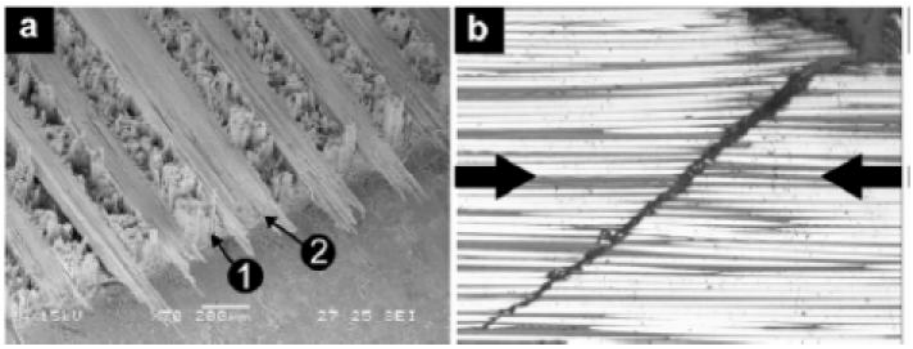

Figure 2.32 Failure mechanisms in FRP: (a) fracture surface including translaminar (1) fibre tensile failure and (2) longitudinal matrix failure (b) shear driven fibre compressive failure (the arrows indicate the loading direction) [50]

2.3.4. Interlaminar and intralaminar failure

In unidirectional fiber composite materials, an interlaminar crack, or delamination, is defined as a discontinuity in the x–y plane between two adjacent plies of a laminate whereas the intralaminar crack is defined as a discontinuity in the y–z plane, which advances through the entire laminate thickness in the direction parallel to the fiber direction [51]. However, nowadays, composite materials can be developed in the form of fabric. The definition of intralaminar becomes counterfeit in the case of woven materials because the crack may grow by rupturing the

fibers transversally. From a different point of view, delamination cracks are more dangerous than in-plane cracks. Such behaviors make the delamination a treacherous phenomenon. The main reason for this conflict is the lack of any reinforcement in the thickness direction. As a result, delamination cracks are easier to form. In addition, the delamination does not directly influence the response if the loading is tension. This characteristic makes the delamination insidious. The delamination may occur in the form of opening, shearing, tearing alone, or a combination of the two and three modes. However, other subcritical degradations may play an important role in the final failure of delamination. In particular, intralaminar cracks because of tensile, compressive and impact loads, generally appearing at relatively low-stress levels, have been shown to act as initiators for delamination [52].

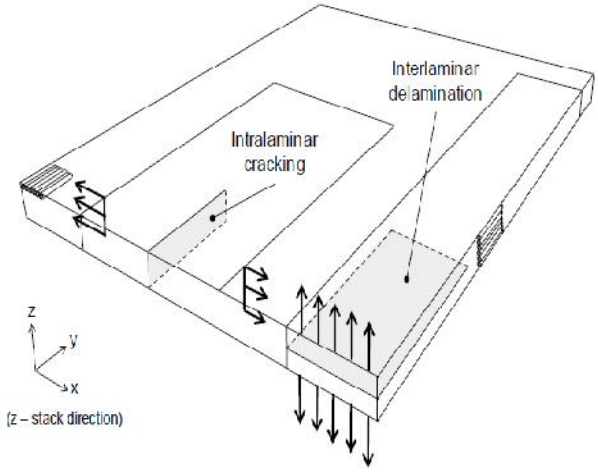

Figure 2.33 Interlaminar versus Intralaminar damage [50]

Unidirectional fiber composite materials damage has three failure modes. As earlier described, the first damage type is the separation of plies, which is parallel to the fiber direction plane. Unless some fiber bridges occur, it is created due either to matrix crack or to debonding between the matrix and the bundle of the fiber, tow. The second type of damage is matrix-cracking parallel to the fibers in the transverse direction of the ply or laminate. The initiation of the crack may be formed in a matrix rich region or from debonding. Nevertheless, the damage may include fibers and matrix. In the ideal case, it follows the matrix region. The third type of damage is perpendicular to the direction of the fiber. The failure includes both the fiber and the matrix.

When the reinforcement material is of the fabric type, the damage combines the above last two types of damage and it is named as a combination of intralaminar and translaminar. The

separation of plies is the same as that of the unidirectional composite material, which is named as interlaminar. Figure 2.34 shows the ideal model for each type of failure [50].

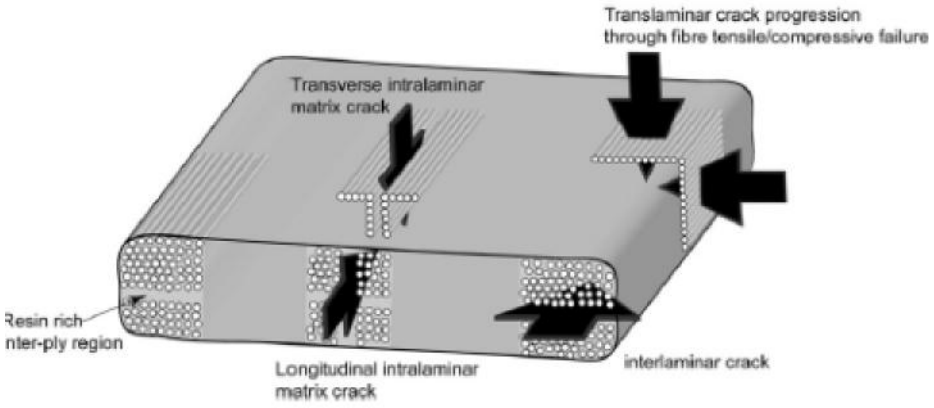

Figure 2.34 Overview of ply-level failure modes [50]

2.3.5. Impact failure

Load direction highly influences the damage mechanisms of materials. One of the load application types is the suddenly applied load that includes both impact and blasting. The impact may create internal damages and, eventually, may cause a severe reduction in the laminate strength/stiffness that, in particular cases, may lead to sudden catastrophic failure of composite structures during services [53]. In laminated composites, different damages such as delamination, matrix cracks, fiber-matrix debonding, and fiber fracture can be caused as a consequence of impact loading of foreign pieces of stuff (in-service conditions and maintenance operations) [54]. As already explained, delamination is one the most important failure among these damages which is easily made even in a very low-velocity impact. Like tension, compressive, and twisting loads, impact load affects the material by combining all damages i.e. matrix, fiber, particle and separation of plies together. The impact creates damage in both the out-of-plane and in-plane directions. This means that damage occurring in impacted laminates consists of a combination of intralaminar damage mechanisms (such as matrix cracking or plasticity, fiber/matrix debonding and fiber fracture) and interlaminar failure, which develops at the interface between adjacent plies in the form of debonding between layers (delamination) [55]. The intralaminar damages represent the in-plane compression and tension.

2.3.6. Summary

Unlike observed in the isotropic crystalline materials, there are various types of failures in composites. Often, damage develops from manufacturing-induced flaws for both homogenous

and heterogeneous/or composite materials [56]. The damage caused by manufacturing-induced flaws may be enlarged when a laminated composite panel is loaded. Principal stresses are magnified due to the presence of inclusions or structure features like notches and holes. Broadly, the intralaminar and interlaminar failures summarize the whole damages as shown in Figure 2.35. This is due to the heterogeneous structure of composites. Thus, more precise and more reliable methods are required to handle progressive damage and to predict the behaviour of laminated composite components.

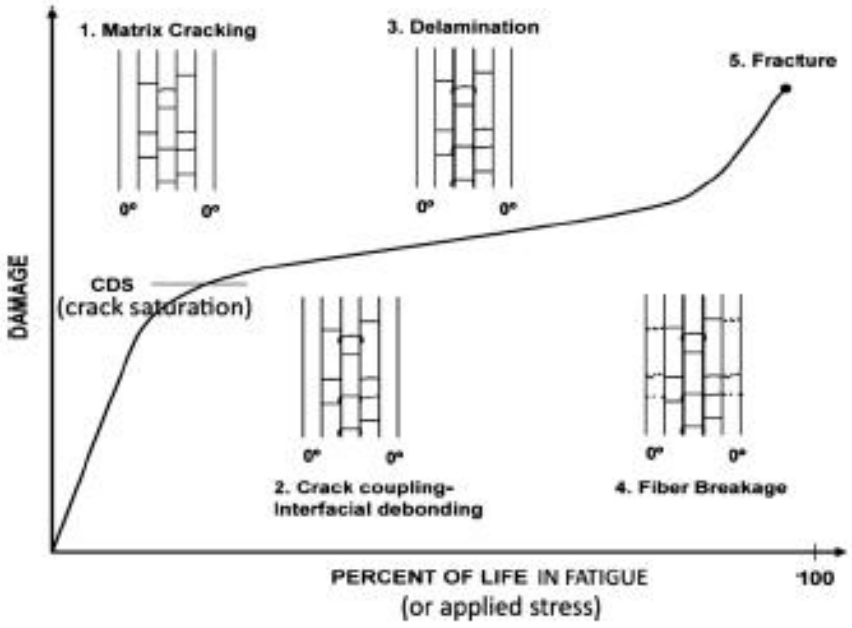

Figure 2.35 A schematic depiction of progression of failure events in a general laminate subjected to axial static or cyclic tension [37]

In addition, the damage resistance or retardation may be improved by improving the interfacial strength of fiber-matrix and between plies in the out of plane directions. The prevention methods are based on the addition of extra reinforcements to the matrix such as enhancement obtained by using very small particles. Stitching and z pinning may be also valuable methods to minimize the out of plane failures between plies.

2.4. Enhancement of Composite Material Properties

2.4.1. Introduction to nanoparticles

As it was already mentioned in section 2.3, within the fiber-reinforced composite family, ordinary laminated composite materials are the most common type. Fibers reinforce in layer plane directions [8, 57], but mechanical properties are poor in out of the plane direction. One of the constituents of these composite materials is the matrix. The most common matrix type is epoxy i.e. a type of polymer used both as adhesive and as the matrix for fiber-reinforced composites. These polymeric matrices are used in structural engineering applications owing to their low moisture absorption, relatively high modulus, and relatively high-temperature performance even if they generally come with the undesirable property of brittleness with relatively poor strength and low fracture resistance because of their structure [58, 59]. Nowadays, various types of reinforcing materials, including hard and soft particles [57],give enhanced mechanical performances to polymeric matrices. These novel enhancing particles are Nano sized materials (nanoparticles) which can be easily combined with the polymeric matrices and the combined resulting materials are named nanocomposites. These nanoparticles are significantly larger than individual atoms and molecules but they have high surface area per volume unit compared to macro-level materials. These nanocomposites are a class of materials in which one or more phases, with nan scale dimensions (0-D, 1-D, and 2-D), are embedded in a metal, ceramic, or polymer matrix [60]. The general idea behind the addition of the nan scale second phase is to create a synergy between the various constituents, such that novel properties result capable of meeting or exceeding design expectations [61]. The properties of nanocomposites relay on a range of variables; particularly the matrix reinforcing materials, which can exhibit nan scale dimensions, loading (percentage by volume, or percentage by weight), degree of dispersion, size, shape, and orientation of the nan scale second phase and interactions between the matrix and the second phase[60, 62]. The nano-sized materials can be produced from metals, metallic oxide, silicates, carbon, and polymers. Some of the used nanoparticles are both metallic based such as Silver, Copper, Gold, Iron, Platinum, TiO_2, ZnO, Fe_2O_3, and non-metallic based such as Nano-clays, $CaCO_3$, fullerene, graphene, carbon nanotube (CNT), carbon black, rubber, nitrile, nano-cellulose [60, 62-64]. Currently nanoclay, CNT and graphene have been widely studied to enhance the various properties of the bulk composite materials.

Nano sized coalesced materials modify the physical and mechanical properties of the composite materials. Therefore, this review focuses principally on the influence of nanoparticles on the mechanical properties (such as stiffness and strength), fracture toughness and damage behaviors of composite materials as it will be described in the following sections. This review addresses also related factors that affect the effectiveness of Nano fillers to obtain the desired mechanical properties of the targeted composite material; a percentage of Nano sized coalesced materials by weight, the percentage by volume, morphology and size effects of the particles, are of particular relevance.

Nanoparticles are those materials having a size of particles up to 100 micrometers. Figure 2.36 was taken from a video documentary entitled 'making stuff smaller' which was prepared by David Pogue and it shows the size comparison of materials with various ever known sizes.

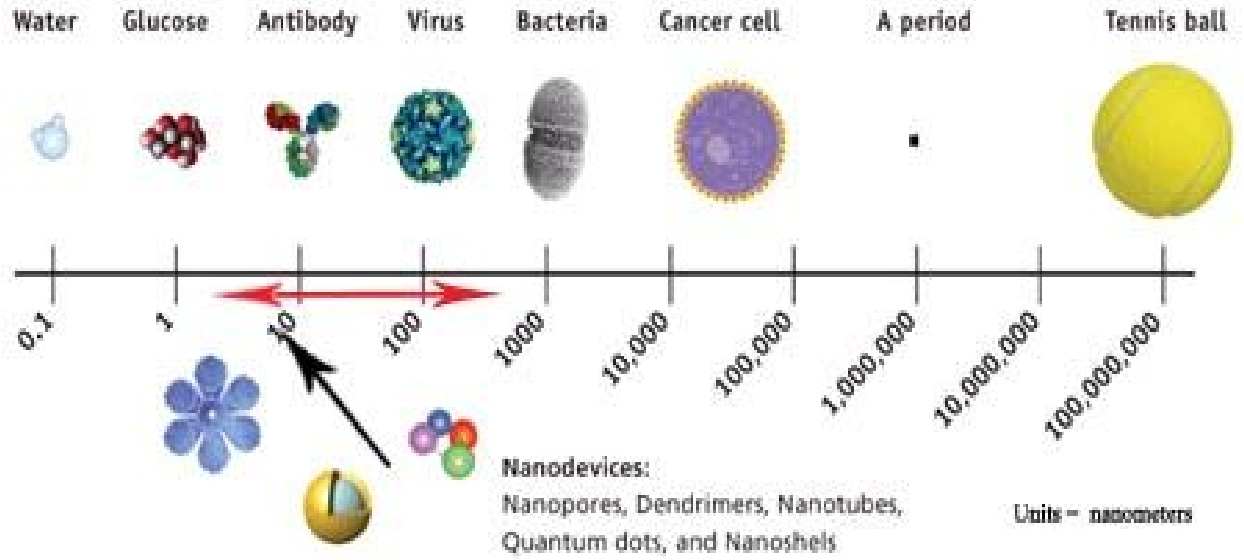

Figure 2.36 Size representations of nanoparticles

2.4.2. Influence of nanoparticles on mechanical properties of composite materials

Mechanical property improvements have resulted in a major interest in nanocomposites. Nanocomposites are the outcome of innovative technologies with great potential to create new multifunctional materials, characterized by enhanced physical and mechanical properties and new improved products for various fields of application [101]. Factors like type and concentration, dispersion and distribution of nanoparticles affect the property of composite material characteristics. Agglomeration which is caused by poor dispersion of nanoparticles may cause inhomogeneity and, eventually, uncured resin zones while imposing extra energy into the

mixing process to obtain fine dispersion under sonication may also cause early curing of the resin, which leads the resultant composite to be brittle [102]. Thus, by adding the optimum amount of nanoparticles, the material mechanical properties such as tensile strength, flexural strength, modulus of elasticity and the physical properties like thermal stability and barrier properties can improve remarkably for such a type of composite materials [71]. Mechanical properties of nanoparticles may reach the theoretical strength, which are one or two orders of magnitude higher than that of single crystals in the bulk form. The enhancement in mechanical strength is simply due to the reduced probability of defects. Thus, in the following subtopics, the influences of various types of nanoparticles on the mechanical properties of composite materials were reviewed.

2.4.2.1. Effects of nanoclay loadings

One of the nanoparticles type considered quite frequently is nanoclay, that stays under the category of silicate and it is relatively cheap. The ability of nanoclay to induce enhancement in the physical, chemical and mechanical properties of the composite material in comparison with what is possible to obtain from conventionally filled composites is largely reported in the literature [61, 65-66]. Clay is a weathering product resulting from the disintegration and chemical decomposition of igneous rocks with the fine texture of particle size. Clay polymer nanocomposites (CPNC) became one of the important fields of nanotechnology since Toyota produced the first application in the automobile industry [67]. Nanoclay fillers induce great improvement in the mechanical, thermal and barrier properties. Epoxy clay nanocomposites can be used for many specific applications such as in aerospace, defense, and automobile industries. The materials have been used in high performance structural and functional applications such as laminates and composites, adhesives, sealants, tooling, molding, casting, electronics, and construction. Mechanical properties of polymer-clay nanocomposites depend on the microstructure in which the clay particles are dispersed in the polymer matrix as well as on the finesse of their dispersion. Generally, the fine dispersion of the clay particles into the polymer matrix yields enhanced tensile modulus, storage, and loss modulus (relevant in case of dynamic loading of viscoelastic materials) and tensile strength [68]. The greatest improvement of the mechanical characteristics of these materials often comes with an exfoliation degree. In the following, the effect of nanoclay loadings reviewed.

Nanoclay is available in various forms, among them, platelets (Cloisite 30B) is one of the most common types. Assaedi, et al. [69] studied the effects of nanoclay (Cloisite 30B) on the mechanical and thermal properties of fly ash geopolymer by adding nano-clay platelets with different loadings from 1 wt.%, to 2 wt.%, and to 3 wt.%. The mechanical properties of geopolymer nanocomposites were considerably influenced. The flexural modulus was increased by 15.9%, 25%, and 20.45% as the result of nano-clay loadings of 1 wt.%, 2 wt.%, and 3 wt.% respectively; similarly, the flexural strength was increased by 13.33%, 24.44%, and 15.55% for the given nano-clay loadings respectively. Moreover, the compressive strength and the hardness increased by 5.9%, 23.38%, 8.06% and by 2.8%, 12.68%, 4.23% respectively as the result of the mentioned additions of nanoclays. It is evident that the improvement in the mechanical properties is not linear with the increment of the percentage of nanoclay addition in weight but the maximum effect is identified in correspondence of the 2 wt.% addition. On the other side, the addition of 2 wt.% in the weight of nanoclay decreased the porosity and this increased the nanocomposite's resistance to water absorption significantly. Furthermore, Assaedi and co-workers also found the conditions for the optimum thermal stability of nanoclay. The addition of nanoclay in a geopolymer affected the material properties as the temperature varied. The thermal stability was determined using thermo-gravimetric analysis (TGA) and it was studied in terms of the weight loss percentage as a function of temperature. The weight loss decreased at the higher temperature (e.g. 600^{o}C to 700^{o}C) with the increment in the nanoclay fraction. The highest enhancement to the thermal stability of the geopolymer matrix was with a loading of 2 wt.% of nanoclay. A higher amount of nanoclay caused agglomeration and poor dispersion, which resulted in increased porosity.

Other researchers, Eesaee et al. [70] dealt with natural montmorillonite (CN) and organically modified montmorillonite (CB). The nanoclay improved the mechanical performance of novolac phenolic resin (PF)/woven glass-fiber (GF) composites due to the nano dispersion and good interfacial interaction with the matrix. The nanoparticles' loadings were 0.5 wt.%, 1.5 wt.%, and 2.5 wt.%. As indicated in Figure 2.37 (a & b), 2.5 wt.% of the clays enhanced the elastic modulus up to 38% for CN and 43% for CB. PF/GF composites submitted to aging processes with various aqueous solutions such as water, brine, and acidic environments, increased stiffness from 100 to 250% with respect to the base composite. However, aging led to the reduction of strength caused by matrix degradation due to hydrolysis and interfacial debonding. Both clays

diminished the durability of PF/GF composites probably due to their hydrophilic nature enhancing water absorption.

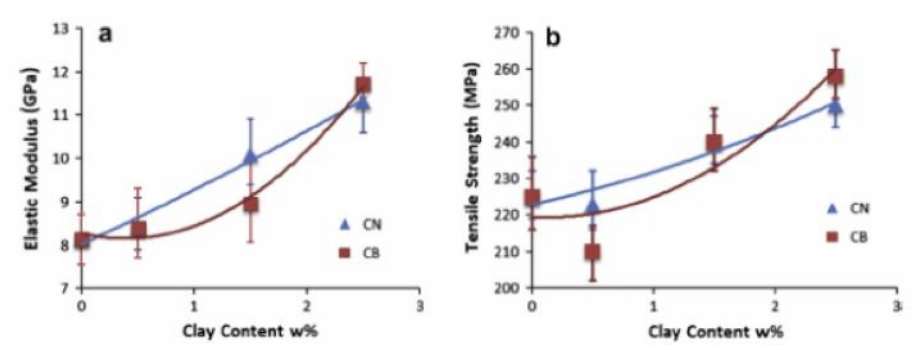

Figure 2.37 - Effect of montmorillonite nano-clay content on elastic modulus (a), tensile strength (b), [70]

Hakamy et al. [63] worked on the effect of calcined nanoclay (CNC) with the chemical treatment of the microstructure and mechanical properties of treated hemp fabric-reinforced cement nanocomposites. The optimum hemp fabric content for these nanocomposites was 6.9 wt.% (6 fabric layers). Mechanical properties were improved by the calcined nanoclay (CNC) loading, tests were done with additional quantities of 1 wt.%, 2 wt.% and 3 wt.% and an optimum replacement of ordinary Portland cement with 1 wt.% CNC was observed.

Binu et al. [71] studied the significant effect of nanoclay, Cloisite 15A, on the mechanical properties of Glass Fiber Reinforced Polyester for 0.5 wt.%, 1 wt.%, 1.5 wt.% and 2 wt.% nanoparticle additional quantities. The highest tensile modulus and strength were obtained within the addition range from 0.5 wt.% to 1 wt.% nanoclay as indicated in Figure 2.38; while for 1.5 wt.% and 2 wt.% nanoclay addition, the modulus value became lower. On the other hand, optimum impact strength and storage modulus were exhibited at 1 wt.% nanoclay. Nanoclay loadings as those considered by John et al. [72], led to substantial improvements in mechanical properties i.e. tensile, flexural, compressive strengths and moduli. According to their work, the addition of 2 vol.% and 4 vol.% nanoclay in cyanate ester syntactic foam registered tensile strength improvement by 63 and 94%, respectively.

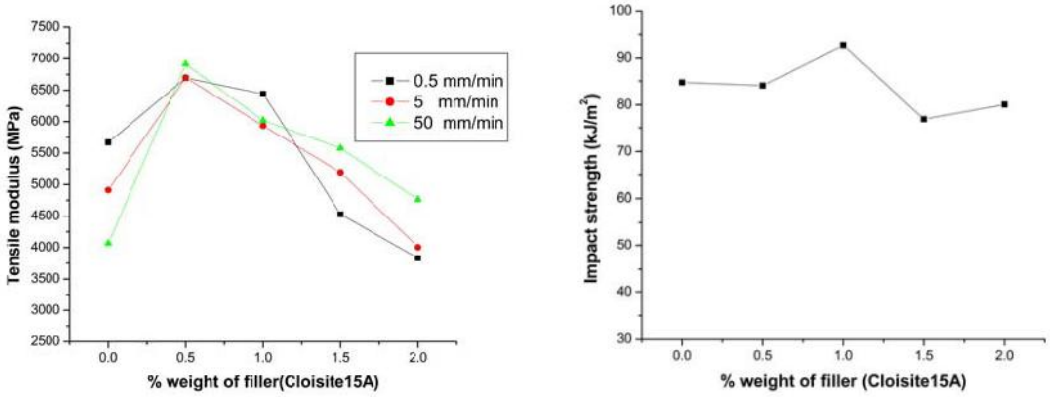

Figure 2.38- Effect of Closite15A content on Tensile Modulus (a) and Impact strength (b) [71]

Table 2.2 - Modulus and ultimate strength enhancement as a consequence of the specified loading of nanoclay inside Araldite GY251 epoxy [102].

Sample	Young modulus (MPa)	Percentage improvement (%)	Mean of Ultimate Strength (MPa)	Percentage improvement (%)
Pristine epoxy	2120	0	52.4	0
1 wt.%	2474	16.68	58.02	10.72
3 wt.%	2625	23.81	58.49	11.23
4 wt.%	2772	30.72	60.72	15.88
5 wt.%	2841	34.00	65.22	24.47
7 wt.%	3334	57.24	54.43	3.87
9 wt.%	2432	14.70	32.82	-43.43

However, thermal properties were not significantly altered by the addition of nanoclay particles. Glass transition temperature decreased due to the increased plasticization of the matrix caused by the organic modifier present in the nanoclay. Similarly, Maharsia et al. [72] conducted the

hybridizations by using the volume fraction in the range from 2 vol.% to 5 vol.%. The nanoclay reinforcement of syntactic foams enhanced the tensile strength of up to 22%. Chan et al. [102] reported another interesting finding: the Araldite GY251 epoxy resin and hardener HY956 in the ratio of 5:1 were used to produce nanoclay/epoxy composites. As indicated in Table 2.2, the increment in Young's modulus and tensile strength of a composite sample with 5 wt.% were 34% and 25%, respectively. Further increment of the content of nanoclay would result in decreasing the mechanical properties of the enhanced composites. The results for 9% wt.% clearly indicate that there is a maximum acceptable value for the amount of loading, beyond which the addition of nanoparticles is ineffective. Withers et al. [73] considered epoxy glass–fiber composites with an organo-modified surface, Cloisite 30B nanoclay was dispersed in the epoxy at 2 wt.% and 4 wt.% levels to improve the mechanical properties. The researchers concluded that the nanoclays apparently toughened the epoxy matrix and strengthened the fiber-matrix interfaces in the composite to achieve the above-mentioned mechanical property improvements.

Sharma et al. [74] dealt with glass fiber reinforced polymer-clay nanocomposites. Their work showed better dispersion of clay in epoxy for samples with 1 wt.% and 3 wt.% clay loadings while agglomerates were found in 5 wt.% samples. Tensile and bending tests performed on nanocomposites showed that with the addition of nanoclay up to 3 wt.%, the tensile strength increased and then decreased with a 5 wt.% loading, while the flexural strength increased with the addition of nanoclay up to 5 wt.%.

Loading of nanoclay ranges is of interest not only for mechanical property enhancement, but morphology also has a great impact on the customization of composite materials. Phong et al. [78] worked on morphology and they found that with the addition of nanoclay to polymer matrices, a good degree of exfoliation was obtained for concentrations of 6.6 wt.% while the mechanical properties, such as Young modulus, were increased of 54%. As a conclusion, all the mentioned papers, excluding morphological issue, have shown that the loadings (i.e. the % in weight addition) of nanoclay have to be less than 5 wt.%, which is similar to the conclusion of other review papers, see for example that published by Azeez et al. [68] and Ravandi et al. [75]. This implies that the optimal amount of nanoclay should not exceed 5 wt.% to enhance mechanical properties.

2.4.2.2. Effect of other nanoparticles loadings particle size, adhesion and morphology

Mechanical properties, including Young's modulus, ultimate tensile strength, ductility, etc., of the epoxy matrix can be enhanced by loadings of carbon nanotubes, graphene and silica fillers like nanoclay. According to Domun et al. [65], the carbon nanotube families (CNT), single-walled CNT (SWCNT), double-walled CNT (DWCNT) and multi-walled CNT (MWCNT) modified the epoxy mechanical property considerably. The Young's modulus is enhanced from 80 to 130% for CNT additions within the range from 0.04 wt.% to 5 wt.% and from 94% to 148% for graphene additions within the range from 0.03 wt.% to 4.5 wt.% respectively. Further silica enhanced Young's modulus from 86 to 158% for additions within the range from 0.05 to about 25% in weight. The diagram reported in Figure 2.39 [65] shows the superposition of the different nano-particle clouds that describe the possible enhancement of the ultimate tensile strength from 72.5 to 145% produced by graphene loadings within the range from 0.03 wt.% to 3 wt.% and from 92 to 130% for CNT loadings within the range from 0.045 wt.% to 0.7 wt.% respectively. Silica, under a cluster of loadings between 1 wt.% and 25 wt.% enhanced the ultimate tensile strength from 60 to 132%.

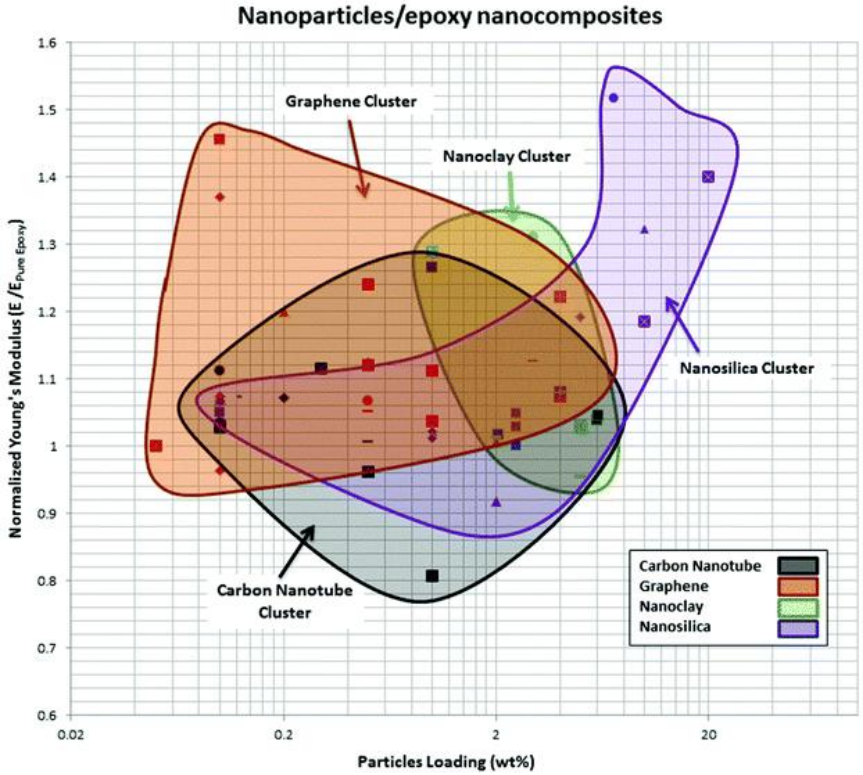

Figure 2.39 Map of the stiffness of nanoparticles/epoxy nanocomposites with respect to particle loading [65].

Shuvo et al. [76] published another interesting work. Graded nanoclay (nanoclay, montmorillonite clay surface modified with 15-35 wt.% in octadecylamine and 5 wt.% aminopropyltriethoxysilane) and non-graded nanoclay were used as reinforcements of polyester. Upon addition of non-graded nanoclay to pure polyester, the tensile strength, and modulus decreased by about 30% while with graded nanoclay increased by about 10%. Flexural strength also increased by about 15%. Ghadami et al. [77] studied nanoclay and alumina nanoparticles. The tensile strength of epoxy-clay nanocomposite specimens gradually enhanced by increasing nanoclay up to 5 wt.% content due to good dispersion process, also Young's modulus of epoxy-nanoclay nanocomposite increased significantly. These results were obtained through the addition of the various wt. percentage of nanoclay in a resin that is made of hot-cured epoxy resin (LY556), anhydride-curing agent (Aradur 917) and imidazole accelerator (DY070). With the addition of alumina nanoparticles higher than 3 wt.%, tensile strength decreased alternately for the specified epoxy resin. This behavior can be explained by the increasing viscosity of uncured compound that causes to trap more porosity during mixing, casting, and finally curing of nanocomposite specimens.

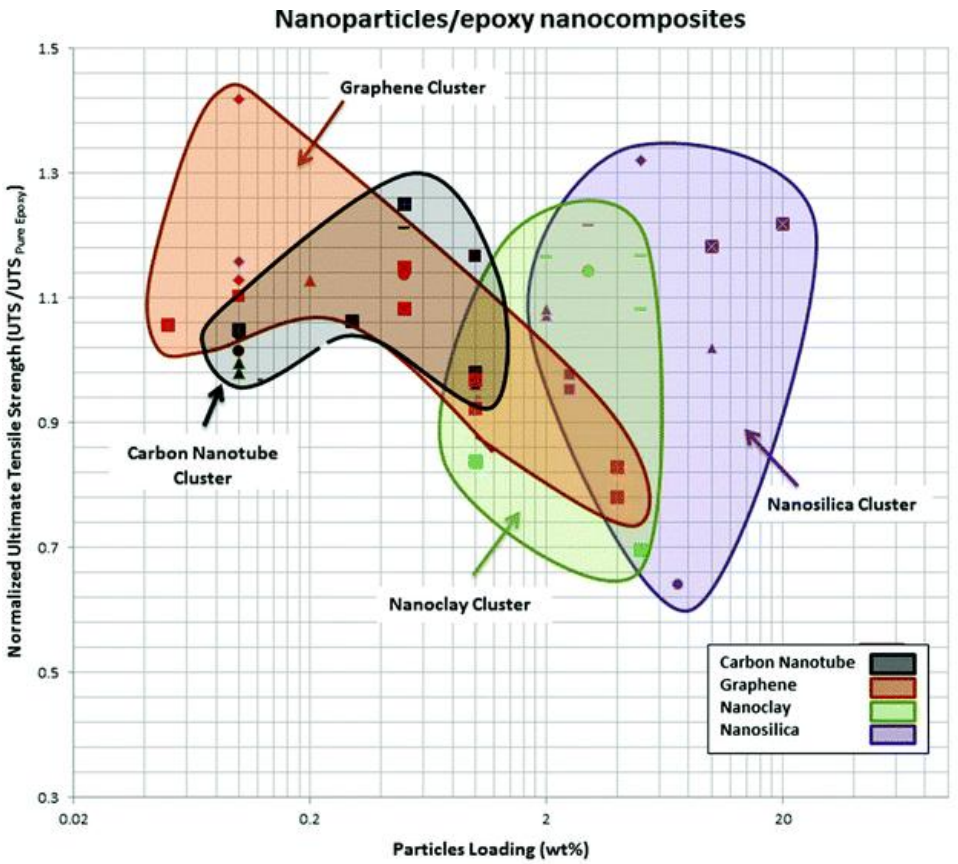

Figure 2.40 Map of the ultimate tensile strength of nanoparticles/epoxy nanocomposites with respect to particle loading for different types of nano-particles [65]

Other researchers, Phong et al [78] observed the effects of loadings made with nano-polyvinyl alcohol (nPVA). Polyvinyl alcohol powder was added to the matrix of a composite reinforced with plain-woven carbon cloth (TR3110M), the matrix was made of Epoxy resin (Epikote 828), while modified aliphatic polyamines was used as curing agent. Randomly–aligned web of PVA nano-fibers whose diameter was about 40–80nm, with four different values of loading percentage, namely 0 wt.%, 0.03 wt.%, 0.05 wt.% and 0.1 wt.%, resulted to affect the strength. In particular, the tensile strength was increased by about 5% with the addition of 0.05 wt.% of nPVA.

Another work published by Gantenbein et al. [79] considered the size effects of the particles; the research concluded that the increment in size of the particles affected the enhancement in strength due to lower surface to volume ratio. Similarly, to the size of particles, the distribution of the nanoparticles alters the enhancement of the bulk material mechanical properties. Iman et al. [80] observed the cross-linking agent, which improved the physicochemical properties such as mechanical, thermal, flame retardancy and dimensional stability. Moreover, Matusik et al. [81]

and Awad et al. [82] demonstrated how the improvement of the mechanical parameters could be related to very good particle dispersion. The effects of particle loading and size (in the range 4.5–62 micrometer) on the elastic modulus of epoxy/spherical glass particle composites with low volume fractions of glass beads (10–18 vol.%) were studied, it came out that the modulus is almost independent on particle size. Strength and toughness exhibited dependency on adhesion quality. Fu et al. [62] observed the adhesion property of nanoparticles. According to their work, for silica, adhesion showed magnificent tensile strength result at 5 wt.% but the tensile strength drastically changed as the loading increased above 5 wt.%.

2.4.3. Influence of nanoparticles on fracture toughness of composite materials

Failure of composite materials in the out of plane direction is the most concerning type of failure due to the inherent fragility of the epoxy matrix [57, 58, 60, 78, 83, 84]. The improvements of layered composite material property in the out of plane direction were dealt using different methods such as stitching [75, 85-90], 3D weaving, braiding and z-pinning [86, 91]. However, while stitching, 3D weaving, braiding, and z-pinning improved the composite fracture toughness considerably, these methods affected negatively the in-plane mechanical properties (tensile strength and stiffness) [85, 91]. Alternative methods have been explored in order to obtain improvements in the composite fracture toughness and at the same time avoid decrement in the in-plane properties.

2.4.3.1. Effect of nanoparticles loadings

The fracture toughness behavior of composite materials was improved by various nanoparticles loadings. Maharsia et al. [72] made experiments for syntactic foams. According to their work, the addition of 5 vol.% nanoclay particles increased the toughness up to 58%.

Other researchers, Kim et al. [93], studied material with modified bisphenol - A type of epoxy resin. The material was used to test the mode I fracture toughness, K_{IC} using 3- point bending method with SENB specimens. The nanoclay (Cloisite 93A) with a loading of only 0.5 wt.% up to3.0 wt.% enhanced the K_{IC} value by 20%, up to 50% on the average, respectively, at room temperature. Nevertheless, the toughness decreased as the temperature increased; the researchers concluded that the intermolecular forces between polymer networks of the epoxy have been more dominant than the toughening effect of the mixed nano-particles.

In another study by Ghadami et al [77], a material consisting of hot-cured epoxy resin (LY556), with an anhydride curing agent (Aradur 917) and imidazole accelerator (DY070) resin, was modified by loading of Nanoclay (Cloisite 15A) and Al_2O_3nano-particles with the particle size of 100 nm, to modify the fracture toughness. The fracture behavior was tested using single-edge-notch specimens in three-point bending geometry. The results showed that the nanoclay improved fracture toughness progressively up to 5 wt.% addition, while alumina registered maximum improvement at 3 wt.%. Increasing the volume fraction of the alumina nano-particles more than 3 wt.% leads to a gradual decrement of the fracture toughness. The explanation was the presence of micro-cracks that initiated from undispersed Al_2O_3nano-particles and micro-porosities.

Further researches instigated the influences of silicates (Nano-clays, $CaCO_3$), carbon (fullerene, graphene, CNT, carbon black) and polymer (Rubber, nitrile, Nano cellulose) based nanoparticles respect to this relevant specific sub-topic. Specifically, rubber particles have demonstrated to be able to control significantly the enhancement of the fracture toughness. One-way for further enhancing the fracture toughness of epoxies could be the use of other toughening mechanisms such as hybrid application of soft particles and rigid fillers as Liang [94] discussed it. Interlaminar toughness improvement for carbon fiber/epoxy laminates was achieved by the incorporation of nano-particles by Zeng et al. [57]. Two types of nanoparticles were added 40 wt.% sol-gel nano-silica with approximately 20 nm-sized SiO_2 and nano-rubber/bisphenol A with 25 wt.% approximately 100 nm-sized core-shell rubbers. Fracture toughness was tested for mode I by means of the double cantilever beam. The toughening effect of rubber resulted to be more significant. Laminates with 10 wt.% rubber particles gave the highest improvement in toughness that is almost 250% with respect to the base material, while silica modified laminates show only a moderate increase in toughness of 20–30% as shown in Figure 2.41. Zeng et al. summarized the toughness transfer mechanism of the nano-particles modified bulk epoxies in composite laminates by its complicated fibre bridging across the delaminating crack-wake. Therefore, they reasoned out that this effect added to the toughening effects of rubber cavitations and void expansion in epoxies and silica particle debonding in epoxies.

Tsai et al. [96] studied the toughness performance of Glass/Epoxy composites for application in wind blades. The Glass/Epoxy composite toughness property was enhanced by the addition of silica nano-particles and rubber particles. In particular, promising results were obtained on the

enhancement of mode I fracture toughness. While Epoxy with Silica (10 wt.%) increased the fracture toughness by 47%, Epoxy with reactive liquid rubber (CTBN 10 wt.%) improved by 516% and Epoxy with core-shell rubber (CSR 10 wt.%) by 647%. Similarly, the hybrid Epoxy with Silica (10 wt.%) and CTBN(10 wt.%) increased fracture toughness by 390%, while Epoxy with Silica(10 wt.%) and CSR(10 wt.%) influenced positively by 442%. For epoxy with silica (20 wt.%), the improvement grew to 84% as Tsai et al. indicated.

Wetzel et al. [103] studied the loadings and the size effects of particles over toughness both within the Nano size and out of the Nano sized ranges. Thus, the addition of Aluminum oxide (Al_2O_3) with the particle size of about 13 nm and of Titanium dioxide (TiO_2) with particle sizes between 200 and 500nm (out of nanoparticles range) were done for standard epoxy resin (DER331) cured by a cycloaliphatic amine curing agent in order to improve the fracture toughness. The toughness tests were conducted using compact tension specimens. Filler contents of 5 vol.% and 10 vol.% Al_2O_3 increased the fracture toughness by 60% and 120% respectively, while the improvement of lower magnitude has been obtained with TiO_2 fillers for the same volumetric addition percentages. As it was already reviewed for what concerns the mechanical properties, Phong et al. [78] also dealt with the toughness effects of polyvinyl alcohol powder (nPVA). According to their process, polyvinyl alcohol powder was added in a composite of plain-woven carbon cloth (TR3110M) with Epoxy resin (Epikote 828) that was modified aliphatic polyamines (Japan Epoxy Resins). Randomly–aligned web of PVA Nano fibers with a diameter of about 40–80 nm were loaded in the matrix with different weight percentages as shown in Figure5: 0 wt.%, 0.03 wt.%, 0.05 wt.% and 0.1 wt.%. Results in Figure 2.42 show that the material resistance against both the initiation G_{IC} and the propagation G_{IP} of interlaminar fractures, i.e. the material toughness characteristic in mode I, was significantly increased with the addition of 0.1 wt.% nPVA by about 65% and 73%, respectively.

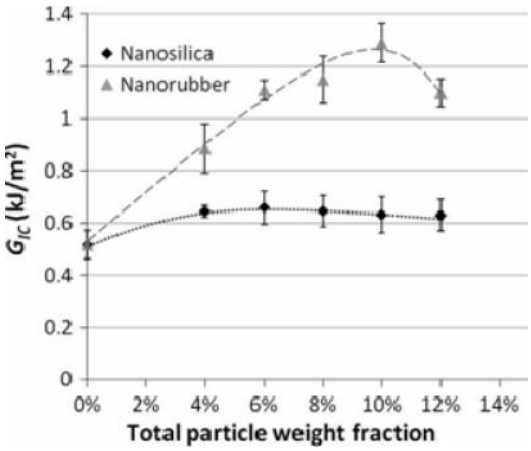

Figure 2.41 - Delamination fracture toughness of composite laminates with binary matrix as a function of the particle weight fraction [57]

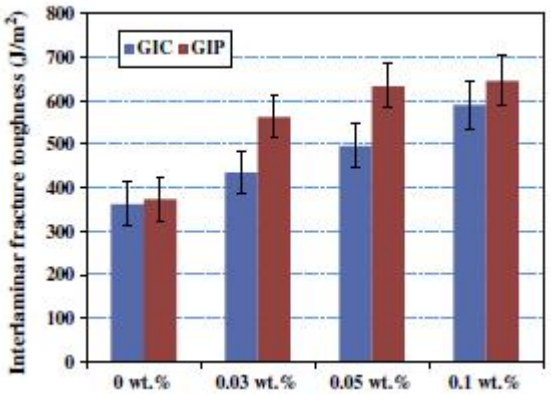

Figure2. 42 - Initiation GIC and propagation GIP fracture toughness in mode-I of CF/EP composite with various contents of nPVA [78]

2.4.3.2. Effect of particle size, adhesion and morphology

Kelkara et al. [97] analyzed the effects of stitching, z pinning and nanomaterial addition with respect to the fracture toughness of composite materials. Addition of alumina nano-particles (110nm) which were dispersed using high energy mixing procedures (using ultrasonication, high shear mixing, and pulverization) and nano-fibers, which were manufactured using an electro spinning technique to woven fiberglass (s_2) composite. The process improved interlaminar fracture toughness. The reason was that electro spinning technology relied on the creation of Nano fibers with an improved molecular orientation at a reduced concentration of fiber imperfections and crystal defects. The test was conducted with the classical double cantilever beam scheme to identify the interlaminar fracture toughness enhancement (51.7%) and to compare these results with those obtainable from stitching and z-pinning. The fracture toughness increased drastically as the particle diameters decreased [92]. This idea was further developed by

Fu et al. [62]. They studied the effects of particle size and volume fraction on the fracture toughness of alumina trihydrate powder-filled epoxy composites at room temperature. They found out that the most important factor is the particle/matrix adhesion, there is also a positive influence of the particles' size diameter increment on the fracture toughness, however, this trend is not always confirmed if the particles are in the Nano sized range and the applied load are characterized by high dynamic rate. However, this does not mean that higher particle loading necessarily leads to higher toughness: optimum value has been found at 22 vol.% while fracture toughness reduces on either side of this optimum point.

Domun et al. [65] did the other compiled study related to toughness. Their review summarized results for various loadings and nanoparticles types as shown in Figure 2.43. Based on their review, nanoclay and nanosilca may increase the fracture toughness from 120 to 270% for 0.7 wt.% to 6 wt.% loadings, and from 100 to 290% for 0.4 wt.% to 20 wt.% loadings respectively. Similarly, graphene and carbon nanotube (CNT) may enhance fracture toughness from 110 to 300% for 0.04 to 6 wt.% loadings and from 100 to 230% for 0.06 wt.% to about 3 wt.% loadings, respectively. For what concerns the morphological properties of the fractured surfaces, Raja et al. [98] examined a number of surfaces using FESEM and revealed that the nano fly ash has better interaction with matrix than other types of particles, and this leads to better stress transfer and thereby avoiding the formation of cracks. Likewise, Moustafa [99] dealt with dispersion and compatibility processes between polymer and nano-filler during the formation of the intercalated and/or exfoliated nanocomposites that leads to better toughening.

Thus nanoclay family enhances both mechanical properties and fracture toughness for 5 wt.% loadings, while silica is appropriate up to 20 wt.%. At the same time, graphene and CNT enhance both mechanical properties and fracture toughness for about 6 wt.% and 3 wt.% loadings respectively. However, it is difficult to put a conclusion in such forms because of parameter inconsistency.

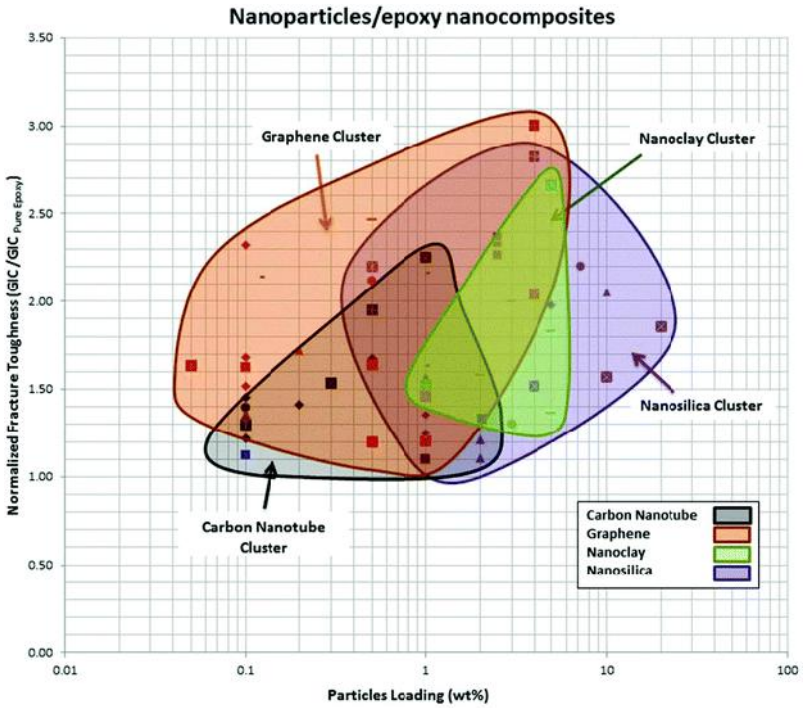

Figure 2.43- Map of fracture toughness of nanoparticles/epoxy nanocomposites with respect to particle loading [65]

2.4.4. Influence of nanoparticles on damages of composite materials

High surface to volume ratio is one of the main characteristics of nanoparticles because of their sizes and minimized surface defects. This property helps nanoparticles to reflect the stress wave (damage progression) which comes from the other phases. The fillers influenced the damage path either by reflecting or by bridging [44] as shown in Figure 2.44. The increment of the particle size may have no significant effects in the process of protection in case of the failure due to the presence of defects on the surface of the filler that may cause the initiation of the damage by itself. Particles having irregular shapes (real situation)[104] also can be easily damaged; however, the bulk property determines the result of the process considerably. Adhesion strengths of polymer composites were enhanced by adding modified clay fillers, which indicates that the phenomenon can reduce the failure because of good stress transfer between phases [98, 99]. Quaresimin et al. [100] to investigate the influence of clay-modified epoxies and their glass-reinforced laminates on fracture and interlaminar properties conducted the research. The result indicated a significant improvement in the fracture toughness and crack propagation threshold of clay-modified epoxy. However, due to the Nano filler morphology, the behavior of clay-modified laminates was still almost comparable with that of the base laminates. Thus morphology, particle

size, interfacial strength, and type of bulk materials influence the damage/failure condition of nanoparticles filled composite.

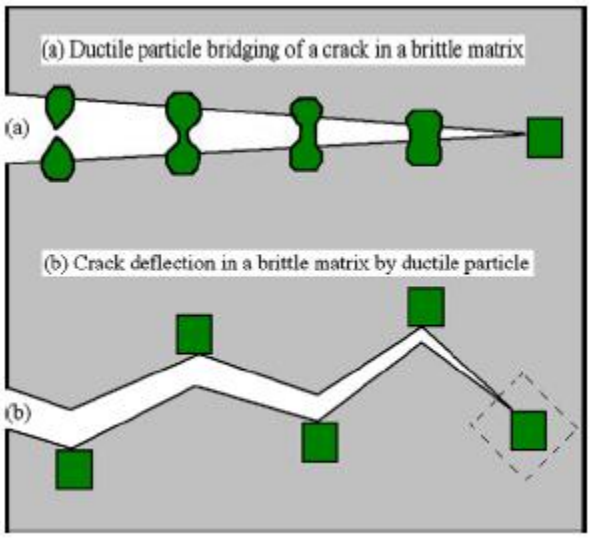

Figure 2.44 - Schematic illustrations of ductile particle toughening mechanisms in MCC: (a) ductile particle bridging; (b) crack deflection by ductile particle [44]

2.4.5. Summary

This review was aimed to summarize the effect of several factors and for various types of nanoparticles on the mechanical characteristics of composite materials with the polymeric matrix. Due to a lack of detailed research results for specific bulk materials and specific nanoparticles with the report of all the relevant parameters, it is difficult to establish a general conclusion about the influence of nanoparticles on the mechanical properties of composite materials. In addition, property variations of nanoparticles may happen due to manufacturing, sonication, curing, and modification processes.

However, particular conclusions can be drawn from the above discussion.

- Composite strength and toughness are strongly affected by loadings (wt.% and vol.%), particle size, particle/matrix adhesion, morphology.
- Strength depends on effective stress transfer between filler and matrix, and toughness/brittleness is controlled by adhesion.
- Inclusion of nanoclay in the composite matrix for the enhancement of the mechanical properties and fracture toughness becomes effective for low percentage in weight (i.e.

lower than 5 wt.%) of particle loadings, especially when particle dispersions are fine and, sometimes, modification helps to enhance the adhesion property with the bulk materials.

- Graphene and CNT enhance mechanical properties with a very low percentage by weight; however, fracture toughness can be enhanced relatively with a higher amount of loadings. Nevertheless, all the other parameters should be considered for better results.
- Nano silica particles can enhance fracture toughness and mechanical properties in a better way with loadings up to 22.5 wt.% and 25 wt.% respectively.
- Nanoparticles may affect the bulk negatively unless they are treated properly. It includes avoiding agglomeration, appropriate thermal condition, curing the combined materials, loadings, etc. the large size, poor compatibility, and poor adhesions enhance the damage progress of the composite materials.

Generally, addition of nanoparticles in composite materials enhances the mechanical properties, fracture toughness if the application type, suitable process, loadings, size, type of nanoparticles, etc. are implemented appropriately. If not it could be the cause of damage and it may affect determinately the bulk material's behavior. On the other hand, the review helps the researchers to some extent giving a guide on how the nanoparticles can be selected for the fracture toughness and main mechanical properties of heterogeneous materials.

2.5. Conclusion

The reviewed literature is summarized as pointed out below.

- The coming material science can be managed by customization, specific properties, and lightness, which make the need for composite materials in the emergent stage.
- Composite materials application covers a wide manufacturing field starting from home appliances to spacecraft structures, which pushes researchers to refine the development of qualified materials with respect to physical, mechanical, chemical, thermal, etc. properties.
- The material, structure, and technology history registered progressive advancement together with accidents. According to the literature, as the sophistication of technology and design bump up, more catastrophic failure happed at the beginning stage of each move. The damages in composite materials are initiated in large percentage either because of poor adhesion between the constituents or because of manufacturing

imperfections. This implies that the sophistication of composite material needs research in the composite materials' damage of constituents, interfacial behavior between the constituents, failure conditions of the structure, intralaminar damage, interlaminar failure, and enhancement in every aspect of the properties. Familiarity with the behavior of failures leads to originate better design methodology.

- Damage out of degradation can be prolonged by applying new technological advancement. The intralaminar/translaminar, interlaminar, and interfacial damage resistance can be enhanced by using nanoparticles. However, a number of nanoparticles can improve the positive behavior of the composite material-specific nanoparticles are used for particular applications. Based on the loadings and type of nanoparticles optimized properties can be achieved with respect to the load applications.

Therefore, the above points instigate to study the damage behavior and the influence of enhancement for particular applications.

2.6. References of chapter two

[1] Hosemann P, Frazer D, Fratoni M, Bolind A, Ashby MF, Materials selection for nuclear applications: Challenges and opportunities, ScriptaMaterialia 143 (2018) 181-187

[2] Ashby MF, Materials Selection in Mechanical Design, Fourth Edition, Elsevier Ltd, 2011

[3] Kühnel M, The global CFRP market 2016, Experience Composites, Augsburg, September 2016, JeC Group

[4] Shubha GN, Tejaswini ML, Lakshmi KP, Advanced Material for Newer Applications, Materials Today: Proceedings 5 (2018) 2541–2546

[5] Lin KY, Composite Materials: Materials, Manufacturing, Analysis, Design and Repair, 2014

[6] Kaw AK. Mechanics of composite materials, 2nd edition, Taylor & Francis Group, LLC 2006

[7] Warde S,Golder L, The life of a composite: Turning materials data into materials knowledge, Reinforced Plastics feature, Elsevier Volume 60, Number 5 September/October (2016) 324-328

[8] Wimmera G, Schuecker C, Pettermann HE, Numerical simulation of delamination in laminated composite components – A combination of a strength criterion and fracture mechanics, Composites: Part B 40 (2009) 158–165

[9] Burton WS, ComputAKN , Assessment of continuum models for sandwich panel honeycomb cores, Methods Appl. Mech. Engrg. 145 (1997) 341-360

[10] Peng L, Xu J, Zhang J, Zhao L, Mixed mode delamination growth of multidirectional composite laminates under fatigue loading, Engineering Fracture Mechanics 96 (2012) 676–686

[11] Karger-Kocsis J, Mahmood H, Alessandro Pegoretti, Recent advances in fiber/matrix interphase engineering for polymer composites, Progress in Materials Science 73 (2015) 1–43

[12] Mazumdar SK**,** Manufacturing Materials, Product, and Process Engineering, (2002) 43 CRC Press LLC

[13] Middleton B, Design and Manufacture of Plastic Components for Multifunctionality, (2016)53-102 Elsevier/ http://dx.doi.org/10.1016/B978-0-323-34061-8.00003-X

[14] Elmarakbi A , Advanced composite materials for automotive applications : structural integrity and crashworthiness, John Wiley & Sons, Ltd, 2014

[15] Frketic J, Dickens T, Ramakrishnan S, Automated manufacturing and processing of fiber-reinforced polymer (FRP) composites: An additive review of contemporary and modern techniques for advanced materials manufacturing, Additive Manufacturing 14 (2017) 69–86

[16] Middleton B, Design and Manufacture of Plastic Components for Multifunctionality, (2016)53-102 Elsevier/ http://dx.doi.org/10.1016/B978-0-323-34061-8.00003-X

[17] Balasubramanian KK, Sultan MTH, Rajeswari N, Sustainable Composites for Aerospace Applications., (2018)55-67 Elsevier/ https://doi.org/10.1016/B978-0-08-102131-6.00004-9

[18] Dixit D, Pal R, Kapoor G, Stabenau M, Lightweight Ballistic Composites, (2016)157-216 Elsevier/ http://dx.doi.org/10.1016/B978-0-08-100406-7.00006-4

[19] US department of energy, office of energy efficiency & renewable energy advanced manufacturing office, Bandwidth study on energy use and potential energy saving opportunities in U.S glass fiber reinforced polymer manufacturing, September 2007

[20] Maillet I, Michel L, Rico G, Fressinet M, Gourinat Y, A new test methodology based on structural resonance for mode I fatigue delamination growth in an unidirectional composite, Composite Structures 97 (2013) 353–362

[21] Chen J, Fox D, Numerical investigation into multi-delamination failure of composite T-piece specimens under mixed mode loading using a modified cohesive model, Composite Structures 94 (2012) 2010–2016

[22] Naqvi SR, Prabhakara HM, Bramer EA, Dierkes W, Akkerman R, Brem G, A critical review on recycling of end-of-life carbon fibre/glass fibre reinforced composites waste using pyrolysis towards a circular economy, Resources, Conservation & Recycling 136 (2018) 118–129

[23] Yancey RN, Lightweight Composite Structures in Transport (2016)35-52, Elsevier Ltd/ http://dx.doi.org/10.1016/B978-1-78242-325-6.00002-5

[24] Witten E, Sauer M, Kühnel M , Composite Market Report 2017 market developments, trends, challenges and opportunities, 2017 AVK - IndustrievereinigungVerstärkteKunststoffee.V

[25] Domun N, Kaboglu C, Paton KR, Dear JP, Liu J, Blackman BRK, Liaghat G, Hadavinia H, Ballistic impact behaviour of glass fibre reinforced polymer composite with 1D/2D nanomodified epoxy matrices, Composites Part B 167 (2019) 497–506

[26] Das S, Warren J, West D, Schexnayder SM, Global Carbon Fiber Composites Supply Chain Competitiveness Analysis, Technical Report, May 2016 Clean Energy Manufacturing Analysis Center/ http:/www.osti.gov/scitech

[27] Karatas MA, Gokkaya H, A review on machinability of carbon fiber reinforced polymer (CFRP) and glass fiber reinforced polymer (GFRP) composite materials, Defence Technology 14 (2018) 318-326

[28] Wilson A, Vehicle weight is the key driver for automotive composites, Reinforced Plastics Volume 61, Number 2 March/April 2017, Elsevier /www.reinforcedplastics.com

[29] Nickels L, Composites driving the auto industry, Reinforced Plastics d Volume 62, Number 1 January/February 2018

[30] Herbert GMJ, Iniyan S, Sreevalsan E, Rajapandian S, A review of wind energy technologies, Renewable and Sustainable Energy Reviews 11 (2007) 1117–1145

[31] Yang R, He Y, Zhang H, Progress and trends in nondestructive testing and evaluation for wind turbine composite blade, Renewable and Sustainable Energy Reviews 60 (2016)1225–1250

[32] Thomas L, Ramachandra M, Advanced materials for wind turbine blade- A Review, Materials Today: Proceedings 5 (2018) 2635–2640

[33] Sutherland LS, A review of impact testing on marine composite materials: Part I – Marine impacts on marine composites, Composite Structures 188 (2018) 197–208

[34] Neser G, Polymer Based Composites in Marine Use: History and Future Trends, Procedia Engineering 194 (2017) 19 – 24

[35] Ávila AF, Neto AS, Junior HN, Hybrid nanocomposites for mid-range ballistic protection, International Journal of Impact Engineering 38 (2011) 669-676

[36] ShieldStrand Woven Fabrics, 2010, Owens corning composite materials, LLC/ www.owenscorning.com

[37] Talreja R, Assessment of the fundamentals of failure theories for composite materials, Composites Science and Technology 105 (2014) 190–201

[38] Talreja R, Singh CV, Damage and failure of composite materials , Cambridge University Press, 2012

[39] Daniel IM, Failure of Composite Materials under Multi-axial Static and Dynamic Loading, Procedia Engineering 88 (2014) 10 – 17

[40] Zubillaga L, Turon A, Maimí P, Costa J, Mahdi S, Linde P, An energy based failure criterion for matrix crack induced delamination in laminated composite structures, Composite Structures 112 (2014) 339–344

[41] Short GJ, Guild FJ, Pavier MJ, The effect of delamination geometry on the compressive failure of composite laminates, Composites Science and Technology 61(2001) 2075–2086

[42] Sørensen BF, Jørgensen E, Debel CP, Jensen FM, Jensen HM, Jacobsen TK, Halling KM, Improved design of largewind turbineblade of fibrecomposites basedonstudies of scale effects(Phase 1) –SummaryReport, 2014

[43] Mulugeta H, Alem B, Fracture analysis of pressure vessel under dynamic loading and thermal effect, M. Sc. Thesis, 2009

[44] Liu Y, Zhou J, Shen T, Effect of nano-metal particles on the fracture toughness of metal–ceramic composite, Materials and Design 45 (2013) 67–71

[45] Li Y, Zhou M, Prediction of fractures toughness of ceramic composites as function of microstructure:II analytical model, Journal of the Mechanics and Physics of Solids 61 (2013) 489–503

[46] Orifici AC, Herszberg I, Thomson RS, Review of methodologies for composite material modelling incorporating failure, Composite Structures 86 (2008) 194–210

[47] Gargano A, Pingkarawat K,Blacklock M, Pickerd V, Mouritz AP, Comparative assessment of the explosive blast performance of carbon and glass fibre-polymer composites used in naval ship structures, Composite Structures 171 (2017) 306–316

[48] Warren KC, Lopez-Anido RA, Goering J, Experimental investigation of three-dimensional woven composites, Composites: Part A 73 (2015) 242–259

[49] Walter TR, Subhash G, Sankar BV, Yen CF, Damage modes in 3D glass fiber epoxy woven composites under high rate of impact loading, Composites: Part B 40 (2009) 584–589

[50] Laffan MJ, Pinho ST, Robinson P, McMillan AJ, Translaminar fracture toughness testing of composites: A review, Polymer Testing 31 (2012) 481–489

[51] Czabaj MW, Ratcliffe JG, Comparison of intralaminar and interlaminar mode I fracture toughnesses of a unidirectional IM7/8552 carbon/epoxy composite, Composites Science and Technology 89 (2013) 15–23

[52] Abisset E, Daghia F, Sun XC, Wisnom MR, Hallett SR, Interaction of inter- and intralaminar damage in scaled quasi-static indentation tests: Part 1 – Experiments, Composite Structures 136 (2016) 712–726

[53] Belingardi G, Beyene AT, Jichuan D, Energy absorbing capability of GMT, GMTex and GMT-UD composite panels for static and dynamic loading – Experimental and numerical study, Composite Structures 143 (2016) 371–387

[54] Saghafi H, Ghaffarian SR, Salimi-Majd D, Saghafi HA, Investigation of interleaf sequence effects on impact delamination of nano-modified woven composite laminates using cohesive zone model, Composite Structures 166 (2017) 49–56

[55] Feng D, Aymerich F, Finite element modelling of damage induced by low-velocity impact on composite laminates, Composite Structures 108 (2014) 161–171

[56] Borkowski L, Chattopadhyay A, Multiscale model of woven ceramic matrix composites considering manufacturing induced damage, Composite Structures 126 (2015) 62–71

[57] Zeng Y, Liu HY, Mai YW, Du XS, Improving interlaminar fracture toughness of carbon fibre/epoxy laminates by incorporation of nano-particles, Composites: Part B 43 (2012) 90–94

[58] Short GJ, Guild FJ, Pavier MJ, The effect of delamination geometry on the compressive failure of composite laminates, Composites Science and Technology 61(2001) 2075–2086

[59] Chandrasekaran S, Sato N, Tölle F, Mülhaupt R , Fiedler B, Schulte K, Fracture toughness and failure mechanism of graphene based epoxy composites, Composites Science and Technology 97 (2014) 90–99

[60] Tang Y, Ye L, Zhang Z , Friedrich K, Interlaminar fracture toughness and CAI strength of fibre-reinforced composites with nanoparticles – A review, Composites Science and Technology 86 (2013) 26–37

[61] Valentini L, Bon SB, Lopez-Manchado MA, Verdejo R, Pappalardo L, Bolognini A, Alvino A, Borsini S, Berardo A, Pugno NM, Synergistic effect of graphenenanoplatelets and carbon black in multifunctional EPDM nanocomposites, Composites Science and Technology 128 (2016) 123-130

[62] Fu SY, Feng XQ, Lauke B, Mai YW, Effects of particle size, particle/matrix interface adhesion and particle loading on mechanical properties of particulate–polymer composites, Composites: Part B 39 (2008) 933–961

[63] Hakamy A, Shaikh FUA, Low IM, Effect of calcined nanoclay on microstructural and mechanical properties of chemically treated hemp fabric-reinforced cement nanocomposites, Construction and Building Materials 95 (2015) 882–891

[64] John B, Nair CPR, Ninan KN, Effect of nanoclay on the mechanical, dynamic mechanical and thermal properties of cyanate ester syntactic foams, Materials Science and Engineering A 527 (2010) 5435–5443

[65] Domun N, Hadavinia H, Zhang T, Sainsbury T, Liaghat GH, Vahid S,Improving the fracture toughness and the strength of epoxy using nanomaterials – a review of the current status, Nanoscale 7(2015) 10294-10329

[66] Nguyen QT, Baird DG, An improved technique for exfoliating and dispersing nanoclay particles into polymer matrices using supercritical carbon dioxide, Polymer 48 (2007) 6923-6933

[67] El-Sheikhy R, Al-Shamrani M, Interfacial bond assessment of clay-polyolefin nanocomposites CPNC on view of mechanical and fracture properties, Advanced Powder Technology 28 (2017) 983–992

[68] Azeez AA, Rhee KY, Park SJ , Hui D, Epoxy clay nanocomposites – processing, properties and applications: A review, Composites: Part B 45 (2013) 308–320

[69] Assaedi H, Shaikh FUA, Low IM, Effect of nano-clay on mechanical and thermal propertiesof geopolymer, Journal of Asian Ceramic Societies 4 (2016) 19–28

[70] Eesaee M, Shojaei A, Effect of nanoclays on the mechanical properties and durability of novolac phenolic resin/woven glass fiber composite at various chemical environments, Composites: Part A 63 (2014) 149–158

[71] Binu P P, George KE, Vinodkumar MN, Effect of nanoclay, Cloisite15A on the Mechanical Properties and Thermal behavior of Glass Fiber Reinforced Polyester, Procedia Technology 25 (2016) 846 – 853

[72] Maharsia RR, Jerro HD, Enhancing tensile strength and toughness in syntactic foams through nanoclay reinforcement, Materials Science and Engineering A 454–455 (2007) 416–422

[73] Withers GJ, Yu Y, Khabashesku VN,Cercone L, Hadjiev VG, Souza JM, Davis DC, Improved mechanical properties of an epoxy glass–fiber composite reinforced with surface organomodified nanoclays, Composites: Part B 72 (2015) 175–182

[74] Sharma SM, Chhibber R, Mehta R, Glass Fiber Reinforced Polymer-Clay Nanocomposites: Processing, Structure and Hygrothermal Effects on Mechanical Properties, Procedia Chemistry 4 (2012) 39 – 46

[75] Chan M, Lau K, Wong T, Ho M, Hui D,Mechanism of reinforcement in a nanoclay/polymer composite, Composites: Part B 42 (2011) 1708–1712

[76] Shuvo SN, Shorowordi KM, Processing and Mechanical Characterization of Graded and Non-graded Nanoclay Composites, Procedia Engineering 105 (2015) 928 – 932

[77] Ghadami F, Dadfar MR, Kazazi M, Hot-cured epoxy-nanoparticulate-filled nanocomposites: Fracture toughness behavior, Engineering Fracture Mechanics 162 (2016) 193–200

[78] Phong NT, Gabr MH, Okubo K, Chuong B, Fujii T, Improvement in the mechanical performances of carbon fiber/epoxy composite with addition of nano-(Polyvinyl alcohol) fibers, Composite Structures 99 (2013) 380–387

[79] Gantenbein D, Schoelkopf J, Matthews GP, Gane PAC, Determining the size distribution-defined aspect ratio of platy particles, Applied Clay Science 53 (2011) 544–552

[80] Iman M, Maji TK, Effect of crosslinker and nanoclay on starch and jute fabric based green nanocomposites, Carbohydrate Polymers 89 (2012) 290– 297

[81] Matusik J, Stodolak E, Bahranowski K, Synthesis of polylactide/clay composites using structurally different kaolinites and kaolinite nanotubes, Applied Clay Science 51 (2011) 102–109

[82] Awad WH, Beyer G, Benderly D, Ijdo WL, Songtipya P, Jimenez-Gasco MM, Manias JGE, Wilkie CA, Material properties of nanoclay PVC composites, Polymer 50 (2009) 1857–1867

[83] Sun XC, Wisnom MR, Hallett SR, Interaction of inter- and intralaminar damage in scaled quasi-static indentation tests: Part 2 – Numerical simulation, Composite Structures 136 (2016) 727–742

[84] Zhao Y, Chen ZK, Liu Y, Xiao HM, Feng QP, Fu SY, Simultaneously enhanced cryogenic tensile strength and fracture toughness of epoxy resins by carboxylic nitrile-butadiene nano-rubber, Composites: Part A 55 (2013) 178–187

[85] Ravandi M, Teo WS, Tran LQN, Yong MS, Tay TE, The effects of through-the-thickness stitching on the Mode I interlaminar fracture toughness of flax/epoxy composite laminates, Materials and Design 109 (2016) 659–669

[86] Wood MDK, Sun X, Tong L, Katzos A, Rispler AR, Mai YW, The effect of stitch distribution on Mode I delamination toughness of stitched laminated composites – experimental results and FEA simulation, Composites Science and Technology 67 (2007) 1058–1072

[87] Mouritza AP, Leongb KH, Herszberg I, A review of the effect of stitching on the in-plane mechanical properties of fibre-reinforced polymer composites, Conqwsires Part A 28A (1997) 979-99 I

[88] Dransfield KA, Jain LK, Mai YW, On the Effects of Stitching in CFRPs-I. Mode I Delamination Toughness, Composites Science and Technology 58 (1998) 81-827

[89] Jain LK, Dransfield KA, Ma YW, On the Effects of Stitching in CFRPs-II. mode II Delamination Toughness, Composites Science and Technology 58 (1998) 829-837

[90] Sun X, Tong L, Wood MDK, Mai YW, Effect of stitch distribution on mode I delamination toughness of laminated DCB specimens, Composites Science and Technology 64 (2004) 967–981

[91] Mouritz AP, Review of z-pinned composite laminates, Composites: Part A 38 (2007) 2383–2397

[92] Adachi T, Osaki M, Araki W, Kwon SC, Fracture toughness of nano- and micro-spherical silica-particle-filled epoxy composites, ActaMaterialia 56 (2008) 2101–2109

[93] Kim BC, Park SW, Lee DG, Fracture toughness of the nano-particle reinforced epoxy composite, Composite Structures 86 (2008) 69–77

[94] Liang YL, Pearson RA, The toughening mechanism in hybrid epoxy-silica-rubber nanocomposites (HESRNs), Polymer 51 (2010) 4880-4890

[95] Tsai JL, Huang BH, Cheng YL, Enhancing Fracture Toughness of Glass/Epoxy Composites for Wind Blades Using Silica Nanoparticles and Rubber Particles, Procedia Engineering 14 (2011) 1982–1987

[96] Wetzel B, Rosso P, Haupert F, Friedrich K, Epoxy nanocomposites – fracture and toughening mechanisms, Engineering Fracture Mechanics 73 (2006) 2375–2398

[97] Kelkara AD, Mohan R, Bolick R, Shendokar S, Effect of nanoparticles and nanofibers on Mode I fracture toughness of fiber glass reinforced polymeric matrix composites, Materials Science and Engineering B 168 (2010) 85–89

[98] Raja RS, Manisekar K, Experimental and statistical analysis on mechanical properties of nanoflyash impregnated GFRP composites using central composite design method, Materials and Design 89 (2016) 884–892

[99] Moustafa H, Darwish NA, Effect of different types and loadings of modified nanoclay on mechanical properties and adhesion strength of EPDM-g-MAH/nylon 66 systems, International Journal of Adhesion&Adhesives61(2015)15–22

[100] Quaresimin M, Salviato M, Zappalorto M, Fracture and interlaminar properties of clay-modified epoxies and their glass reinforced laminates , Engineering Fracture Mechanics 81 (2012) 80–93

[101] Zappalorto M, Salviato M, Quaresimin M, Mixed mode (I + II) fracture toughness of polymer nanoclay nanocomposites, Engineering Fracture Mechanics 111 (2013) 50–64

[102] Chan ML, Lau KT, Wong TT, Ho MP, Hui D, Mechanism of reinforcement in a nanoclay/polymer composite, Composites: Part B 42 (2011) 1708–1712

[103] Wetzel B, Rosso P, Haupert F, Friedrich K, Epoxy nanocomposites – fracture and toughening mechanisms, Engineering Fracture Mechanics 73 (2006) 2375–2398

[104] Sellappan P, Guin JP, Rocherulle J, Rouxel FCT, Riedel R, Influence of diamond particles content on the critical load for crack initiation and fracture toughness of SiOC glass–diamond composites, Journal of the European Ceramic Society 33 (2013) 847–858

Part I: Investigation on the Influence of Nanoclay on Strengths, Modulus of Elasticity and Interlaminar Fracture Toughness of Glass Fiber Reinforced Plastic (GFRP)

Part I discusses the effects of nano-modification on S-glass woven fiber reinforced plastic material. The epoxy was enhanced by addition of particles of the nanoclay family, specifically Cloisite 20B. The research covered four types of materials with different nanoclay concentrations. The study focuses on two major basic types of experimental works. The first part (chapter three) is devoted to material characterization, which dealt with tensile and compressive behaviors. Specifically, it includes tensile strength, compressive strength, tensile modulus, compressive modulus, Poisson ratios in both warp and weft directions. The second part (chapter four) deals with interlaminar fracture characterization that focuses on fracture toughness and resistance curves.

Chapter 3: Material Characterization of Plain-Woven Composite Materials

In this chapter, the effect of nanoclay, Cloisite 20B inclusion on the mechanical behavior of a woven type glass fiber reinforced plastic (GFRP) composite was experimentally investigated. Specifically, the study examined the effect of nanoclay with various weight percentages on the tensile strength, compressive strength, compressive modulus of elasticity and tensile modulus of elasticity of GFRP in both weft and warp directions. The chapter includes background discussion, manufacturing, experimental procedures and discussions about the results.

3.1. Introduction

Nowadays structures, which are vulnerable to blast loading, explosion, ballistic and fire accidents during a crash, require for materials characterized by suitable related properties. Therefore, composite materials have to be developed from the constituents that have properties

of better heat distortion temperature, barrier characteristics and flame retardanceperformances. Besides that, among the fiber-reinforced composites, ordinary (conventional micro scale composites) laminated composite materials are the most common. The fibers reinforce in-plane directions (within the lamina) [1, 2], while, generally, the through-thickness direction is the weak one. Therefore, one relevant research target is to improve the structural behavior of composite materials with respect to the out of plane properties (along with the through-thickness direction), the shear loading transfer behavior of matrix/fiber and between the layers in the laminate. In this perspective, different approaches like stitching, z-pinning, toughening, etc. could be evaluated. Considerably, property enhancement or toughening of the polymeric fraction plays a great role overall property of the composite material.

One of the utilized approaches consists in adding nanoparticles (see figure 3.1) like nanoclay, Nano silica, nanotubes [3, 4] to the matrix. Two of the major causes of composite material failures in weak directions are debonding and delamination [5]. Debonding and delamination resistance can be improved by adding nanoclay. The ability of nanoclay to induce enhancement in the physical, chemical and mechanical properties of the composite material in comparison with what is possible to obtain from conventionally filled composites is largely reported in the literature [6-8]. In particular, the recent work [7] by Azeez et al. gives a review of the available research results.

Therefore, addition of nanoclay to the weaker constituent of composite material -the matrix - enhances specifically the mechanical and physical properties [5]. As the mechanical properties of the matrix increases, the delamination resistance is consequently improved. Similarly, the debonding resistance can be improved by increasing the interfacial adhesion between matrix and fibers. Thus, the nanoclay enhances the interfacial shear strength by increasing the contact area and wettability between fibers and matrix [9, 10]. In addition to this, the nanoclay heals the defects of the fibers by filling voids and scratches.

The enhancement of the matrix is produced by the combination of nanoparticles/ nanoclay and the new enhanced material is named nanocomposites [4]. The nanoclay requires well dispersion and good distribution throughout the matrix to have better-enhanced nanocomposites. Clay is a weathering product resulting from the disintegration and chemical decomposition of igneous rocks with the fine texture of particle size. Clay-polymer nanocomposites (CPNC) became one of the important fields of nanotechnology since Toyota produced the first application in the

automobile industry [11]. Nanoclays are aluminum silicate, primarily composed of fine-grained minerals having a natural structure with sheet-like geometry (Figure 3.1) besides they are naturally occurring, inexpensive and eco-friendly materials and have found multifarious applications [12,13]. The nanoclay addition improvement of composite materials property should be dealt by taking properly into accounts the specific applications, and tasks to avoid that the new enhancement affects negatively over other important pristine properties. In this chapter, the effect of specific nanoclay, Cloisite 20B, inclusion on the mechanical behavior of a woven type S-glass fiber reinforced plastic (GFRP) composite was experimentally investigated. Specifically, the study examined the effect of nanoclay with various weight percentages on the tensile strength, compressive strength, compressive modulus of elasticity and tensile modulus of elasticity of GFRP in both weft and warp directions. The chapter includes background discussion, manufacturing, experimental procedures and discussions about the results.

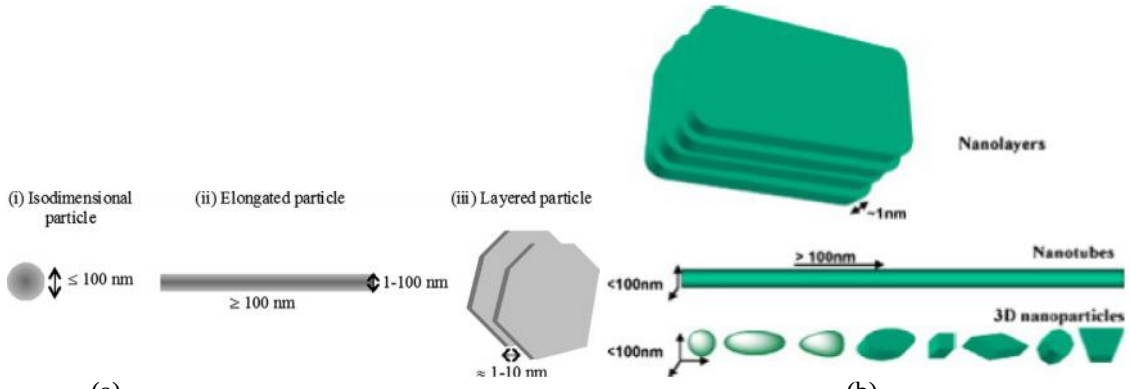

Figure 3. 1. Nanoparticles(a)Schematic representation of the three categories of nanoparticles [12] (b) various types of nan scale materials [13]

The important previous findings related to nanoclay enhancement effects are compiled. Wetzel et al. [14] dealt with the effect of nanoclay in epoxy resin (DER331 by DOW). Their study indicated that 2 wt.% of nanoclay loading provided a denser microstructure, decreases the porosity and subsequently improves the flexural strength and toughness. Korichoet al. [15] found a considerable enhancement in energy absorption capability and lower strain rate sensitivity at various energy levels with 1 wt.% loading of nanoclay. According to Hamitouche et al. [16], who studied the mechanical properties of glass fiber reinforced polyester, highest tensile modulus and tensile strengths were obtained with 0.5 wt.% to 1 wt.% loading of Cloisite15A nanoclay, while opposite results were obtained with 1.5 wt.% to 2 wt. %. In the study done by Assaedi et al. [17], the nanoclay added at 2 vol.% and 4 vol.% in cyanate ester syntactic foam had led to an

improvement of the tensile strength by 63 and 94%, respectively. Natural montmorillonite (CN) and organically modified montmorillonite (CB) improved the mechanical performance of novolac phenolic resin (PF)/woven glass-fiber (GF) composites due to the Nano dispersion and good interfacial interaction with the matrix, at 2.5 wt.% of the clays enhanced the elastic modulus up to 38% for CN and 43% for CB as reported by Binu et al. [18]. Similarly, the results of the research done by John et al. [19] showed that the nanoclay platelets (Cloisite 30B) added at 2.0 wt.% and 4.0 wt.% improved the mechanical properties of the considered cyanate ester syntactic foams. The tensile, flexural and compressive strength improved by 63%, 55% and 73% with 2.0 wt.% and by 94%,97% and 150% with 4.0 wt.%, respectively. Also, an impressive improvement of the fracture toughness, measured by the energy absorbed during the tensile strength, respectively 66%, and 105%, was reported. According to their extensive work, the addition of more nanoclay showed no further increase in these properties due to agglomeration. For unidirectional basalt fiber/epoxy composites, Mostafa et al. [20] reported that, by adding 5 wt.% of silane-modified Na+-montmorillonite nanoclay, the tensile strength, flexural strength, tensile modulus, and flexural modulus increased by 11%, 28%, 23%, and 28% respectively. In a similar study, Khosravi and Farsani [21] made the addition of 5 wt.% nanoclay on syntactic foams, the strength was modified the up to 22%. Azeez et al. [4] showed that 5 wt.% of nanoclay increased the tensile strength considerably. Thus, from the aforementioned, the nanoclay can effectively improve the mechanical properties [22, 23] with loadings that are less than 5 wt.% [17, 24]. Furthermore, all the previously mentioned findings were obtained with the various nanoclay types. Studies related to the enhancement achievable from addition of nanoclay type Cloisites 20B that have a better intercalation behavior and low toxicity, combined with fire retardant properties, when added in composite materials such as S-glass and epoxy, are limited. Epoxies are thermosetting polymers having unique characteristics such as high adhesive strength, neutrality, high strength, and hardness and excellent chemical and heat resistance [25]. One of the constituents, Shield Strand S reinforcing fiber, has an economical advantage, which possibly saves 60% of the cost, attains 40% and 50% weight savings when replacing aluminum and steel respectively [26]. Similarly, epoxy, SC-15 matrix which has low shrinkage, excellent adhesion to carbonaceous materials, and high reactivity with a variety of chemical curing agents [27] can be enhanced with Cloisite 20 that has better melt flow rate and elongation at break(see figure 3.2)

[28, 29]. This property could be one of the alternatives in ballistic applications. Nevertheless, before that, the mechanical properties have to be approachable.

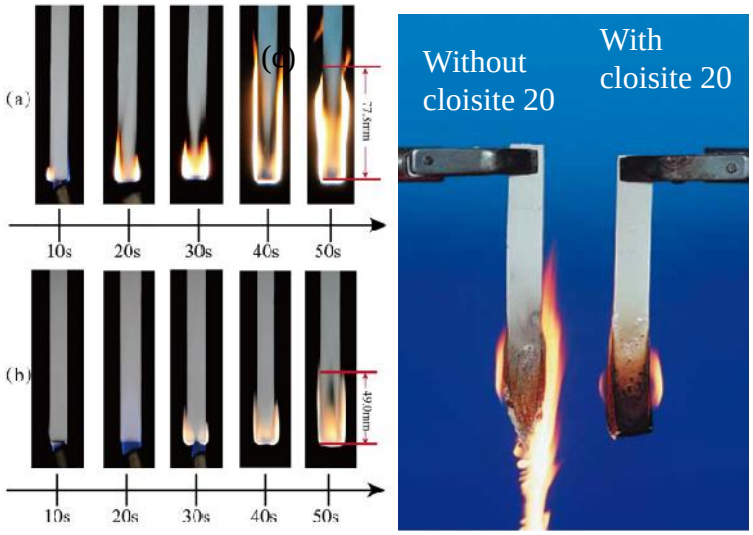

Figure 3.2 (a) unmodified samples [28], (b)Closite20 modified laminate composites [28], (c) difference in melt flow rate and elongation at break[29]

Thus, the main objective of the present work was to develop and study the mechanical properties of pristine and nano modified a particular type of composite a plain-woven S-glass fiber reinforced plastic. Specifically, in this study, the influence of nanoclay, Cloisite® 20B was studied. Three nanoclay weight percentages (wt.%) was added to the resin matrix and their effects compared with the pristine composite material. The percentages by weight added to the base material were 0.5 wt.%, 1 wt.%, and 2 wt.%. The tensile and compressive tests were performed according to the ASTMD3039 [30] and ASTMD6641 [31] standards respectively in the warp and weft directions. The experimental test results were evaluated based on the reaction force-displacement diagram, and the two parameters such as the modulus of elasticity, and strength in the warp and weft directions.

3.2. Experimental procedure

3.2.1. Materials

The material was produced from glass fiber and nanocomposites. The reinforcement was S-glass plain weave fabric with an areal weight of 818g/m^2, which was supplied by Owens Corning Shield Strand S as primary reinforcement. The resin used was two-part toughened epoxy, namely SC-15, obtained from Applied Poleramic, CA. The secondary reinforcing nano-additives were

Cloisite® 20B (Southern Clay Products, Inc., TX). The number of plies used was eight with a symmetric stacking sequence of [0/90/0/90]s having thickness of the laminate, 5mm .

The manufacturing process was undertaken to obtain good nano distributive and dispersive mixing in order to blend throughout the polymeric matrix as well as to minimize agglomeration respectively. Initially, see Figure 3.3(a), part A of SC-15 epoxy was mixed with the desired amount of nanoclay and the resulting compound was sonicated (Vibra-Cell™ sonicator), see Figure 3.3(b), for around 30 minutes until the total applied energy was 30kJ. Intermittent sonicating energy (10s energy, 5s pause) was applied to take under control the rise in temperature of the compound. Once the selected amount of energy (30kJ) was applied, the resulting mixture was cooled at room temperature for 30 minutes, followed by mixing of part B of SC-15 epoxy (control). The solution was mixed thoroughly, degassed before application on each ply using hand layup process. Figure 3.3(c) showed the sonicated nanomodified epoxy material, which was ready for manufacturing the composite materials.

Four types of composite materials were manufactured using the hand layup method, see Figure 3.3(d): Pristine, 0.5 wt.% 20B Cloisite, 1 wt.% 20B Cloisite, and 2 wt.% 20B Cloisite to deal with the effects of Nano filler on the elastic modulus of elasticity and strengths.

(a)

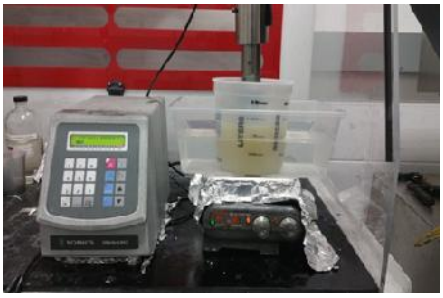

(b)

(c)

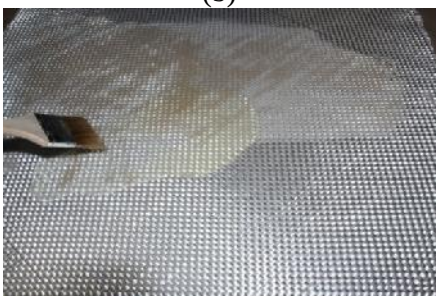

(d)

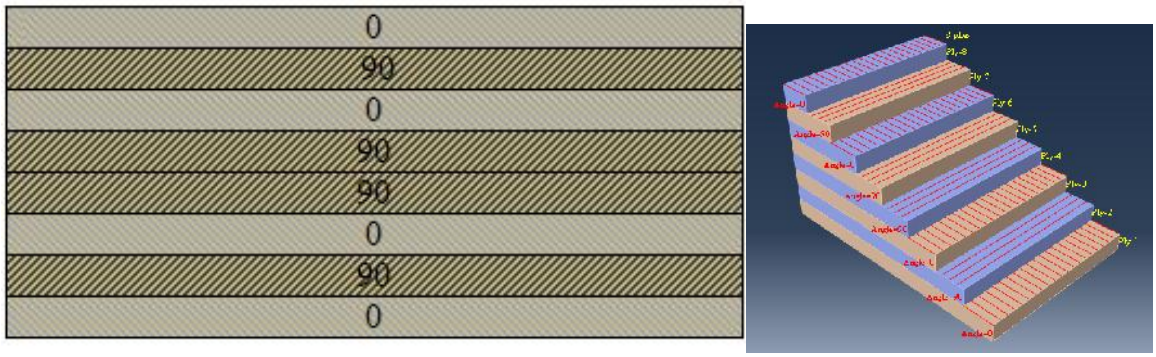

(e) (f)

Figure 3,3 – The panel's preparation process (a) SC-15 epoxy with Cloisite 20B organized for sonication, (b) sonication process, (c) after sonication/ nanocomposite, (d) hand layup coating process, (e) layup, (f) Abacus representation

3.2.2. Experimental test setup

3.2.2.1. Tensile test

First, the base material was characterized to identify the reference performance and study, by comparison, the effects of nanoclay, Cloisite 20B, on the main mechanical properties and to understand the failure mechanism of the material. Two types of specimens were prepared for tensile tests (both warp (L) and weft (T) directions) from the same plates, as shown in Figure 3.4. The tensile test was performed as per ASTM D3039 [30] and 5 samples with gage length 100mm were taken for each of the pristine and the other three nanoclay concentrations in both directions. The samples were instrumented each with two strain gauges, as shown in Figure 3.4c, to measure accurately Young's modulus and Poisson's ratio. Tensile tests were conducted with a 100kN capacity servo-hydraulic testing machine (INSTRON-8801), shown in Figure 3.5b with a crosshead rate of 2 mm/min, specimens were clamped by means of hydraulic wedge grips. The NI WLS-9163 data acquisition board acquired the strain gauges data. The load and crosshead displacement data were also acquired directly from the testing machine transducers by the NI DAQCard-6062E card. All data were acquired with a sampling rate equal to 1 kHz.

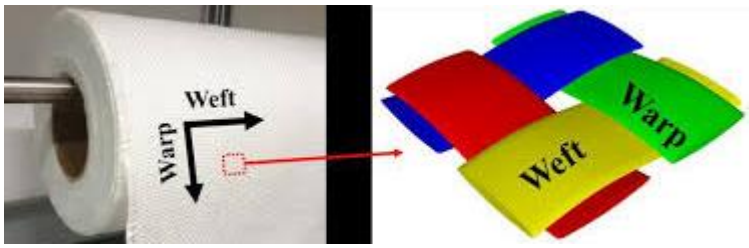

(a)

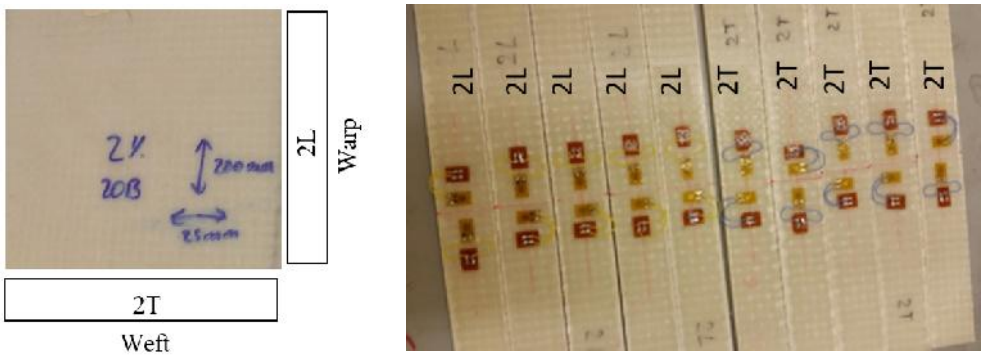

(b) (c)

Figure 3.4 Panel and specimens (a) architectural representation, (b) panel with 2 wt.% Cloisite 20B and (c) the organized warp/weft tensile test specimens instrumented with strain gauges.

(a) (b) (c)

Figure 3.5 –Tensile testing setup (a)NI WLS-9163 data acquisition board, (b) 100 kN capacity servo-hydraulic testing machine (INSTRON-8801) ,(c) enlarged view of one specimen

3.2.2.2. Compression test

As earlier stated, the compression tests were undertaken according to the ASTM D6641M standards [31], samples from each of the pristine and three different Cloisite 20B concentrations, were cut from the same panels where tensile samples were taken, in both warp and weft

directions. The samples were instrumented each with two strain gauges, to measure Young's modulus and Poisson ratio and the crosshead rate of the test was 2 mm/min. Here, since there is not enough space to place the two strain gauges on the same face (as the nominal gage section is 13 mm), it was decided to attach the two strain gauges, i.e. the longitudinal and transverse strain ones, on the opposite faces of the samples, as shown in Figure 3.6 [31].

Buckling and bending at the gage section is the common problem in compressive loading tests, they can occur due to imperfections in the test specimen, the specimen fixture, improper gage section or the testing procedure, and need to be monitored. The occurrence of Euler buckling totally invalidates the test while the eventual presences of bending have to be limited to a maximum of 10% of the difference between the strains measured on the two surfaces.

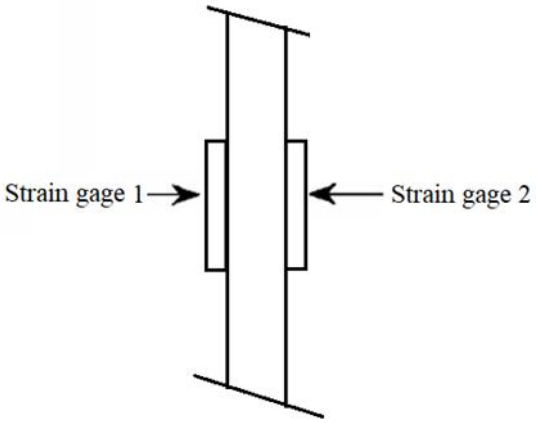

Figure 3.6: A back-to-back strain gauges for buckling and bending percentage test, strain gage 1 in longitudinal directions and strain gage 2 in the transverse directions

Thus, in order to check against the eventuality of such buckling and bending problems, a back-to-back strain gauges placement, i.e. positioning longitudinal strain gauges on both sides of the samples as shown in Figure 3.6, was used for some set of samples of each material and the percentage By of the bending was determined using equation 3.1[31].

$$B_y = percent.bending = \frac{e_1 - e_2}{e_1 + e_2} x100 \qquad (3.1)$$

Having calibrated the test set up, here again, the 100kN capacity servo-hydraulic testing machine (INSTRON-8801), as shown in Figure 3.7, was used together with the specimen fixtures specific for the compressive tests. According to the ASTM D6641/D6641M standards, samples were subjected to monotonic compressive loading with a stroke rate of 1.3mm/min. The strain gage signals were acquired with the NI WLS-9163 data acquisition board while the applied load and

the crosshead displacement data were acquired from the testing machine transducers by the NI DAQCard-6062E card. All data were acquired with a sampling rate equal to 1 kHz.

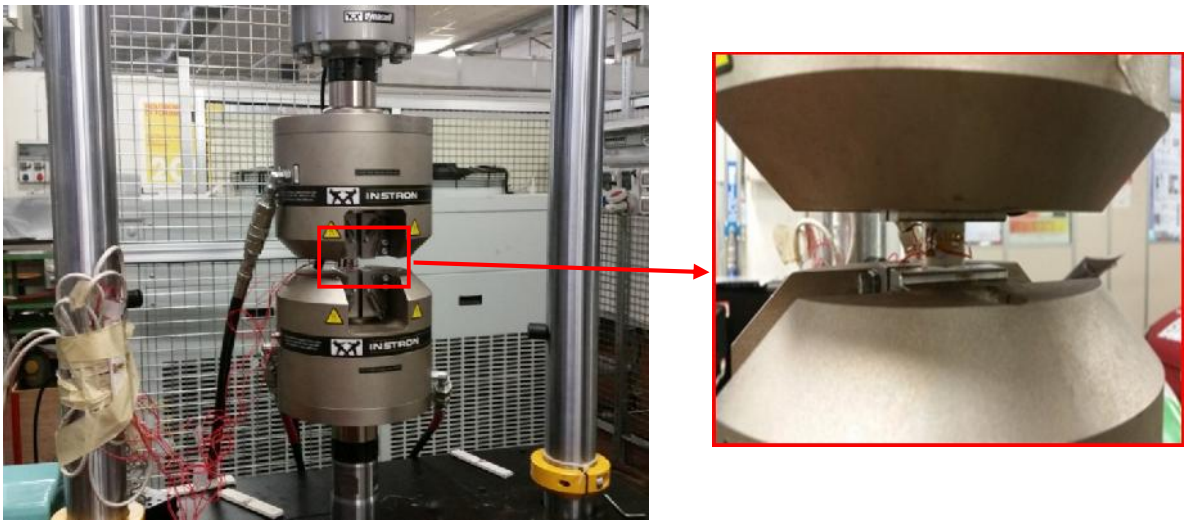

(a) (b)

Figure3.7– Compression test setup (a)100 kN capacity servo-hydraulic testing machine (INSTRON-8801), (b) enlarged section from 90°viewtest specimen

3.3. Results discussion

3.3.1. Tensile tests

Figure 6 shows the force-displacement curves in tensile tests of the considered material modified with 1 wt.% of nano-clay, in the first diagram are grouped the curves for the loading direction coincident with the warp fibers, while in the second diagram are grouped the other curves related to the weft fibers. For instance Figure 3.8(e), the tensile test results indicate that the warp direction specimens reached failure values of the force greater than the weft direction of the specimens (Figure 3.8(f)). In the diagrams shown in Figure 3.8 (e) and (f) respectively, it is visible a first change (decrease) of the stiffness that took place at about 25kN. Then the curves continued linearly, but with a slightly lower slope, until load values very close to the failure point. It is worthy of note that the five curves of all the diagrams are well superimposed and this means high repeatability of the experimental results.

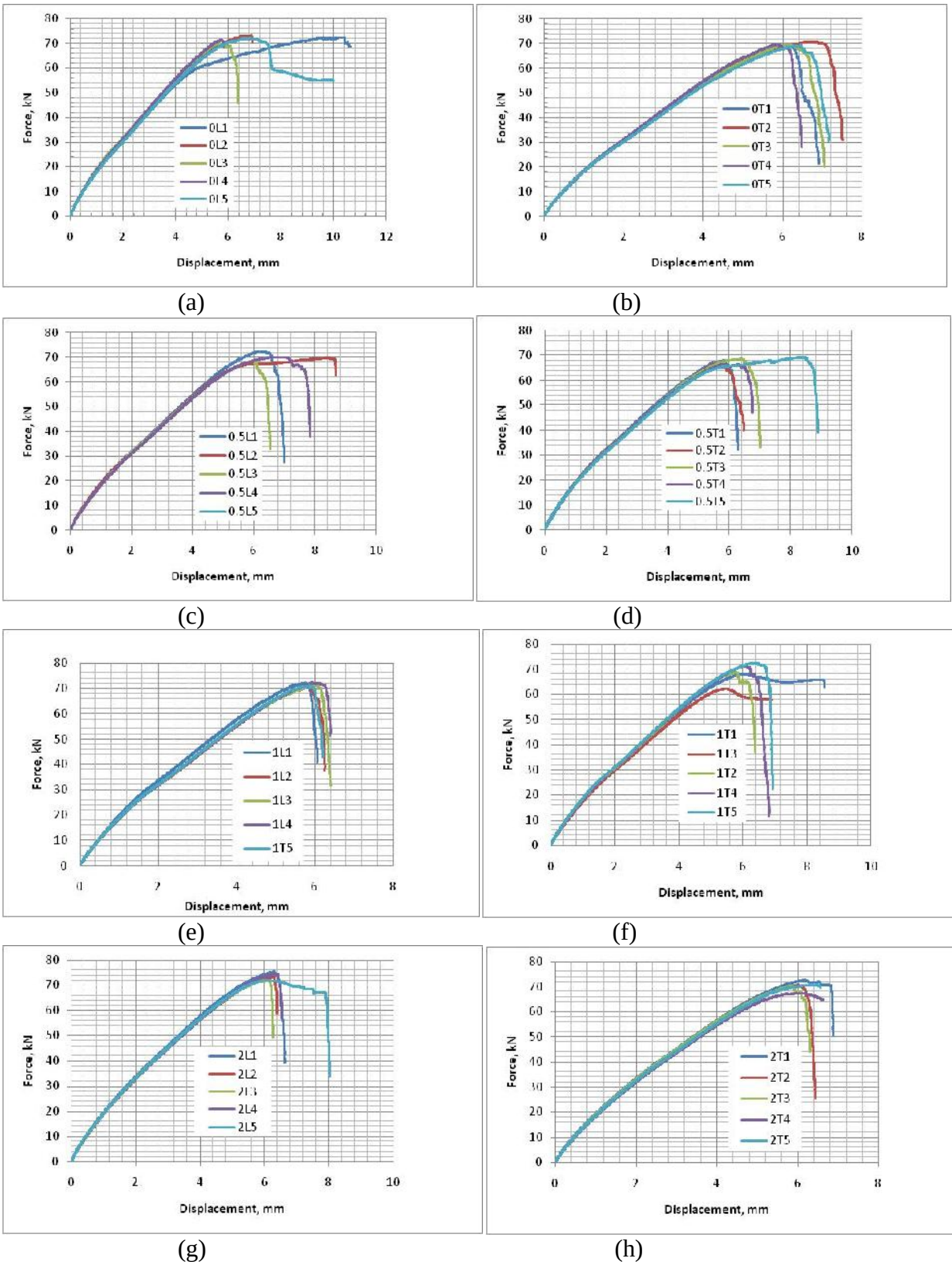

Figure 3.8 –Tensile force displacement diagrams for (a) 0 wt.% the warp , (b) 0 wt.% the weft, (c) 0.5 wt.% the warp, (d) 0.5 wt.% the weft, (e) 1 wt.% the warp, (f) 1 wt.% the weft, (g) 2 wt.% the warp, (h) 2 wt.% the weft directions

The discrepancy among the stiffness values was insignificant. Observation of the curves in Figure 3.8 (a-h) puts in evidence that the modification of the composite matrix by the addition of a small amount of nanoclay has an effect, even if not very relevant, on the material stiffness after the first knee and on the maximum load. Besides that, the stiffness alterations indicate the starting point of the material damage. From the experiment, the failure of the fiber was pulling out phenomenon unlike other E-glass and carbon fiber composites.

The load and crosshead displacement data acquired from the testing machine with the set-up described in section 3.2.2.1 were recorded and then the ultimate tensile strength and the stress at each data acquisition point were calculated using equations 3.2 and 3.3 respectively [30]. As shown in the graphs, the measured data were consistent in both stress data point and ultimate failure load, having

$$\sigma_u = \frac{F_u}{A_t} \tag{3.2}$$

$$\sigma_{t_i} = \frac{F_t}{A_t} \tag{3.3}$$

where

σ_{ut} – Ultimate tensile strength, [MPa]

σ_{ti} – Tensile stress at each data point, [MPa]

F_{ut} – Maximum tensile load at failure, [N]

F_{ti} – Tensile load at each data point, [N]

A_t – specimen gage area, [mm^2]

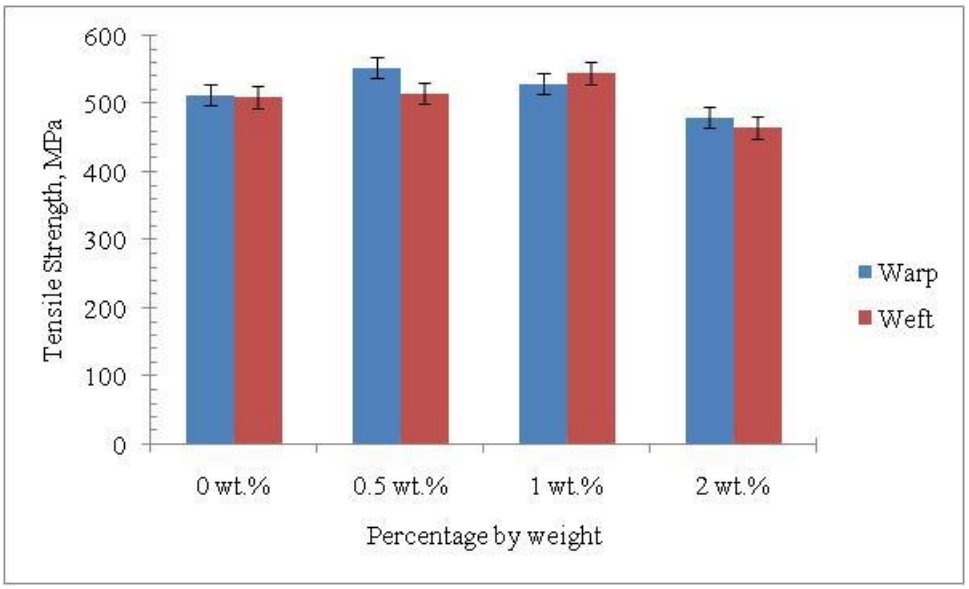

Figure 3.9 Tensile failure stress diagram both in the warp and weft directions for the four different sample types. Scatter values are also reported

Figure 3.9 shows a comparison of the failure strength for the pristine and the nanoclay modified glass fiber reinforced plastic in the warp and weft directions. The material strength reached its maximum which is about 7.59% higher with respect to the pristine characteristic value, at 0.5 wt.% of nanoclay while the failure strength declines on both directions of nanoclay loadings. On the other hand in the weft direction, the maximum strength is reached at 1 wt.%, once again with an increment of about 6.75% with respect to the pristine characteristic value. A possible explanation for these improved properties is that the 0.5 wt.% in warp direction and 1 wt.% in weft direction nanoclay concentration was sufficient for adequate reinforcement of the polymeric matrix, and as well, the nano-clays were well dispersed and exfoliated in the epoxy resin. Nanoclay addition at 2 wt.% caused a decrease in both the strength values for the nano-composite. At higher nanoclay loadings, large aggregates of clay could form within the matrix or there could be poor nanoclay exfoliation that causes a reduction in mechanical properties. The further analyses in this study will be limited to compare the 2 wt.%[24]. All the tensile strength results are reported and compared in Figure 3.9, where it is possible to note that the values for the warp directions are always higher than the values for the weft directions and they are well comparable.

Besides the strength of the material, the effect of nanoclay percentage weights on the tensile

modulus of elasticity and Poisson's ratio was examined. To evaluate Young's modulus and Poisson's ratio, a lab view routine was developed to acquire simultaneously the strains in both warp and weft directions and the applied load.

Having calculated the stress at each data point by using equation 3, these are plotted against the respective strain data. The initial linear part of the data curves see Figure 3.10 (a) & (b) for example, was used to calculate both Young's modulus and Poisson's ratio respectively. Such data analysis was done for each sample and then the results from each type of the five samples were averaged to get the material properties that are displayed in Figure 3.11. Specifically, the modulus elasticity of each sample type is presented.

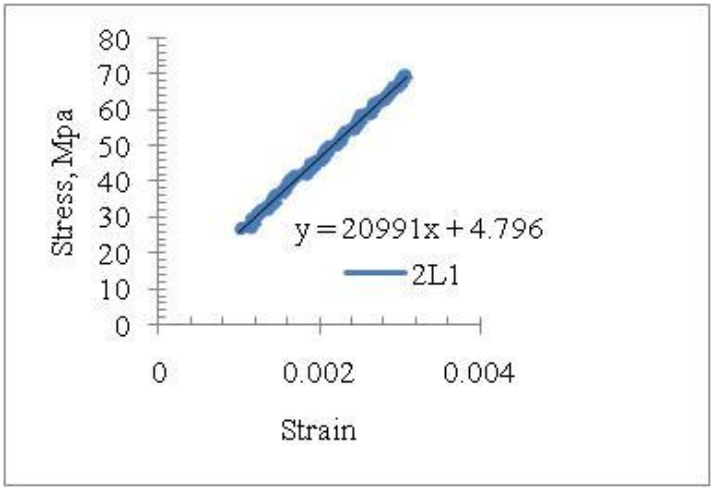

(a)

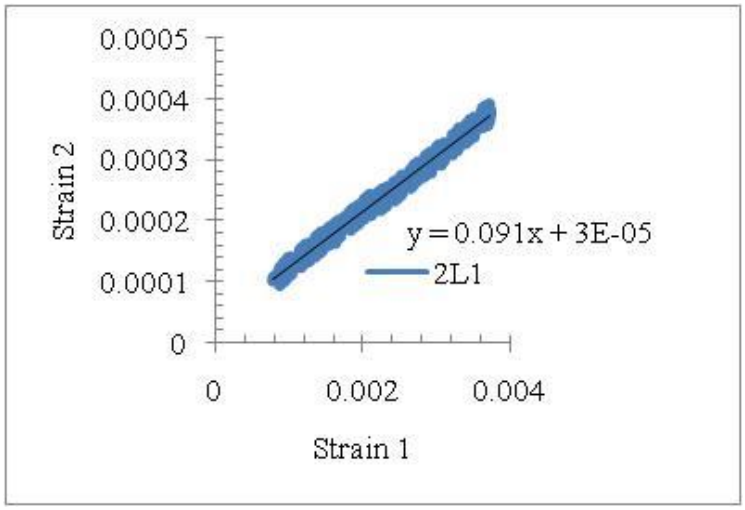

(b)

Figure 3.10–Linear interpolation of the (a) stress-strain and (b) Poisson ratio diagrams in case of the tensile loading of a 2wt.% single sample in the warp direction

Unlike strength property, the modulus of elasticity of all the modified nanoclay samples was affected negatively in the warp direction. However maximum modulus of elasticity was registered at 0.5 wt.% nanoclay concentration for samples in the weft direction.

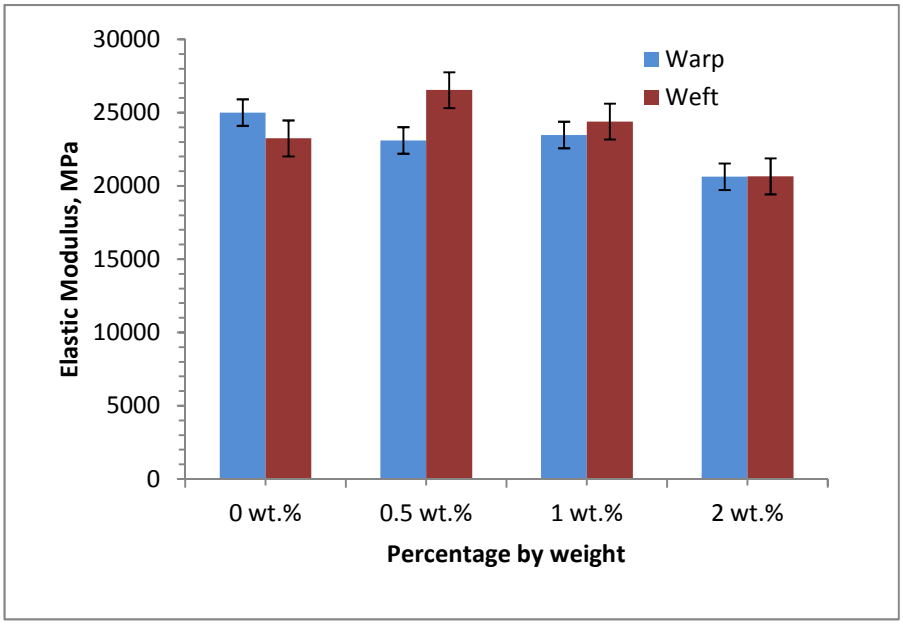

Figure 3.11–Tensile modulus of Elasticity in the warp and weft directions for the four different sample types. Scatter values are also reported

The quantification of tensile results for strength, Modulus of Elasticity and Poisson's ratio for all nanoclay loadings and directions are presented in Table 3.1. As it was mentioned for qualitative results, which were displayed using figures, the results in Table 3.1, were averaged, form each sample according to the specific ASTM standard. The last row of Table 3.1 is dedicated to the values of the Poisson ratio. It comes out that also the Poisson ratio is influenced by the wt. percentage of nanoclay.

Table 3.1 - Tensile results of mechanical material properties

Directions	Warp				Weft			
Loadings	Pristine	0.5 wt.%	1 wt.%	2 wt.%	Pristine	0.5 wt.%	1 wt.%	2 wt.%
Tensile Strength [MPa]	513.9	552.9	529.99	480.99	510.6	515.5	545.1	465.9
Tensile Modulus of Elasticity [GPa]	25.0	23.1	23.5	20.6	23.2	26.5	24.4	20.7
Tensile Poisson Ratio	0.121	0.124	0.089	0.082	0.120	0.153	0.089	0.072

3.3.2. Compression test

As mentioned under section 3.2.2.2, five samples of each material type in both longitudinal and transverse directions, instrumented with strain gauges, were subjected to monotonic compressive loading with a stroke rate of 1.3mm/min up to failure.

The load and crosshead displacement data acquired from the testing machine transducers were recorded as shown in Figure 3.12 and then the ultimate compression strength and the stress at each data point were calculated using equation 3.4 and 3.5 respectively [31]. Figure 3.12 collects 8 diagrams each with four to five curves. Representative Figure 3.12(e) shows the curves for the warp direction, while figure 3.12(f) the curves for the weft direction. Having the ultimate stress of each sample, the average of the five for each material type were calculated and displayed in Table 3.2 and Figure 3.14.

$$\sigma_u = \frac{F_u}{A_t} \tag{3.4}$$

$$\sigma_c = \frac{F_c}{A_t} \tag{3.5}$$

where

σ_{uc} – Ultimate compressive strength, [MPa]

σ_{ci} – Compressive stress at each data point, [MPa]

F_{uc} – Maximum compressive load at failure, [N]

F_{ci} – Compressive load at each data point, [N]

A_t – specimen gage area, [mm^2]

To analyze the effect of the nano-particles loading, a representative comparison of the mechanical properties is established in Figure 3.12(e) & (f) where the force-displacement curves in compression are shown for five and four samples of 1 wt.% nanoclay modified materials in both warp and weft directions. First, it can be noticed that the five curves in each of the two diagrams are nearly identical which means good repeatability of the test results. The curves show a more pronounced nonlinearity to the analogous tensile curves.

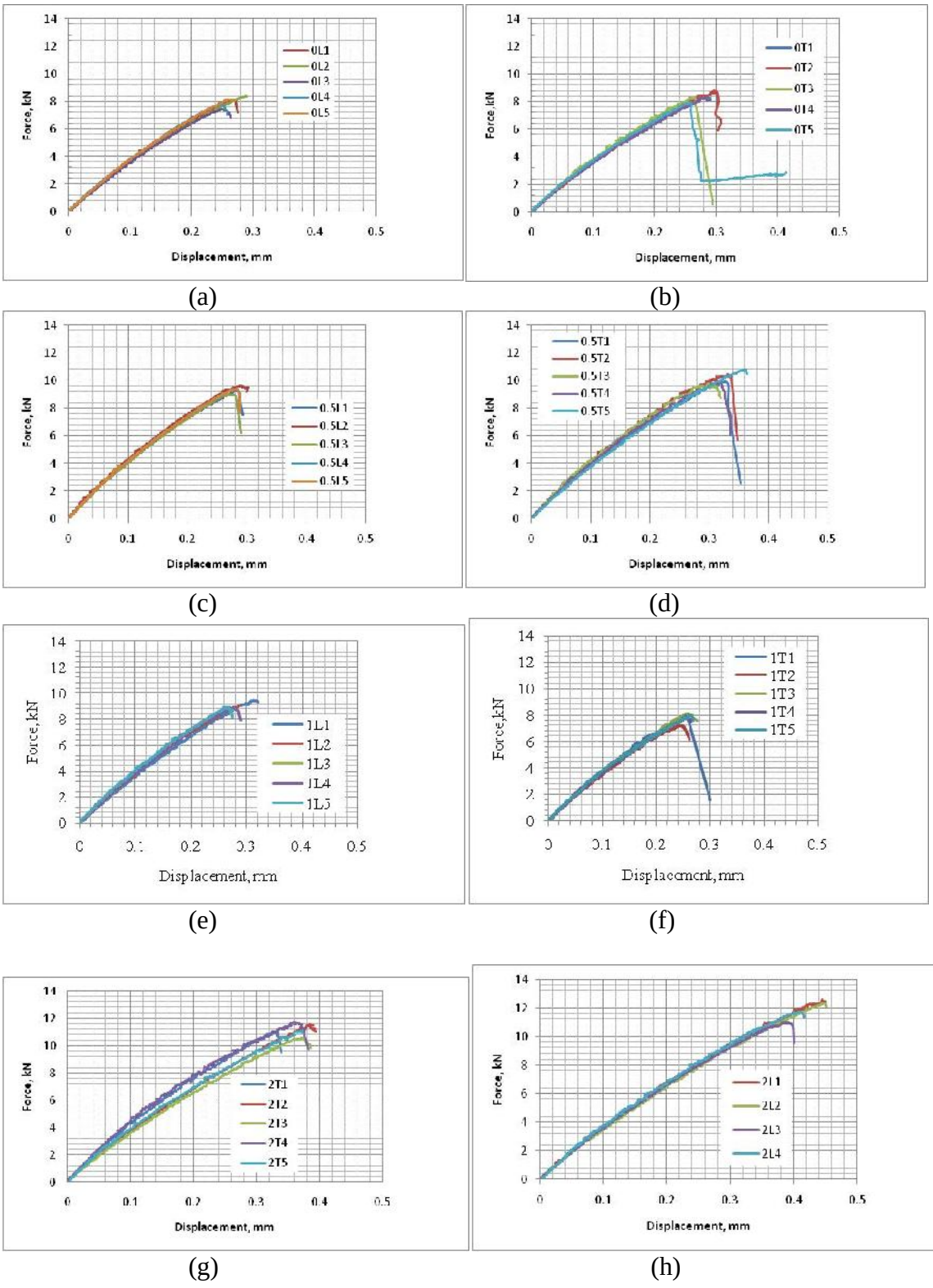

Figure 3.12– Compressive force-displacement diagram for (a) 0 wt.% the warp , (b) 0 wt.% the weft, (c) 0.5 wt.% the warp, (d) 0.5 wt.% the weft, (e) 1 wt.% the warp, (f) 1 wt.% the weft, (g) 2 wt.% the warp, (h) 2 wt.% the weft directions

Similar to the tensile test, the calculated stress at each data point by using equation 3.5 has been plotted against the respective strain data. The initial linear part of the data curves, e.g. Figures 3.13 (a)&(b), was used to calculate both the elasticity and Poisson's ratio respectively. Such data analysis was done for each sample and then the results from the five samples of each type were averaged to get the material properties that are displayed in Figure 3.15 and Table 3.2.

Table 3.2 Compressive results of mechanical material properties

Directions	Warp				Weft			
Loadings	Pristine	0.5 wt.%	1 wt.%	2 wt.%	Pristine	0.5 wt.%	1 wt.%	2 wt.%
Compressive Strength [MPa]	86.3	77.2	83.5	97.7	92.7	77.1	76.9	91.7
Compressive Modulus of Elasticity [GPa]	25.2	25.9	26.3	28.3	24.8	25.1	26.1	22.2
Compressive Poisson Ratio	0.058	0.086	0.060	0.078	0.101	0.091	0.065	0.079

In Figure 3.14 the average values of the compressive strength are reported as a function of the nano-particles loadings in the warp direction and in the weft direction, The compressive strength in the warp directions reaches its maximum at 2 wt.% of loading which was increased 13.17% however at 0.5 wt.% and 1 wt.% gradually decreased relative to the pristine. Like warp directions, the compressive strength in the weft direction gradually decreased for 0.5 wt.% and 1 wt.% with respect to the pristine, but the strength for 2 wt.% nanoclay concentration does not recover the pristine value: the gap is very small but calculated values are still a little bit lower. Figure 3.13 shows the influence of nanoclay contents and the direction of specimen testing positions about the compressive strength behavior. The last row of Table 3.2 is dedicated to the values of the Poisson ratio. The Poisson ratio is influenced by the weight percentage of nano-clay.

It is of interest to compare the data of Table 3.1 and Table 3.2. It can be noticed that the strength values in the case of compressive loads are of the order of 16% those obtained for the tensile loads. On the contrary, as expected, Young's moduli in tensile and compression have comparable values. Moreover, the Poisson's ratio values in case of tensile loads result generally to be larger than in the case of compression loads.

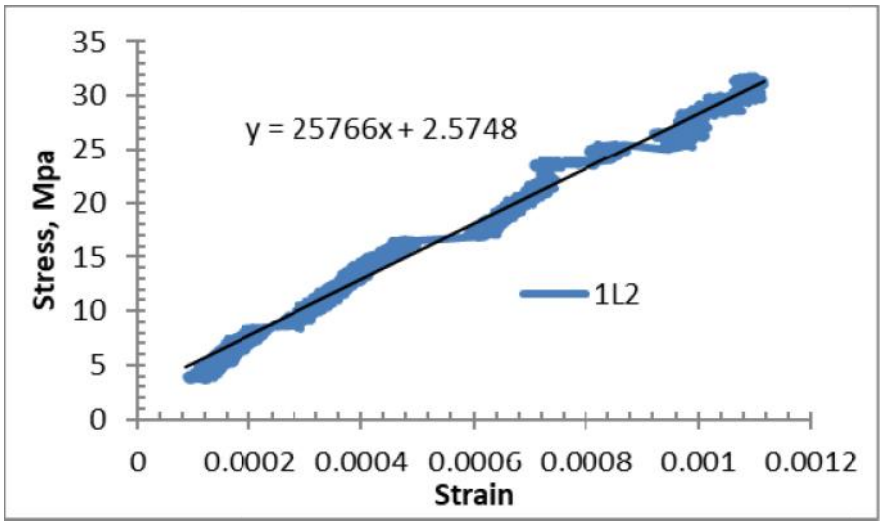

(a)

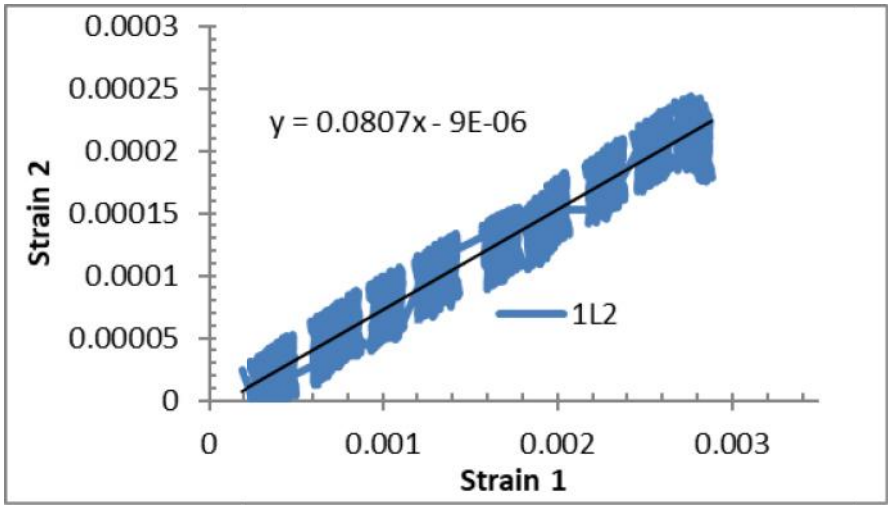

(b)

Figure 3.13–Linear interpolation of the (a) stress-strain and (b) Poisson ratio diagrams in case of the compressive loading of a 1 wt.% single sample in the warp direction

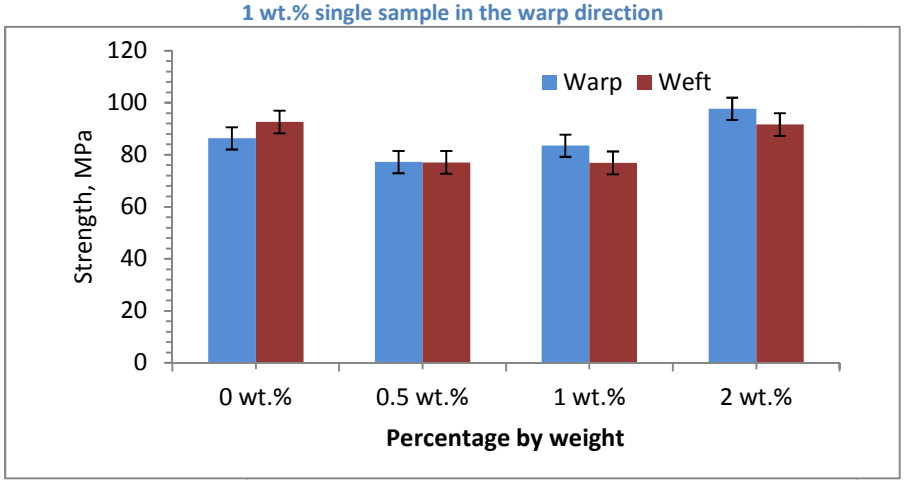

Figure 3.14 - Compressive failure strength diagram of nano modified composite materials in both warp and weft directions.

The compressive modulus of elasticity of the modified materials increased gradually in the weft direction while the maximum modified value was registered at 1 wt.% in the warp direction as shown in Figure 3.15. The 12.6% enhancement obtained at a loading of 2 wt.% of the weft. Though the amount of percentage increase was relatively small, a 5.14% increment was registered at 1 wt.% of the warp.

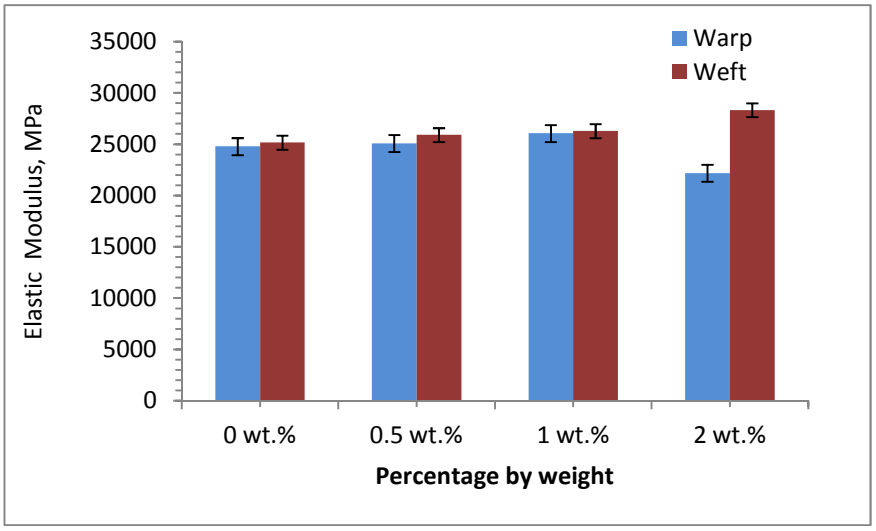

Figure 3.15 - Compressive Modulus of Elasticity diagram of nano modified composite materials in both warp and weft directions

Thus, unlike the tensile test results, the compressive modulus of elasticity exhibited a gradual increment as the filler content increased.

The practical failure conditions of the composite material are matrix crack followed by fiber rupture and debonding followed pull out. The SEM observations, as well as the experimental results, showed this latter condition (Figure 3.16 a-d and e). Damage/ failure is initiated either from poor adhesion between fiber and matrix [32] (see figure 3.17(c)), defects on the surface of the fiber, porosity or agglomeration (see Figure 3.17(c)). The main purpose of the nanoclay is to fill the porosity, increase the surface contact between polymer/fiber [7] and healing the defects of fiber. Pictures in Figures 3.16 (b) and 3.17 (b) showed fewer pullouts than Figures 3.16 (a) and 3.17(a) -the fibers are still bound by the nanocomposite. This implies that the nanoclay was distributed and dispersed properly and healed the porosity/defects. However, the aggregation Cloisite 20B reverses the improvement by reducing the interfacial strength of the fibers and matrix, which reduces the strength of the composite materials. It is worth of note that this result is obtained with the addition of a moderate amount of nanoclay.

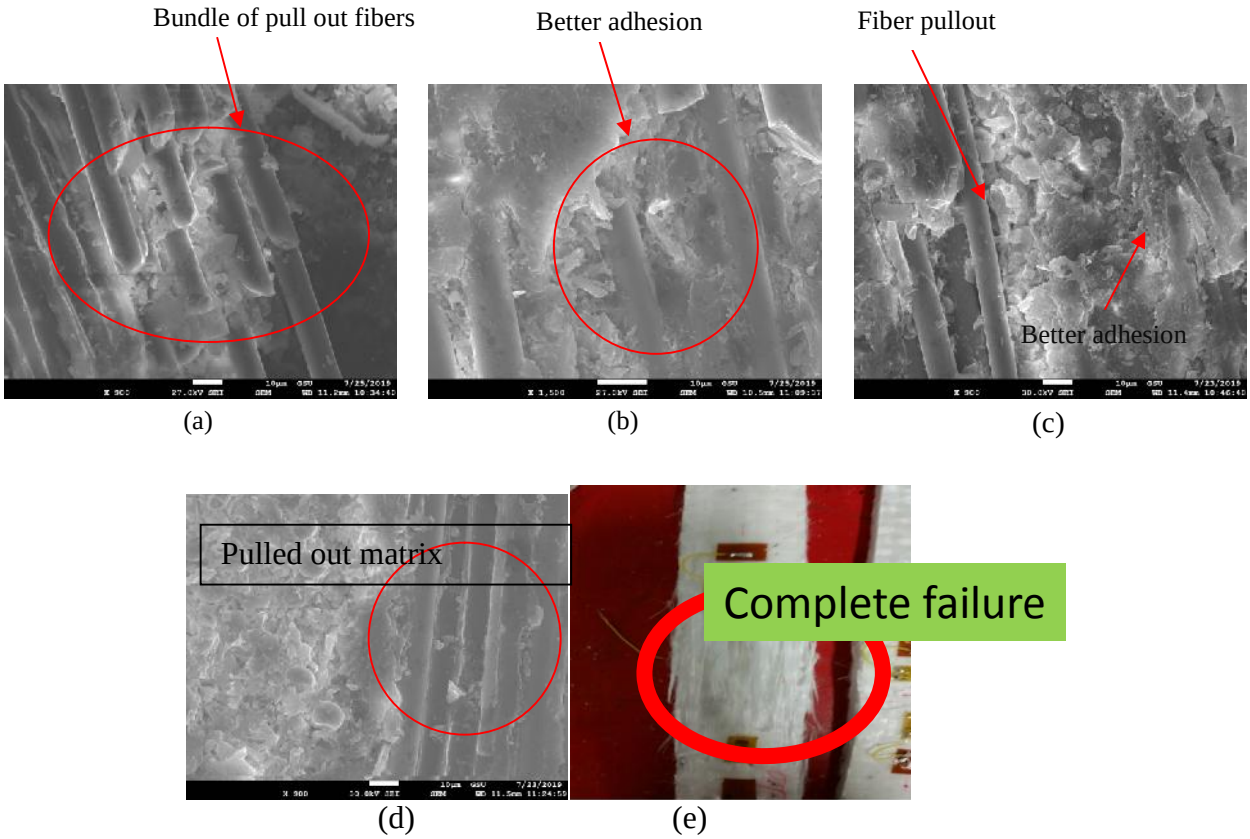

Figure 3.16. SEM images of (a) 0wt.%_ x900 interface and metrics (b) 0.5wt.%_ x1500 interface (c) 1wt%_ x900 interface and metrics (d) 2_ x900 cross section and interface metrics (e) experimental test result(pull out failure)

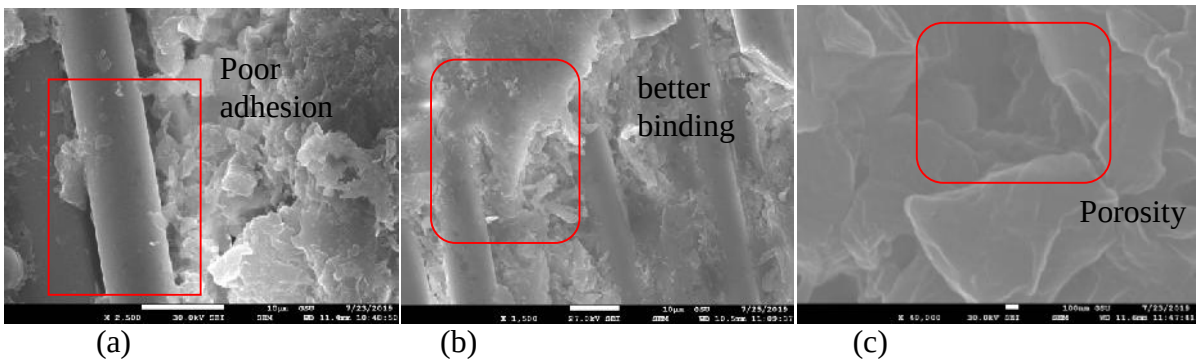

Figure 3.17 Adhesion, matrices porosity and agglomeration (a) 1wt.%_ x2500 interface, (b) 0.5wt%_ x1500 interface metrics, (c)2wt.%_ x40000 metrics

Figure 3.16(c & d) showed extra nanoclay or agglomeration, which resulted in damage initiation and caused lower strength values.

The results of strength in the warp direction (0.5 wt.%) [18, 33] and tensile modulus in weft direction (1 wt.%) agree with qualitative result/idea of literature[18]

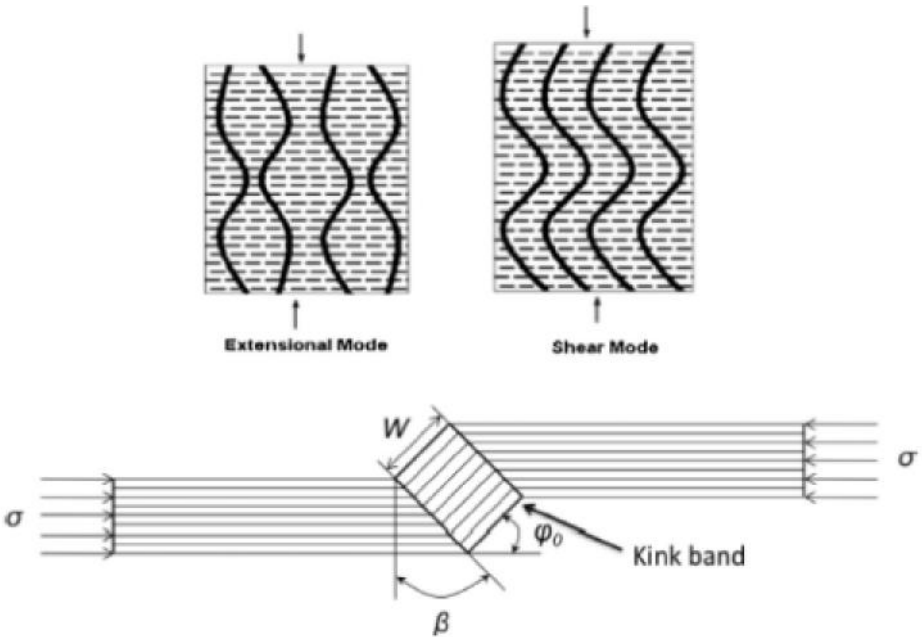

(a)

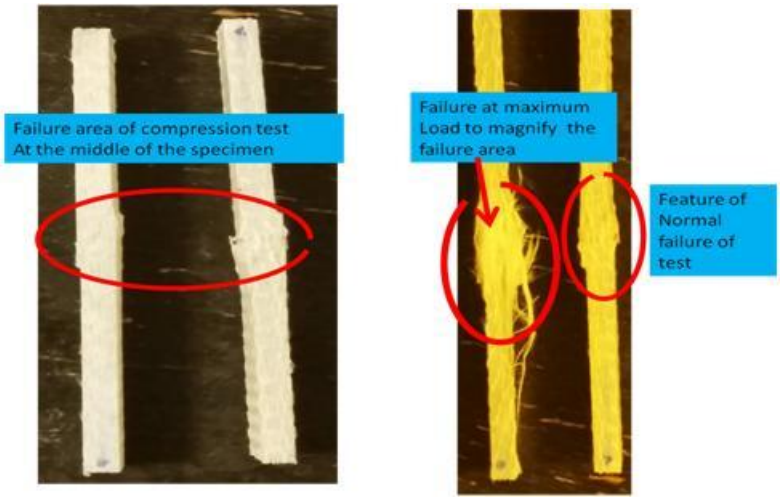

(b)

Figure 3.18 (a) failure modes in unidirectional composite under axial compression [37], (b) compressive test results that shows kinking failure

Unlike the tensile test failed by a pullout, failure due to compressive loads, that was shown in figure 3.18, indicated kink band failure [34, 35], which agreed with literature.

3.4. Conclusions

In this chapter, the effect of the presence of layered nanoclay, Cloisite 20B, on the tensile and compression properties of the glass-fiber-reinforced polymer (GFRP) was studied. The considered GFRP consisted of S-glass plain weave fabric and SC-15 toughened epoxy. Three

nanoclay weight percentages (wt.%) was considered namely: 0.5 wt.%, 1 wt.%, and 2 wt.% and their effects on the mechanical properties of the composite material were studied by comparison with the pristine GFRP. The observed results can be summarized as follow:

- Inclusion of 1 wt.% Cloisite 20B nanoclay into epoxy improved the tensile strength of GFRP by 6.75% in the weft direction. In the warp direction, the maximum tensile strength was found at 0.5 wt.% nanoclay by 7.59% enhancement. Thus, the tensile strength can be positively, even if slightly, affected by the addition of nanoclay.
- Similarly, the maximum compressive failure strength was observed at 2 wt.% in the warp direction with 13.17% enhancement compared with the pristine material. It is worth to mention that the presence of a high concentration of Nano fillers enhanced the compressive strength. This could be explained by the improvement of either interlaminar fracture toughness or shear strength, which are the dominant failure modes prior to buckling and kinking-band failures. The presence of nanoclay fillers could delay the crack formation or arrest the crack propagation during the compressive testing. As a result, the stability of the test specimen could be improved to resist the additional compressive load. Thus, the compressive strength can be positively affected by the addition of nanoclay.
- The maximum and minimum tensile modulus of elasticity was found in the weft direction at 0.5 wt.% with 14.16% of enhancement and at 2 wt.% with 17.5% of reduction compared with the pristine GFRP, respectively. In the warp direction the tensile elastic modulus decreased with the increment of wt.% of Nano fillers. Thus, the sensitivity of the elastic tensile strength can be positively affected by the addition of nanoclay only in the weft direction.
- The maximum compressive modulus of elasticity was found in the warp direction at 2 wt.% with 12.3% of enhancement while in the weft direction at 1 wt.% with 5.2% of increment compared with the pristine GFRP. Thus, the sensitivity of the elastic compressive strength can be positively affected by the addition of nanoclay.
- Finally, the effect of the Cloisite 20B nanoclay on the Poisson ratio was studied. Tensile tests, both in the warp and weft directions, gave a small increment in the case of 0.5 wt.% of Nano filler and then a larger decrement with 1 and 2 wt.%, with respect to the pristine composite. The obtained compressive values for the Poisson ratio are different from the

tensile ones. They are affected by the wt.% of Nano fillers in both the warp and weft directions. In particular, in the warp direction, a maximum is reached at 0.5 wt.%; in weft direction, the maximum value is for the pristine composite with a relevant decrement as a consequence of the Nano filler addition.

Overall, it is possible to conclude that the inclusion of a small amount of Cloisite 20B nanoclay has beneficial, even if limited, effects on the mechanical properties of the considered S-glass fabric/epoxy composite. Slightly smaller/comparable improvement effect obtained if compared with another Cloisites nanoclay family. However, Cloisite 20B can be preferred because of its non-toxicity and flame-retardant behavior.

The investigation of interlaminar fracture, intralaminar fracture and impact behavior of Cloisite 20B modified composite materials are some of the further research directions that would complete the performed analysis by providing a comprehensive frame of advantages and limitations of the proposed materials for vehicle and other engineering applications.

3.5. References of chapter three

1. Wimmer G, Schuecker C, Pettermann HE, Numerical simulation of delamination in laminated composite components – A combination of a strength criterion and fracture mechanics, Composites: Part B 40 (2009) 158–165
2. Zeng Y, Liu HY, Mai YW, Du XS, Improving interlaminar fracture toughness of carbon fibre/epoxy laminates by incorporation of nano-particles, Composites: Part B 43 (2012) 90–94
3. Short GJ, Guild FJ, Pavier MJ, The effect of delamination geometry on the compressive failure of composite laminates, Composites Science and Technology 61(2001) 2075–2086
4. Azeez AA , Rhee KY , Park SJ,Hui D, Epoxy clay nanocomposites – processing, properties and applications: A review, Composites: Part B 45 (2013) 308–320
5. Bazhenov SL, Interlaminar and intralaminar fracture modes in 0/90 cross play glass/epoxy laminate, Composites 26(1995) 125-133
6. Domun N, Hadavinia H, Zhang T, Sainsbury T, Liaghat GH, Vahid S, Improving the fracture toughness and the strength of epoxy using nanomaterials – a review of the current status, Royal society of chemistry, open access online journal, 2015
7. Valentini L, Bon SB, Lopez-Manchado MA, Verdejo R, Pappalardo L, Bolognini A, Alvino A, Borsini S, Berardo A, Pugno NM, Synergistic effect of graphenenanoplatelets and carbon black in multifunctional EPDM nanocomposites, Composites Science and Technology 128 (2016) 123-130
8. Nguyen QT, Baird DG, An improved technique for exfoliating and dispersing nanoclay particles into polymer matrices using supercritical carbon dioxide, Polymer 48 (2007) 6923-6933
9. Dorigato A, Morandi S, Pegoretti A, Effect of nanoclay addition on the fiber/matrix adhesion in epoxy/glass composites, Journal of Composite Materials, 46(2012) 1439–1451
10. Salviato M, Zappalorto M, Quaresimin M, Nanoparticle debonding strength: A comprehensive study on interfacial effects, International Journal of Solids and Structures 50 (2013) 3225–3232
11. El-Sheikhy R, Al-Shamrani M, Interfacial bond assessment of clay-polyolefin nanocomposites CPNC on view of mechanical and fracture properties, Advanced Powder Technology 28 (2017) 983–992

12. Wolf C, Angellier-Coussy H, Gontard N, Doghieri F, Guillard V, How the shape of fillers affects the barrier properties of polymer/non-porous particles nanocomposites: A review, Journal of Membrane Science 556 (2018) 393–418
13. Majeed K, Jawaid M, Hassan A, Bakar AA, Khalil HPSA, Salema AA, Inuwa I, Potential materials for food packaging from nanoclay/natural fibres filled hybrid composites, Materials and Design 46 (2013) 391–410
14. Wetzel B, Rosso P, Haupert F, Friedrich K, Epoxy nanocomposites – fracture and toughening mechanisms, Engineering Fracture Mechanics 73 (2006) 2375–2398
15. Koricho EG, Khomenko A, Haq M, Drzal LT, Belingardi G, Martorana B, Effect of hybrid (micro- and nano-) fillers on impact response of GFRP composite, Composite Structures 134 (2015) 789–798
16. Hamitouche L, Tarfaoui M, Vautrin A, An interface debonding law subject to viscous regularization for avoiding instability: Application to the delamination problems, Engineering Fracture Mechanics 75 (2008) 3084–3100
17. Assaedi H, Shaikh FUA , Low IM, Characterizations of flax fabric reinforced nanoclay-geopolymer composites, Composites Part B 95 (2016) 412-422
18. Binu PP, George KE, Vinodkumar MN, Effect of nanoclay, Cloisite15A on the mechanical properties and thermal behavior of glass fiber reinforced polyester, Procedia Technology 25 (2016) 846 – 853
19. John B, Nair CPR, Ninan KN, Effect of nanoclay on the mechanical, dynamic mechanical and thermal properties of cyanate ester syntactic foams, Materials Science and Engineering A 527 (2010) 5435–5443
20. Eesaee M, Shojaei A, Effect of nanoclays on the mechanical properties and durability of novolac phenolic resin/woven glass fiber composite at various chemical environments, Composites: Part A 63 (2014) 149–158
21. Khosravi HH, Eslami-Farsani R, Enhanced mechanical properties of unidirectional basalt fiber/epoxy composites using silane-modified Naþ-montmorillonite nanoclay, Polymer Testing 55 (2016) 135-142
22. Maharsia RR, Jerro HD, Enhancing tensile strength and toughness in syntactic foams through nanoclay reinforcement, Materials Science and Engineering A 454–455 (2007) 416–422

23. Moustafa H, Darwish NA, Effect of different types and loadings of modified nanoclay on mechanical properties and adhesion strength of EPDM-g-MAH/nylon66 systems, International Journal of Adhesion& Adhesives 61(2015)15–22
24. Ho MW, Lam CK, Lau KT, Ng DHL, Hui D, Mechanical properties of epoxy-based composites using nanoclays, Composite Structures 75 (2006) 415–421
25. Sharmila TKB, Ayswarya EP, Abraham BT, Begum PMS, Thachil ET, Fabrication of partially exfoliated and disordered intercalated cloisite epoxy nanocomposites via in situ polymerization: Mechanical, dynamic mechanical, thermal and barrier properties, Applied Clay Science 102 (2014) 220–230
26. Shield Strand Woven Fabrics, 2010, Owens corning composite materials, LLC/www.owenscorning.com
27. Chen Q, Zhao Y, Zhou Z, Rahman A, Wub XF, Wuc W, Xu T, Fong H, Fabrication and mechanical properties of hybrid multi-scale epoxy composites reinforced with conventional carbon fiber fabrics surface-attached with electrospun carbon nanofiber mats, Composites: Part B 44 (2013) 1–7
28. Chen H, Wang J, Ni A, Ding A, Sun Z, Han X, Effect of novel intumescent flame retardant on mechanical and flame retardant properties of continuous glass fibre reinforced polypropylene composites, Composite Structures 203 (2018) 894–902
29. Nanocomposite Additive for Halogen-free Flame Retardants, Cloisite Technical Information B-RI 10, 2013, BYK Instruments /www.byk.com/additives
30. ASTM D3039/D3039M–08, Standard test method for tensile properties of polymer matrix composite materials, Annual Book of ASTM Standards; Philadelphia (USA): American Society for Testing and Materials; 2008
31. ASTM D6641/D6641M–01, Standard test method for determining the compressive properties of polymer matrix composite laminates using a combined loading compression (CLC) test fixture, Annual Book of ASTM Standards; Philadelphia (USA): American Society for Testing and Materials; 2001
32. Dorigato A, Morandi S, Pegoretti A, Effect of nanoclay addition on the fiber/matrix adhesion in epoxy/glass composites, Journal of Composite Materials 46(2012) 1439–1451
33. Sancaktar E, Kuznicki J, Nanocomposite adhesives: Mechanical behavior with nanoclay International Journal of Adhesion & Adhesives 31 (2011) 286–300

34. Pimenta S, Gutkin R, Pinho ST, Robinson P, A micromechanical model for kink-band formation: Part I — Experimental study and numerical modeling, Composites Science and Technology 69 (2009) 948–955
35. Talreja R, Assessment of the fundamentals of failure theories for composite materials, Composites Science and Technology 105 (2014) 190–201

Chapter 4: Interlaminar Fracture Toughness

Fiber-reinforced plastic materials are able to be customized looking for an accordance between the application and behavior of materials. In this chapter, the effect of meticulous nanoclay, Cloisite 20B, inclusion on the interlaminar fracture toughness glass fiber reinforced plastic (GFRP) composite was experimentally investigated. The mode-I tests were conducted based on a double cantilever beam (DCB) tests using the American society of testing materials standard (ASTM D5528). The chapter discusses the background of fracture behavior of composite materials, experimental procedure, energy release rate calculation, resistance curve and clarification about the results. Finally, the research results showed that the inclusion of nanoclays improved the interlaminar fracture toughness of the GFRP composite in the range of 12.65% and 54.07% as compared with the pristine one, with a progressive increment of the nanoclay weight content (from 0.5 to 2%). A better understanding of the Cloisite filler contribution to improvement of the delamination resistance can lead to design of better melt flow rate and good elongation at break for structures which are made up of composite materials.

4.1. Introduction of interlaminar fracture toughness

For many applications, it is sufficient to determine the maximum static or dynamic stresses and deflection that the material can withstand; and then design the structure to ensure that the operational stresses remain below acceptable limits. However, most critical applications require some kind of defect tolerance analysis. In these cases, the material or structure is considered to contain flaws and it must be decided whether to replace the part or leave it in service under a more tolerable loading for a certain period. This kind of decision is usually made using the methods of fracture mechanics approach.

Unlike conventional materials, the failure/damage characterization of composite materials using a fracture mechanics approach is sophisticated. Nevertheless, the mode of fracture is the same, composite materials crack characterization depends on the plane of the crack growth whether it is parallel to the fiber direction or perpendicular to the fiber plane of layered composite material.

As mentioned in chapter 2, composite structures for automotive, aerospace, wind turbine, spacecraft, sports goods, and marine applications exposed to heavyweight that causes energy

consumption. Moreover, stiffness, strength, fatigue, corrosion, thermal expansions, creeps, and temperature variation resistances are crucial problems [1-5].

Fire engines, military vehicles, fighting planes, nuclear reactor vessels, chemical vessels are susceptible to fire, explosion, blast fragments, and low to high-speed impact while passenger vehicles, airplanes are exposed to crash which causes a fire. Besides in automotive and marine structures, ballistic impact loading from events such as bird strikes, hailstones, shrapnel, runway debris, and bullets may occur[6, 7]. Once a crash or explosion occurs, the structures have to be good enough to retard the fire flame and fast degradation.

However, these heterogeneous materials have enormous advantages; structures made of composite materials need special consideration during design in comparison with conventional materials. Moreover, as for all new ideas, the failures of materials have been increasing through time as the technological sophistication has advanced. So that the failure of composite materials cannot only be approximated using strength approach but the fracture approaches require specific analysis and considerations. Ordinary laminated composite materials are the most common and in which the fibers reinforce in-plane directions (ply plane) [8]. There is no reinforcement in the out of plane direction (perpendicular to the axis of the fiber), which leads to interlaminar crack growth or delamination [1, 2]. Thus, the ability of layered composite materials to resist delamination is very weak [9]. The delamination due to weak strength in the out of plane direction may occur according to one of the three base modes: mode I (opening mode), mode II (sliding shear mode) and/or mode III (tearing shear mode) or it can appear as combinations of two modes, often mode I and II[3, 10]. The causes of delamination may vary with its applications and the load point of application. Blasting load [11], equipments' interaction during maintenance [6], impact load [12], buckling [13], drop of plies [14] are some of the causes of separation of plies. In order to minimize the susceptibility of composite materials for delamination, the improvement of the interfacial strength or the strength in the out of plane direction of the laminate can be of advantage.

Researchers had been discussing the development of various techniques to resolve the failures due to delamination. Among the improvement techniques stitching [15, 16], z pinning [17, 18], weaving, braiding, and knitting were designed to introduce through-the-thickness reinforcement into the laminates to improve the delamination toughness [19, 20]. However, stitching and z pining may reduce the in-plane strength [8, 20, 21]. The other method to improve interlaminar

strength is adding nanoparticles. This method is mainly focusing on the toughening of the matrix because fracture toughness of composite materials increases with an increase in toughness of the matrix [9, 22].

Nanocomposites have been widely studied by the addition of nanoparticles to improve the strength, modulus of elasticity and fracture toughness of composite materials. Among the many nanoparticles, carbon nanotube, nanosilca, and nanoclay are widely used. Thus for mode I fracture toughness laminates with nanoparticles modified epoxy number of researchers showed their enhancement levels. Zeng et al. [8] reported that 10 wt.% rubber particle improved the fracture toughness 2.5 times while silica increases 20 to 30%. Kelkar et al. [23] found 51% improvement in mode I fracture toughness using alumina nanoparticles. According to Adachi et al. [24], spherical silica particle-filled epoxy increased fracture toughness drastically. Kim et al.[25] did enhancement of fracture toughness using carbon nanotubes on material of carbon/epoxy composite and they improved it considerably.

Specifically, nanoclay has been studied on the effects of fracture behaviors of laminated fiber reinforced composite materials. Improvement of fracture toughness should not highly affect the in-plane mechanical properties of the laminate. Therefore, the better weight by percentages has to be considered for specific enhancement. Binu et al.[26] worked on appropriate nanoparticles/nanoclay loadings. In a similar way, epoxy clay nanocomposites showed remarkable improvement in tensile, flexural and fracture toughness properties as Azeez et al. [27] reported. Lim et al. [28] studied nylon 6-based nanocomposites and the fracture toughness of this nylon6/organoclay nanocomposite was significantly improved. Vila et al. [29] investigated the nanoclay modified epoxy resin of a plain-weave woven fiberglass composite related to fracture and porosity behaviors. The research described the direct correlation of void reduction and fracture toughness. Similarly, Khan et al. [30] observed fracture toughness improvement due to the addition of nanoclay.

All the previously mentioned results were found from the various nanoclay types. Studies related to the enhancement that can be obtained from the addition of nanoclay types Cloisites 20B that have a better intercalation behavior and low toxicity combined with fire-retardant properties, in composite materials such as S-glass and epoxy are limited. Epoxies are thermosetting polymers having unique characteristics such as high adhesive strength, neutrality, high strength, and hardness and excellent chemical and heat resistance [31]. Specifically epoxy SC-15 matrix, that

has low shrinkage, excellent adhesion to carbonaceous materials, and high reactivity with a variety of chemical curing agents [32], has been adopted. Cloisite 20 enhances SC-15 to have a better melt flow rate and elongation at break [33]. The other reinforcing constituent, Shield Strand S-glass reinforcing fiber, has an economical advantage, which possibly saves significant weight when replacing aluminum and steel respectively [34]. This property could be one of the alternatives in fire and ballistic applications. On the other hand, the semi-new material that focuses on the fracture toughness characterization has to be approachable. So the effect of the use of appropriate loading of nanoclay on the interlaminar fracture toughness of plain-woven S-glass fiber reinforced plastic (GFRP) has been investigated. Nanoclay, Cloisite 20B (C20B) with three different weight percentages (wt.%) were added and performance compared with the pristine of the composite material. The percentages by weight added to the material were 0.5 wt.%, 1 wt.%, and 2 wt.%.

4.2. Materials

4.2.1. Fabrication of composite laminates

The reinforcement was S-glass plain weave fabric with an areal weight of 818g/m^2, which was supplied by Owens Corning Shield Strand S. The resin used was two-part toughened epoxy, namely SC-15 obtained from Applied Poleramic. The used nano-additives were Cloisite® 20B (Southern Clay Products, Inc. TX). Initially, part A of SC-15 epoxy was mixed with the desired concentration of fillers and the resulting compound was sonicated (Vibra-Cell™ sonicator) for around 30 minutes until the total applied energy was 30kJ. Intermittent sonicating energy (10s energy: 5s pause) was applied to control the rise in temperature of the compound. Once 30kJ was applied, the resulting mixture was cooled at room temperature for 30 minutes, followed by mixing of part B of SC-15 epoxy (see Figure 4.1 (a))

(a) (b)

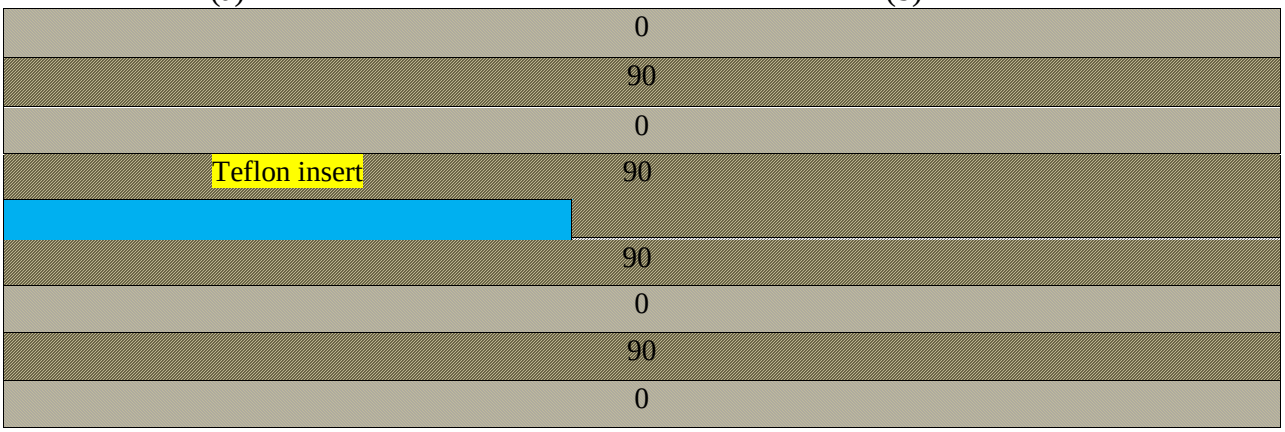

(c)

Figure 4.1 manufacturing process (a) nanocomposite, (b) hand layup coating, (c) layup and location of the Teflon sheet

The solution was mixed thoroughly, degassed before applied on each ply using hand layup process (see figure 4.1 (b)). During the laminate hand layup, a 12.5 micrometer Teflon sheet was incorporated in the middle of the laminate along with thickness (between the fourth and the fifth plies, as shown in figure 4.1 c) at one side of the laminate to introduce a crack for Mode I tests. The resin-infused panel was cured in a convection oven at 60^{o}C for 2 h and post cured at 94^{o}C for 4 h. The manufactured composite plate consisted of eight plain fabric plies (total thickness-5.1 mm) with asymmetric stacking sequence of [0/90/0/90]s and a resin mass content equal to 36.5%(Figure 4.1(c)).

Four types of composite materials were manufactured: Pristine, 0.5 wt.% 20B Cloisite, 1 wt.% 20B Cloisite, and 2 wt.% 20B Cloisite to deal with the effects of Nano filler over the out of plane failure using interlaminar fracture toughness characterization.

4.2.2. Experimental design and test

The specimens for fracture toughness tests according to the DCB standard require placement of a predetermined crack that, in case of a composite laminate, is obtained by inserting a thin layer of non-adhering material, Teflon, at the mid-plane of the laminate. Mode I fracture toughness was determined experimentally by conducting a double cantilever beam (DCB). The DCB test, used to determine mode I fracture toughness, is the most widely used interlaminar fracture toughness test. As mentioned under the section of fabrication, the DCB specimen consists of a laminate with a predetermined crack created at the mid-plane of the laminate during fabrication (see Figure 4.2(a)). During the DCB test, the two arms are usually loaded in bending either using loading hinges or loading blocks at the arm tips. The performed experimental test used loading hinge type as shown in Figure 4.2(b).

The Mode I DCB delamination tests were performed with a 100kN capacity servo-hydraulic testing machine INSTRON-8801 in accordance with ASTM standard D5528 [35]. The specimen size, as shown in Figure 4.2(b), was 150mm length, 5mm height and 25mm width with initial crack length (a_o) = 50mm. The experiment was displacement controlled and the crack tip opening displacement rate was 3mm/min. Three to four samples were tested for each nanoclay wt.% including the pristine. The load-displacement curves were recorded and crack growth was monitored with a digital camera.

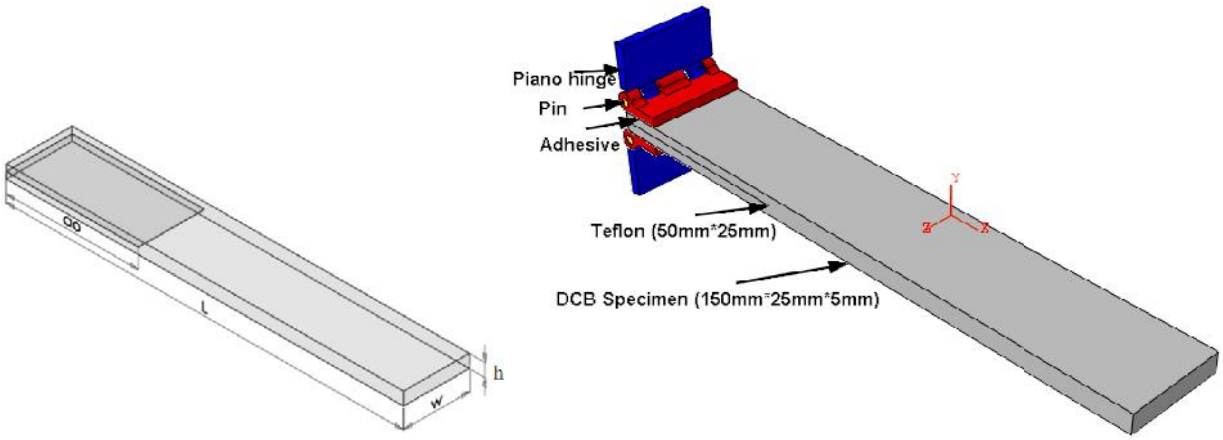

(a) (b)

Figure 4.2. DCB specimen (a) Teflon inserts and dimensions and crack view (b) with fixtures and descriptions

4.2.3. Initiation and reduction methods

4.2.3.1. Initiation methods

According to ASTM D5528 standard [35], the three initiation procedures can be used to calculate the energy release rate.

a. Deviation from linearity (NL) – where the non-linear point in the load-deflection curve is assumed to be where onset occurs,
b. Visual observation (VIS) – where the critical point is determined through direct observation using optics or by recording test images digitally, and
c. 5% offset/maximum load (5%/max) – which uses the larger of the maximum load or the intersection of the load-deflection curve with a secant 5% decrease in initial stiffness.

The non-linear method is typically considered to be the most conservative; however, the criteria used to determine the nonlinear point depends on the material type and it can also alter the results significantly[35, 36].

4.2.3.2. Reduction methods

The Interlaminar Fracture Toughness, which is expressed in the energy release rate (GIC) calculations, was undertaken according to ASTM standard D5528 and using the three reduction methods. These consisted of a modified beam theory (MBT), a compliance calibration method (CC) and a modified compliance calibration method (MCC) using equations 1, 2 and 3 respectively [35].

Modified Beam Theory (MBT) Method: The beam theory expression for the strain energy release rate of a perfectly built-in (that is, clamped at the delamination front) double cantilever beam is as follows:

$$G_{I} = \frac{3P\delta}{2b} \qquad (4.1)$$

Where:

P = load,

δ = load point displacement,

b = specimen width, and

a = delamination length.

In practice, equation (4.1) overestimates the value, because it does not consider the effects of rotations at the crack front. Therefore, the expression should be corrected by slightly increasing the crack length up to a+|Δ|, where 'a' and |Δ| are the measured crack length and the modification of measured crack length (a). |Δ| was be generated from the results of the experiment respectively by generating a least-squares plot of the cube root of compliance, $C^{1/3}$, as a function of delamination length (Figure 4.3(a)). The compliance, C, is the ratio of the load point displacement to the applied load, δ/P. The values used to generate this plot should be the load and displacements corresponding to the visually observed delamination onset on the edge and all the propagation values. The Mode I interlaminar fracture toughness can be calculated as

$$G_{I} = \frac{3P\delta}{2b(a+|\Delta|)} \qquad (4.2)$$

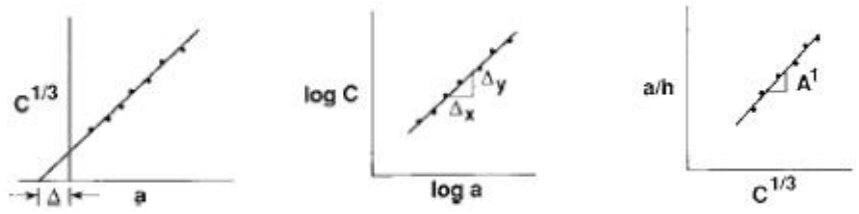

(a) (b) (c)

Figure 4.3 (a)least square plots for MBT, (b) slope for CC and (c) slope for MCC

Compliance Calibration (CC) Method: a least-squares plot of log (δ_i/P_i) versus log (a_i) is generated using the visually observed delamination onset values and all the propagation values. A straight line is drawn through the data that results in the best least-squares fit. The exponent n is then calculated from the slope of this line according to n = Δy/Δx, where Δy and Δx are defined in Figure 4.3(b), in the bi-logarithmic scale diagram. The Mode I interlaminar fracture toughness can be calculated as follows:

$$G_{I} = \frac{n\ \delta}{2b} \qquad (4.3)$$

Modified Compliance Calibration (MCC) Method: a least-squares plot of the delamination length normalized by specimen thickness, a/h, as a function of the cube root of compliance, $C^{1/3}$, is generate as shown in Figure 4.3(c), using the visually observed delamination onset values and all the propagation values. The slope of this line is A_1. The Mode I interlaminar fracture toughness can be calculated as follows:

$$G_{I} = \frac{3P^2\delta C^{2/3}}{2A_1 b} \quad (4.4)$$

The large displacement effects are corrected by the parameter F, evaluated using equation 4.5 [35], in the calculation of G_I, Where t is the distance between the mid plane of the specimen and the center of the piano hinge pin. The parameter, F, accounts the shortenings of the moment arms.

$$F = 1 - \left(\frac{3}{1}\right)\left(\frac{\delta}{a}\right)^2 - \left(\frac{3}{1}\right)\left(\frac{\delta}{a^2}\right) \quad (4.5)$$

4.3. Result and discussion

4.3.1. Load opening displacement response

The interlaminar force-displacement response of the pristine material test and the modified material are shown in Figure 4.4(a-d). Delaminations usually grow in two ways. The first one is stable and slow extension while the second one has a run arrest growth. The former property laid for unidirectional composite materials as the latter is the behavior of fabric arrangements. For this reason, all the load-displacement curves show picks and valleys because of the fiber bridge at fabric interaction of two middle plies and epoxy pockets respectively. The run arrest has smoother trend when it is compared with brittle material and it shows medium crest and valley unlike unidirectional materials, which have continuous and smooth curves. This means that at the pocket, the epoxy strength is improved by the nanoclay addition.

Figure 4.4(e) presents the superposition of representative stiffness curves of the out of plane stress for the four different tested materials. The results show stiffness increment as the concentration of Cloisite increases. Particularly the increment of the stiffness is particularly evident between pristine and 2 wt.% of Cloisite, however very small increment are obtained moving from 0.5 wt.% to 1 wt.%. The concentration increment results in stiffness increment, which means that the nanoclay inclusions were distributed appropriately.

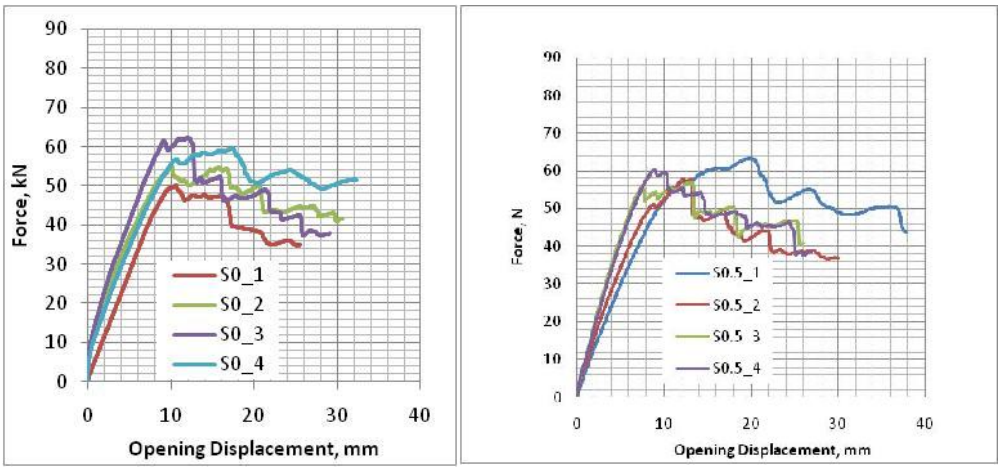

(a) (b)

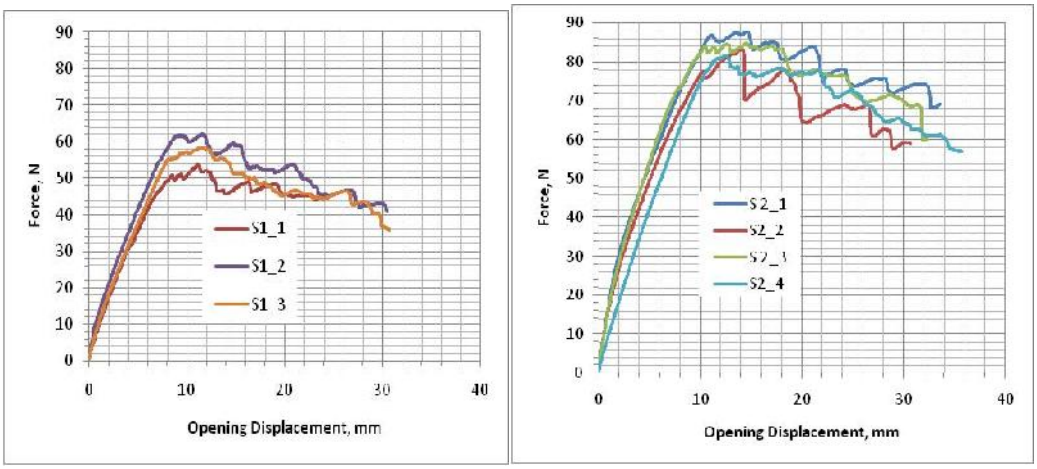

(c) (d)

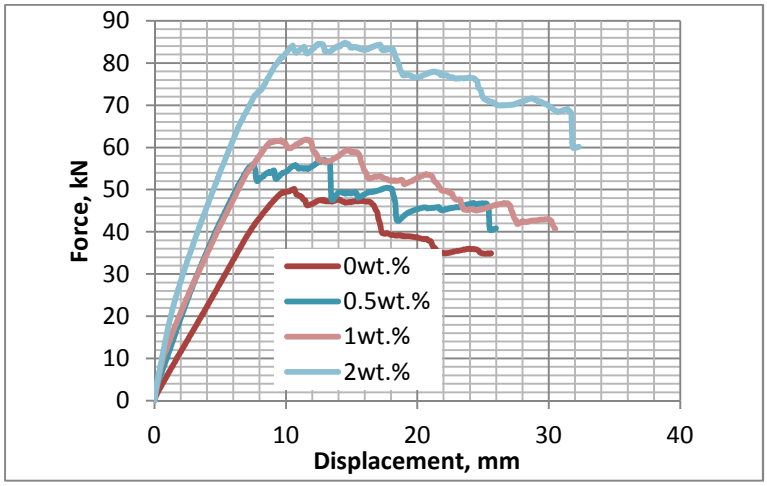

Figure 4.4- Force versus displacement diagrams (a) pristine, (b) 0.5 wt.%, (c) 1 wt.%, (d) 2 wt.%, (e) representative for the four tested materials aimed to stiffness comparison

4.3.2. Fracture toughness

The fracture toughness results were determined using the three initiation value procedures according to ASTM standard [35]. Deviation from nonlinearity (NL), visual observation (VIS) and 5% offset values were determined. The above initiations were selected due to the special (due to pullout/fiber bridging) property of the material. In order to calculate the interlaminar fracture toughness results, the three data reduction methods - the modified beam theory, compliance calibration, and modified compliance calibration -were applied using equations (1), (2) and (3) respectively. To incorporate the uncertainties, the average value of each individual specimen's results was taken. According to literature and ASTM, the fracture toughness results obtained using the reduction methods of MBT were considered conservative. Figure 4.5 (a) shows the fracture toughness, G_{IC} calculated values using MBT, CC, and MCC. The MBT values are 0.336kJ/m^2, 0.378kJ/m^2, 0.408kJ/m^2 and 0.517kJ/m^2 for the pristine, and for the modified with 0.5 wt.%, 1 wt.% and 2 wt.% nanoclays respectively. The obtained VIS values are 0.469kJ/m^2, 0.525 kJ/m^2, 0.543kJ/m^2 and 0.794kJ/m^2 for pristine, and for the modified with 0.5 wt.%, 1 wt.%, and 2 wt.% respectively. Similarly, the energy release rates found using a reduction method of CC are presented in Figure 4.5(b).

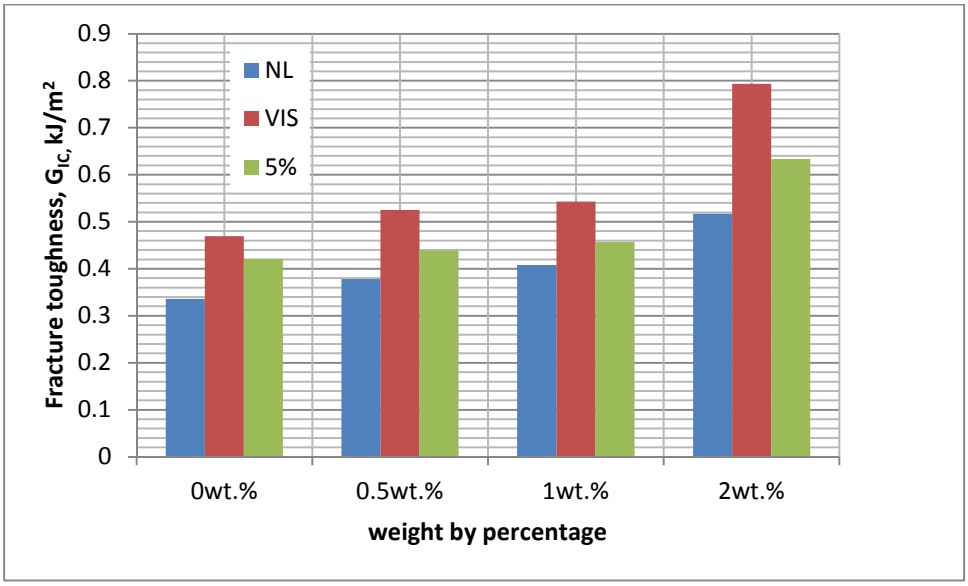

(a)

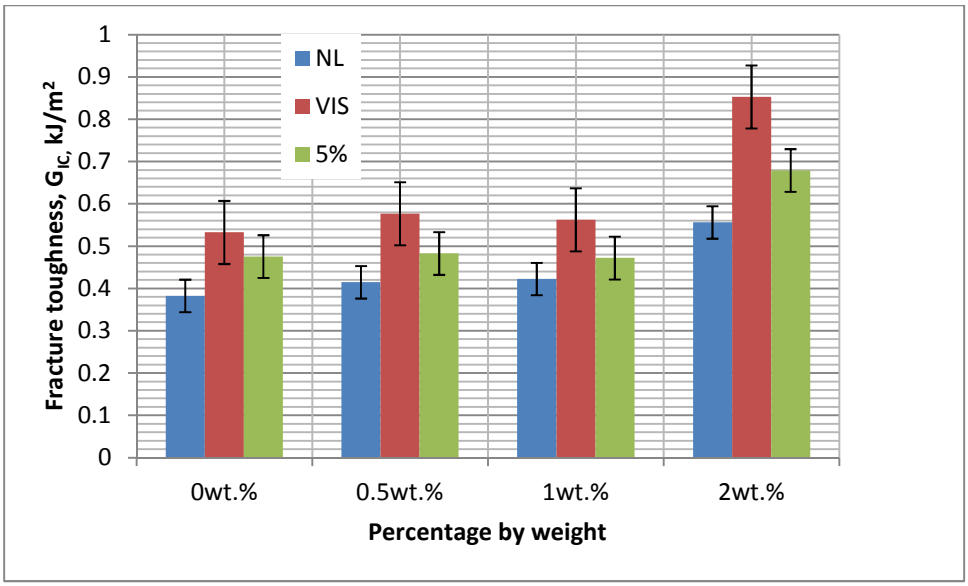

(b)

Figure 4.5- Fracture Toughness of each Nano filler concentration by weight calculated by the procedures (a) MBT and (b) CC

From the indicated results, whatever procedure is adopted for the evaluation, it is clear that the nanoclay improved the values of the interlaminar fracture toughness. Because of the ASTM standard recommendation, the NL initiation values are considered, however, the VIS initiating values are convincing for this specific material. The values are higher than those reported in the literature for the E-glass reinforced plastic [36] for a pristine, while for 2 wt.% Nano filler addition the toughness values are comparable with carbon fiber reinforced plastic(even if these materials have better strength) composite[37].

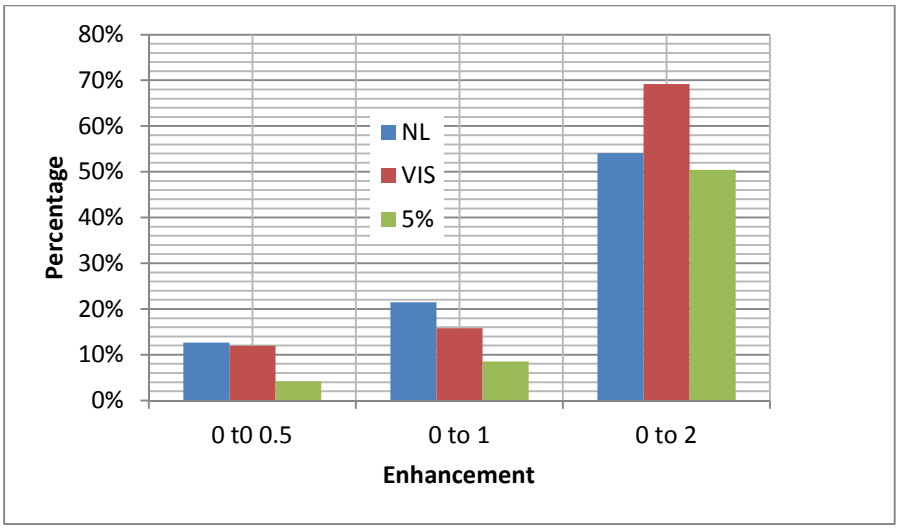

Figure 4.6 Enhancement of the fracture toughness consequent to each concentration by weight addition

Figure 4.6 shows the improvement of the results by percentages. Cloisite 20B enhanced the NL value of the fracture toughness initiation by 12.65% when 0.5 wt.% was added to the pristine and 21.49% with the addition of 1 wt.%. Significant enhancement, 54.07% obtained at 2 wt.% nanoclay addition. Similarly, the nanoclay improved the VIS values of the fracture toughness by 11.96%, 15.78%, and 69.17% for the Cloisite concentrations of 0.5 wt.%, 1 wt.% and 2 wt.% respectively. The improvements at a lower level of concentration, specifically, between 0.5 wt.% and 1 wt.%, are small. This might be due to insufficient sonication for 1 wt.% because, at 2 wt.% concentration, more than 1.5 times enhancement was gained.

4.3.3. Resistance curve

The resistance curve of crack and delamination shows the crack growth behavior of the material in terms of energy release across the surface area of the crack or delamination. The resistance curve for pristine and 2 wt.% are presented in Figure 4.7(a) and (b) while Figure 4.8 shows the comparison of all enhanced materials with respect to pristine.

Unlike the unidirectional composite materials, woven composites yield scattered R curves associated with varying toughness within and away from interlaminar resin pockets as the delamination grows. Since many scatter obtained during crack propagation, taking the average value of each material deviates the actual values and pattern. Therefore, the energy release rates of each specimen were presented to show the actual distribution.

The additional scattering behavior depends on the nanoclay distribution. Literally, the slope of the valley to pick decreases in magnitude due to the toughening effects of the epoxy. Sometimes

the arrest and growth may not be stable which follows the same scatter in energy dissipation. The delamination growth propagated unstably both in the epoxy pocket and the fabric contact. This is either due to the agglomeration of nanoclay at the place of fabric contact and/or tearing of fiber from a matrix having strong bonding. The strong bond causes fiber bridging due to cohesive failure. During fiber bridging, the fiber or matrix could be damaged from either cohesive in matrix or cohesive in fiber. Thus, the highly scattered and the smooth energy release rate distributions cannot be obtained unlike unenhanced brittle woven composite materials and like unidirectional composite materials /or conventional homogeneous materials respectively. The average of the resistance curve values of each material type became almost straight line, which is starting about from 60 mm crack length, which agrees with the basic theories.

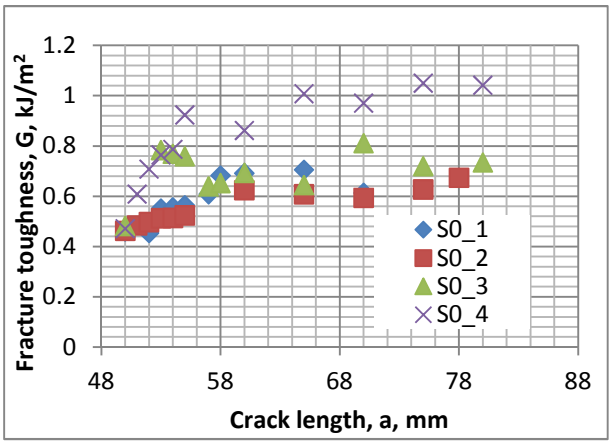

(a)

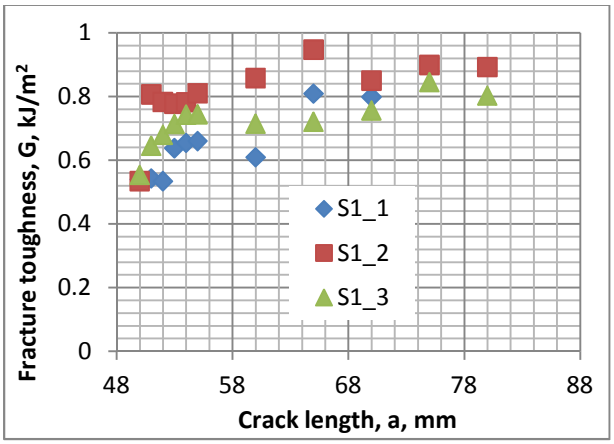

(b)

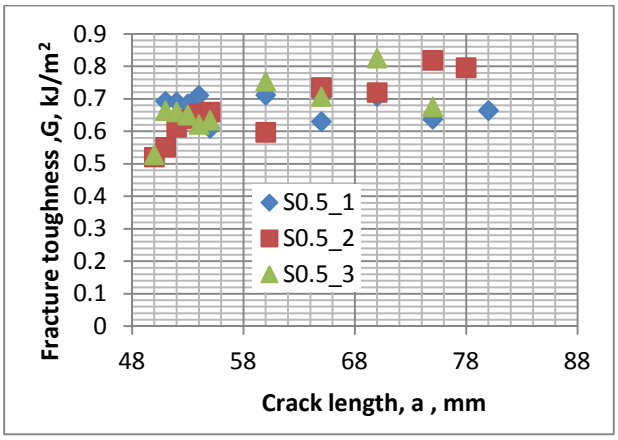

(c)

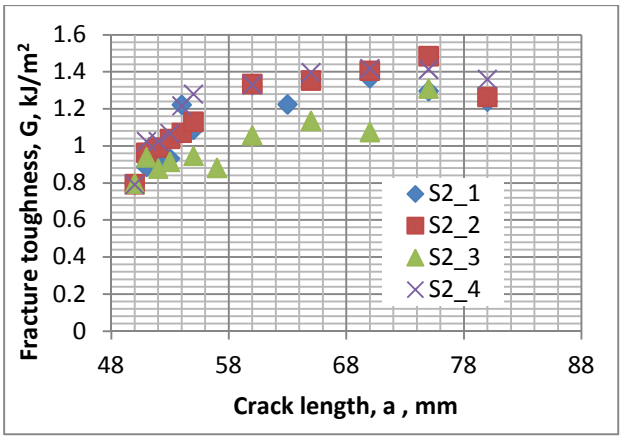

(d)

Figure 4.7 Comparison of the resistance values for (a) pristine, (b) 0.5 wt.% C20B, (c)1 wt.% C20B and (d) 2 wt.% C20B

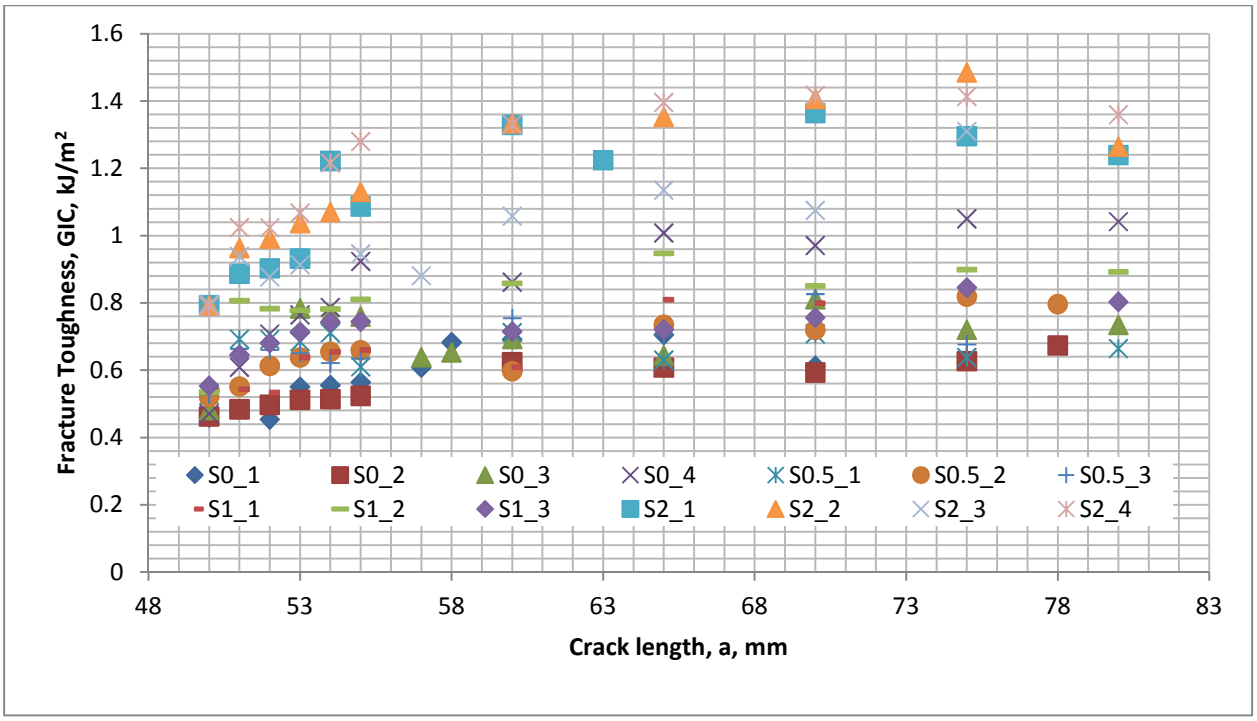

Figure 4.8 Comparisons of resistance curves for pristine, 0.5 wt.%, 1 wt.% and 2 wt.%

The comparison of the trends showed in figures 4.7 and 4.8 the relevant improvement to the resistance values that are obtained with 2 wt.% addition of Cloisite 20B with respect to the pristine material.

3.1. Damage behavior

In order to investigate the influence of the inclusion of nanoclays/Cloisite on the mode of fractures and the resulting surfaces, the delaminated surfaces were observed by SEM. Figure 4.9 shows the micrography of mode-I fracture surfaces of pristine and nanoclays/Cloisite modified GFRP composites. Generally, the failure mechanism for the pristine and nanoclays/Cloisite modified GFRP consisted of voids, fiber-matrix debonding, fiber pullout from fiber bridging. The pristine materials, as shown in Figure 4.9(a), showed a significant number of voids, as compared with the remaining material configurations.

Meanwhile, even though the purpose of the inclusion of nanoclays fillers is to increase the surface contact between fiber and matrix and to improve the interfacial bonding, sometimes dry region could occur, as it can be observed in 1 wt.% Cloisite modified GFRP, Figure 4.9(c). On the other hand, the presence of the highest energy release rate exhibited by 2 wt.% Cloisite

modified GFRP, as depicted in Figure 4.5(a), could be explained by the presence of a good interfacial bonding between the fiber and the matrix and fiber bridging that resulted in fiber breakage, as shown in Figure 4.9(d).

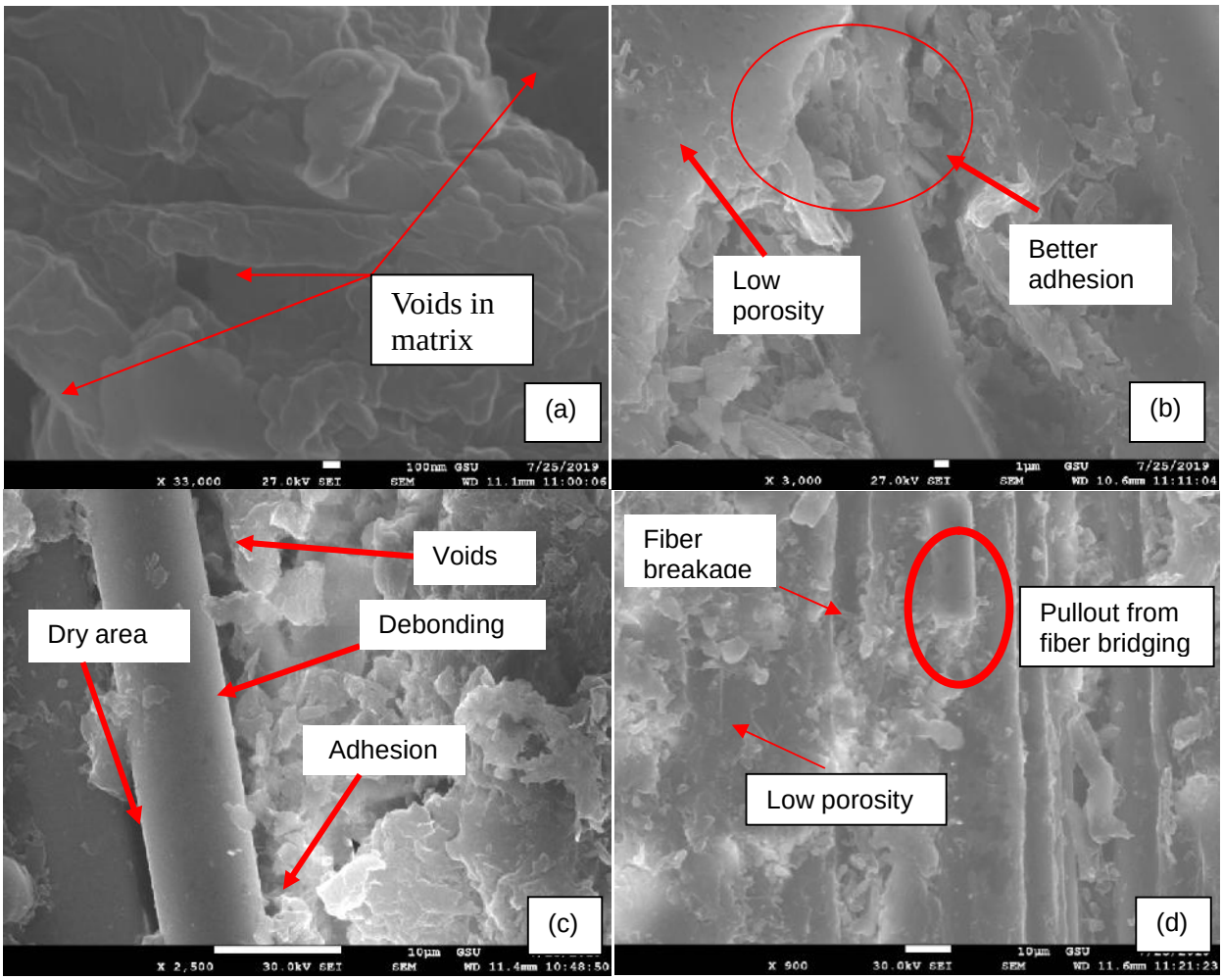

Figure 4.9 SEM images of: (a) Pristine at x33,000, (b) 0.5wt.%Cloisite 20B at x3000, (c) 1wt%Cloisite20B at x2500, (d) 2 wt.% Cloisite 20B at x900 magnification

4.4. Conclusions

The research shows the effect of the presence of layered nanoclay, Cloisite 20B, on interlaminar fracture toughness of glass-fiber-reinforced polymer (GFRP). The considered GFRP consisted of S-glass plain weave fabric and SC-15 toughened epoxy. Three nanoclay weight percentages (wt.%) namely 0.5 wt.%, 1 wt.%, and 2 wt.%. were considered and their effects were compared

with the pristine GFRP. Tests have been performed with the DCB technique according to the ASTM standard. The observed results can be summarized as follows:

- The force-displacement response at the initial crack obtained by the Teflon insert, shows medium scatter because of the toughening behavior of the material and small changes as the inclusion of Cloisite 20B increased.
- The delamination stiffness increases by up to 43% as the weight by the percentage of nanoclay increases by up to 2 wt.%.
- The toughness value trends are consistent whatever of the three reduction methods defined by the ASTM standard is adopted for the fracture toughness evaluation. The fracture toughness values increase as the nanoclay weight by percentage increases. Both the NL and VIS initiation values improved at 2 wt.% nanoclay toughening.
- Inclusion of 0.5 wt.%, 1 wt.%, and 2 wt.% Cloisite 20B nanoclay into epoxy improved the interlaminar toughness of GFRP by 12.65%, 21.49%, and 54.07% respectively, according the NL initiation procedure.
- The resistance curve shows a stable energy release rate distribution starting at about 55mm as crack length increases. The average line tends to become horizontal which agrees with the general theory of the resistance curve of the composite materials.
- Generally, the voids that cause damage initiations decreases as the weight by percentage of Cloisite 20B addition increases.

Overall, it is possible to conclude that the inclusion of a small amount of nanoclay has beneficial effects on the fracture behavior of the considered S-glass fabric/epoxy composite. From literature data, it can be noted that good improvements have been achieved in comparison with other

particles of the Cloisites family. Furthermore, the adopted Cloisite 20B is highly preferable because of its non-toxicity, better melt flow rate, low elongation at break and flame-retardant behavior.

Finally, the investigation of intralaminar fracture characteristics, dynamic fracture behavior, the low and medium speed impact behavior of Cloisite modified composite materials is the potential promising research direction in order to complete the analysis and provide a comprehensive picture of advantages and limitations of the proposed materials for vehicles and other engineering applications.

4.5. References of chapter four

[1] Wimmer G, Schuecker C, Pettermann HE, Numerical simulation of delamination in laminated composite components – A combination of a strength criterion and fracture mechanics, Composites: Part B 40 (2009) 158–165

[2] Yuan H , Wang G, Mai Y, Zeng Y, On fracture toughness of nano-particle modified epoxy, Composites: Part B 42 (2011) 2170–2175

[3] Maillet I, Michel L, Rico G, Fressinet M, Gourinat Y, A new test methodology based on structural resonance for mode I fatigue delamination growth in an unidirectional composite, Composite Structures 97 (2013) 353–362

[4] Chen J, Fox D, Numerical investigation into multi-delamination failure of composite T-piece specimens under mixed mode loading using a modified cohesive model, Composite Structures 94 (2012) 2010–2016

[5] Peng L, Xu J, Zhang J, Zhao L, Mixed mode delamination growth of multidirectional composite laminates under fatigue loading, Engineering Fracture Mechanics 96 (2012) 676–686

[6] Belingardi G, Beyene AT, Jichuan D, Energy absorbing capability of GMT, GMTex and GMT-UD composite panels for static and dynamic loading – Experimental and numerical study, Composite Structures 143 (2016) 371–387

[7] Domun N, Kaboglu C, Paton KR, Dear JP, Liu J, Blackman BRK, Liaghat G, Hadavinia H, Ballistic impact behaviour of glass fibre reinforced polymer composite with 1D/2D nanomodified epoxy matrices, Composites Part B 167 (2019) 497–506

[8] Zeng Y, Liu H, Mai Y, Du X, Improving interlaminar fracture toughness of carbon fibre/epoxy laminates by incorporation of nano-particles, Composites: Part B 43 (2012) 90–94

[9] Bazhenov SL, interlaminar and intralaminar fracture modes in 0/90 cross play glass/epoxy laminate, composites 26 ,1995 125-133

[10] Czabaj MW, Ratcliffe JG, Comparison of intralaminar and interlaminar mode I fracture toughnesses of a unidirectional IM7/8552 carbon/epoxy composite, Composites Science and Technology 89 (2013) 15–23

[11] Gargano A, Pingkarawat K, Blacklock M, Pickerd V, Mouritz AP, Comparative assessment of the explosive blast performance of carbon and glass fibre-polymer composites used in naval ship structures, Composite Structures 171 (2017) 306–316

[12] Kim J, Sham M, Impact and delamination failure of woven-fabric composites, Composites Science and Technology 60 (2000) 745±761

[13] Short GJ, Guild FJ, Pavier MJ, The effect of delamination geometry on the compressive failure of composite laminates, Composites Science and Technology 61(2001) 2075–2086

[14] Irisarri FX, Lasseigne A, Leroy FH, Riche RL, Optimal design of laminated composite structures with ply drops using stacking sequence tables, Composite Structures 107 (2014) 559–569

[15] Dransfield KA, Jainb LK, Mai Y, On the effects of stitching in cfrps-i. mode i delamination toughness composites Science and Technology 58 (1998) 815-827

[16] Francesconi L, Aymerich F, Numerical simulation of the effect of stitching on the delamination resistance of laminated composites subjected to low-velocity impact, Composite Structures 159 (2017) 110–120

[17] Mouritz AP, Review of z-pinned composite laminates, Composites: Part A 38 (2007) 2383–2397

[18] Huang HS, Waas AM, Quasi-static mode II fracture tests and simulations of Z-pinned woven composites, Engineering Fracture Mechanics 126 (2014) 155–165

[19] Sun X, Wood MDK, Tong L, A parametric study on the design of stitched laminated DCB specimens, Composite Structures 75 (2006) 72–78

[20] Mouritza AP, Leong KH, Herszberg I, A review of the effect of stitching on the in-plane mechanical properties of fibre-reinforced polymer composites, Conqwsires Part A 28A (1997) 979-991

[21] Ravandi M, Teo WS, Tran LQN, Yong MS, Tay TE, The effects of through-the-thickness stitching on theMode I interlaminar fracture toughness of flax/epoxy composite laminates, Materials and Design 109 (2016) 659–669

[22] Ye Y, Chen H, Wu J, Chan CM. Interlaminar properties of carbon fiber composites with halloysite nanotube-toughened epoxy matrix. Compos Sci Technol71 (2011) 717–723

[23] Kelkar AD, Mohan R, Bolickb R, Shendok S, Effect of nanoparticles and nanofibers on Mode I fracture toughness of fiber glass reinforced polymeric matrix composites, Materials Science and Engineering B 168 (2010) 85–89

[24] Adachi T, Osaki M, Araki W, Kwon S, Fracture toughness of nano- and micro-spherical silica-particle-filled epoxy composites, ActaMaterialia 56 (2008) 2101–2109

[25] Kim M, Hong J, Kang S, Kim C, Enhancement of the crack growth resistance of a carbon/epoxy composite by adding multi-walled carbon nanotubes at a cryogenic temperature, Composites: Part A 39 (2008) 647–654

[26] Binu PP, K.E. KE, Vinodkumar MN, Effect of nanoclay, Cloisite15A on the Mechanical Properties and Thermal behavior of Glass Fiber Reinforced Polyester, Procedia Technology 25 (2016) 846 – 853

[27] Azeez AA, Rhee KY, Park SJ, Hui D, Epoxy clay nanocomposites – processing, properties and applications: A review, Composites: Part B 45 (2013) 308–320

[28] Lim S, Dasari A, Yu Z, Mai Y, Liu S, Yong MS, Fracture toughness of nylon /organoclay/elastomer nanocomposites, Composites Science and Technology 67 (2007) 2914–2923

[29] Vila AFA, Morais DTS, Modeling nanoclay effects into laminates failure strength and porosity, Composite Structures 87 (2009) 55–62

[30] Khan SU, Iqbal K, Munir A, Kim J, Quasi-static and impact fracture behaviors of CFRPs with nanoclay-filled epoxy matrix, Composites: Part A 42 (2011) 253–264

[31] Sharmila TKB, Ayswarya EP, Abraham BT, Begum PMS, Thachil ET, Fabrication of partially exfoliated and disordered intercalated cloisite epoxy nanocomposites via in situ polymerization: Mechanical, dynamic mechanical, thermal and barrier properties, Applied Clay Science 102 (2014) 220–230

[32] Chen Q, Zhao Y, Zhou Z, Rahman A, Wub XF, Wuc W, Xu T, Fong H, Fabrication and mechanical properties of hybrid multi-scale epoxy composites reinforced with conventional carbon fiber fabrics surface-attached with electrospun carbon nanofiber mats, Composites: Part B 44 (2013) 1–7

[33] Chen H, Wang J, Ni A, Ding A, Sun Z, Han X, Effect of novel intumescent flame retardant on mechanical and flame retardant properties of continuous glass fibre reinforced polypropylene composites, Composite Structures 203 (2018) 894–902

[34] Shield Strand Woven Fabrics, 2010, Owens corning composite materials, LLC/www.owenscorning.com

[35] ASTM D5528-01 Standard Test Method for Mode I Interlaminar Fracture Toughness of Unidirectional Fiber-Reinforced Polymer Matrix Composites. Annual Book of ASTM Standards; Philadelphia (USA): American Society for Testing and Materials; 2007

[36] Blake SP, Berube KA, Lopez-Anido RA, Interlaminar fracture toughness of woven E-glass fabric composites, Journal of Composite Materials 46(13) 1583–1592

[37] Fanteria D, LazzeriPanettieri E, Mariani U, Rigamonti M, Experimental characterization of the interlaminar fracture toughness of a woven and a unidirectional carbon/epoxy composite, Composites Science and Technology 142 (2017) 20-29

Part II: Intralaminar Fracture Toughness and Resistance Curve of Semi Impregnated Micro Sandwich (SIMS) and GMT Composite Materials

The vehicle industry is demanding lightweight at acceptable costs, with particular attention toward non-conventional materials, to match global environmental regulation and demand. New and enhanced materials have been developed to fulfill the requirements. Meanwhile, safety of passengers is still crucial target for these new technologies. Thus, an Italian company Delta tech and a Switzerland company Quadrant have developed better materials that have better structural properties. Delta tech developed innovative semi impregnated micro sandwich structures while Quadrant developed glass mat thermoplastic and modified into glass mat thermoplastic with a unidirectional reinforcement. This part of the research dealt with the intralaminar fracture behavior of these two materials suitable for automotive application.

Chapter 5: Intralaminar Fracture Toughness

The intralaminar fracture toughness and crack behavior of GMT, GMT-UD, C-SIMS, and G-SIMS were tested based on the modified testing process, based on a Compact Tension (CT) specimen. The description of materials, manufacturing methods, experimental procedure, and reduction methods were discussed and explained. Results about the load-displacement response, fracture toughness, and damage of materials/ fractography had was presented for each type of material. The resistance curves were specifically discussed for G-SIMS, C-SIMS, and GMT-UD. The fractography part was incorporated and elucidated to point out the crack propagation with particular reference to the propagation direction.

5.1. Introduction of intralaminar fracture toughness

When composite materials are used as a primary load-carrying structural component, structures must overcome all the damage and failure conditions for the intended time. Failure due to applied stress and impact are subject of a wide number of research activities and available

papers. However, the structural behavior of composite materials when a crack or similar defect is already existing as a consequence of single or frequent applied loads, impact or defects originated during manufacture, the analysis of damage progress until failure become important factors. Unless we determine and know the fracture behavior, the uncertainty of engineering solutions may have gapes to save a life, property, and economic impact. Vehicle structures, aircraft fuselage, ship body, sports equipment, electronic covers are exposed to impact loads, which cause damages, sometimes barely visible damages. The damages can be taken as the initiation of through stationary crack and/or growing cracks. Through cracks that are perpendicular to the plane of the structure named as an intralaminar fracture. The intralaminar crack behavior includes debonding, delamination, fiber rapture, matrix cracking, fiber pullout, etc. in various directions.

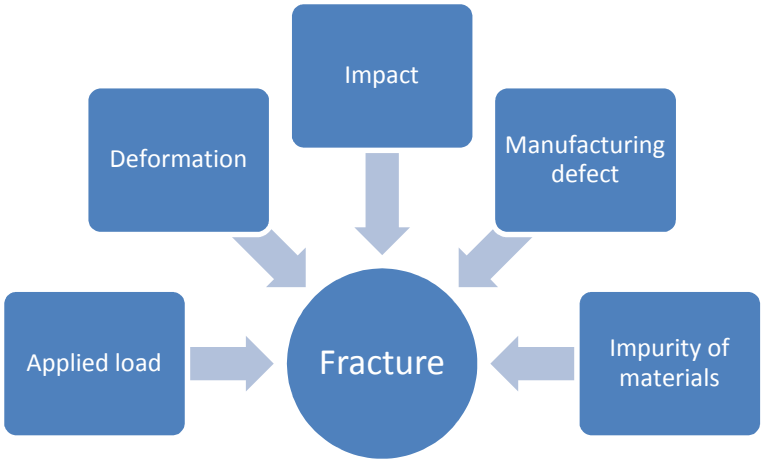

Figure 5.1 Causes of fracture

Composite materials failure can be dealt with in using two approaches as discussed in chapter 2. The first one is the strength approach while the second lies in the fracture approach. Using the fracture approach, composite materials may fail as a consequence of either interlaminar damage or intralaminar damage. The interlaminar situation was previously mentioned and discussed in chapter four. This chapter discusses intralaminar failure mechanics.

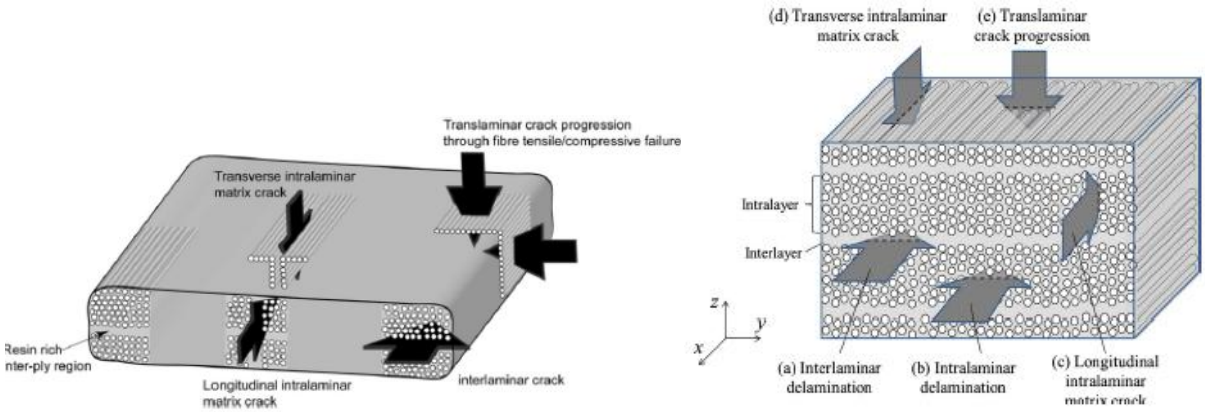

(a) **(b)**

Figure 5.2(a) Overview of ply-level failure modes [1], (b) all failure directions [2]

The intralaminar fracture approach deals with the fracture behavior of matrix cracking between tows or fibers and across fibers. The cracking situation of intralaminar is either transversal or longitudinal. Since most composite material laminates have been manufactured using multidirectional and woven structures, a large amount of the fracture characterization follows the approach of both intralaminar and translaminar at the same time (see figure 5.2(a) and (b)) [1, 2]. Thus, intralaminar fracture approach considers the fiber rupture, matrix cracking, fiber pulled out, and combinations of all these damages. The cause of failure may be impact load, fatigue load, bending load, tensile and compressive load followed by bending, etc.

The intralaminar fracture problem can be studied using bending specimen (SEB), disk-shaped compact tension specimen (DCT), arc-shaped tension specimen (AT), arc-shaped bend specimen (AB), and compact tension (CT). Compact tension (CT), compact compression (CC) and over-height compact (OCT) tension specimens can be considered in experimental tests [3]. The experimental test can determine the stress intensity factor K, the energy release rate G, and the J integrals.

Intralaminar fracture test investigation for composite material does not have specific standards. Some researchers have rarely used ASTM D5045-99[4] in which the standard was produced for plastic materials and the others usually used ASTME399–09 [5], which was produced for metallic (isotropic) materials. The researchers who considered ASTM D5045-99 not the right standard for composite materials, developed new specimens like over height specimens [6] to minimize the damage of the specimen during testing and they proposed double tapered compact

tension [7] (see figure 5.3 (b)). Thus selecting the appropriate specimen type is the first task that has to be done.

Specifically for compact tension specimen, Pinho et al. [5] used compact tension, Li et al. and Xu et al.[8] prepared over height compact tension specimen (OCT), Gzabaj et al. [9] dealt with compact tension, Blanco et al.[7, 10] part I and part II, and Li et al. [6] modified two-sided tapered compact tension specimen (2TCT) (see figure 5.3 (d)). However, the traditional compact tension specimen and over height compact tension specimen have advantages and disadvantages to obtain the appropriate results for dealing with the fracture toughness of the materials. Sizes, damages, and supports are still the main issues. ASTM 5045-99 (for plastic materials) standard is not preferable because of the large thickness of the material specimen, which is equivalent to metals dimension, while the thicknesses for composite material laminates are comparatively thin.

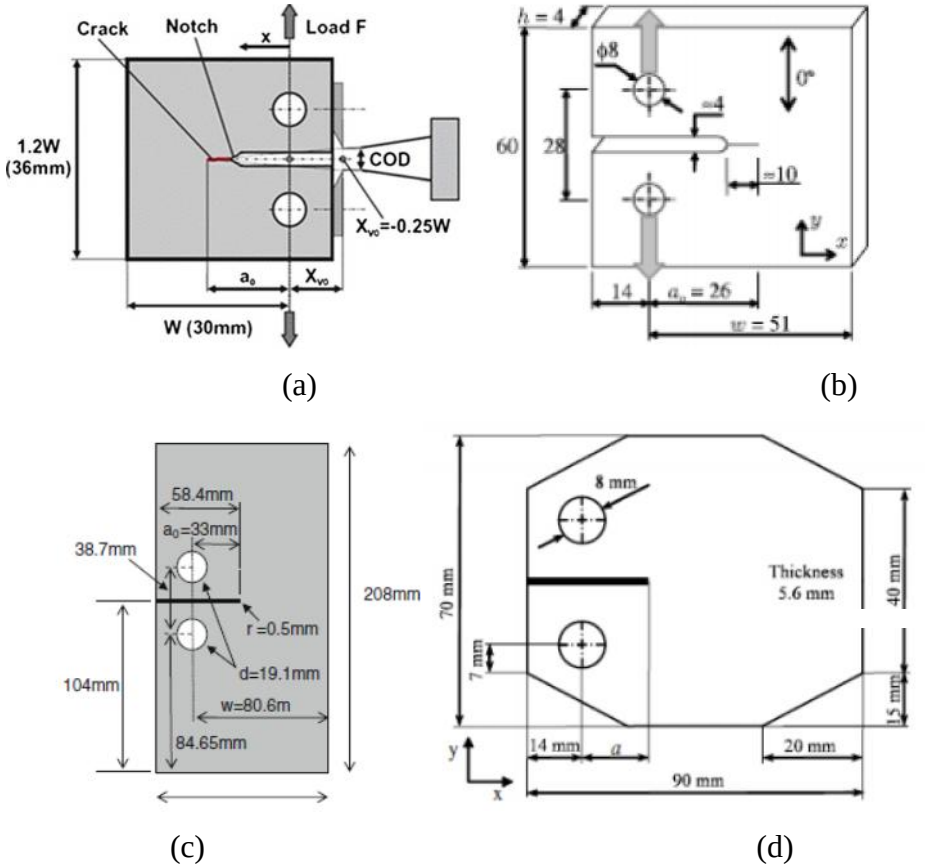

Figure 5.3 Different geometries considered for CT tests - (a) Plastic material specimen [4], (b) metallic material specimen [5], (c) over height specimens[6], (d) double tapered specimens[7, 10]

Similarly, over height, compact tension specimens have the problem of possible specimen bending or warping during the test, which results in damages. Therefore, these specimens could require supports, which create uncertainties in results (see figure 5.4(a-c)).

To consider the problem of damages and sizes, Blanco et al.[7] dealt with compact tension (CT) and the extended compact tension (ECT)specimens. Then, the authors prepared specimens characterized by three geometries, specifically the widened compact tension (WCT), the tapered compact tension (TCT) and the double-tapered compact tension (2TCT). Furthermore, the same authors studied the critical damage zones for the three types of specimens. Figure 5-4(d) shows a scheme for the possible problems and the related critical areas. As a result of this study, based on the damage index analysis, the doubly-tapered compact tension (2TCT) was recommended because of damage minimization during the experimental test at the loading point and at the opposite edge to loading points. The current experimental study prefers to follow the double tapered compact tension specimens because of it minimizes the problems put in evidence in the case of use of the ASTM 5045-99 and over height specimens.

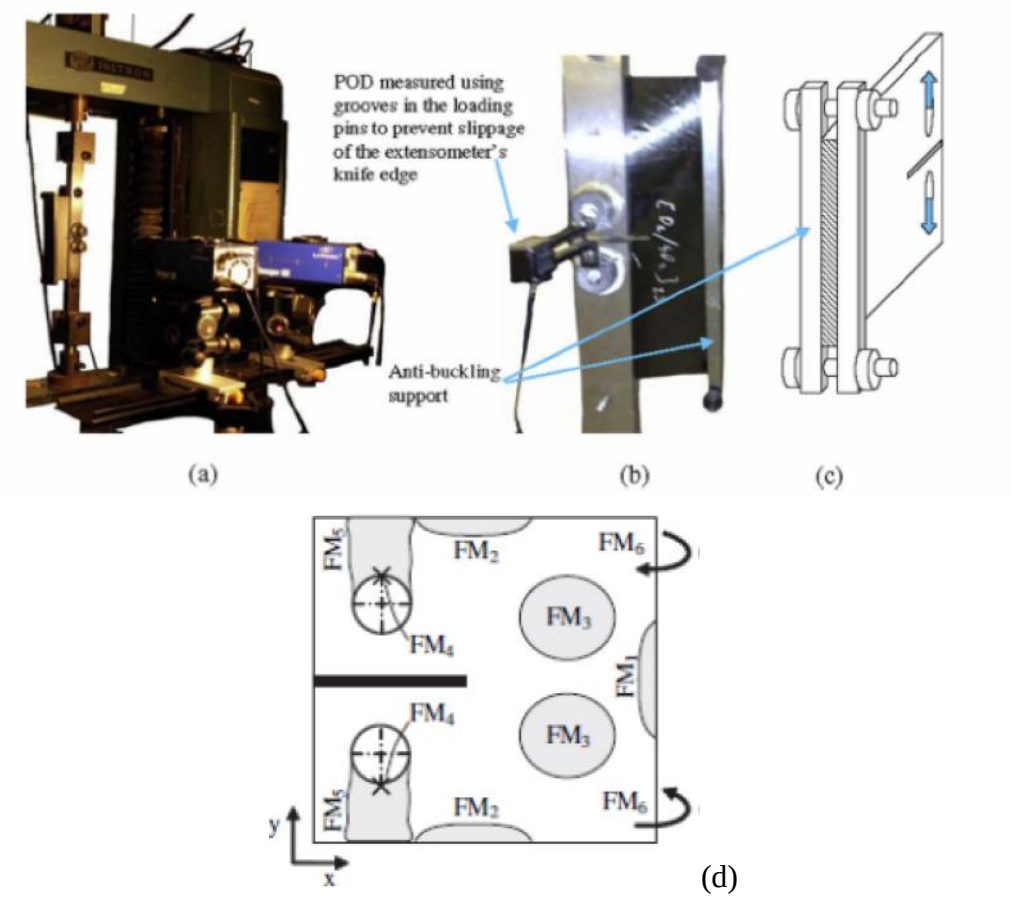

Figure 5.4 OCT specimen (a) set-up, (b) back view of specimen, (c) with anti-twisting support [6],(d) zones of damages [7]

5.2. Materials

The automotive industry demands for lightweight and excellent energy absorption materials. Researchers and companies develop various types of energy-absorbing composite materials like glass mat reinforced thermoplastics (GMT) [11], sandwiches [12] and semi impregnated micro-sandwich structures (SIMS) [13] composite materials. In this work, SIMS and GMT types of materials were examined. These materials contained two types of SIMS that were supplied by Delta tech and the other two types of GMT families, which were supplied by Quadrant.

SIMS and GMT that have better energy absorption materials are good candidates of the automotive industry because the automotive structures are exposed to low and medium speed impact loads. In the case of the gravel, tools, light crash, low-speed impact of the car, temperature changes, pressure change shock, impact, and repeated cyclic stresses, cracks may be induced on the body of the automobile. These cracks are serious problems and failure of the automobile body could take place.

5.2.1. Semi impregnated micro sandwich, SIMS

Sandwich structures are a type of composite materials, which are fabricated using two thin skins and thick core. The core is placed between the two thin skins to provide the sandwich structure to have better bending stiffness and strength together with low density. SIMS is a type of sandwich material that has a number of layers containing different levels of dry fiber within the nonwoven sandwich thickness, see figure 5.5 (a). SIMS is intended to have good energy absorption and thus be a good candidate in all transport sectors (automotive, railway, aerospace, etc.). SIMS can be also applicable to fire, smoke, and toxicity. The panels have outstanding impact strength, which makes them good candidates for the application of automotive external panels and/or composite laminates for personal protection [14].

SIMSs are made up of either using glass fiber or carbon fiber types. A carbon-fiber semi impregnated micro sandwich(C- SIMS) and glass fiber semi impregnated micro sandwich (G-SIMS) materials are used. Belingardi et al. [13] made extensive characterization of these materials about the main mechanical properties such as tensile tests (both longitudinal and transverse directions), compressive tests (both longitudinal and transverse directions), plane shear tests (both longitudinal and transverse direction), and the energy absorption using drop-dart tests. The fracture toughness and crack behaviors are required to have the whole picture of

these materials. Thus, fracture toughness investigation of these materials fills the gap in the characterization of the mechanical behaviors of the materials.

5.2.2. Manufacturing of SIMS laminates

SIMS is a combination of two distinct elements (fabric material and non-fabric fleece see figure 5.5(a)). Thus, the plate with the required thickness was made by adding numbers of SIMS. The procedure of C-SIMS manufacturing was started by treating the flat metal surfaces with a releasing agent. Material 1 was laid on a flat metal surface treated with releasing agent followed by another layer of material 1. As a third layer, material 2 was laid on the second layer of material 1, then with upturned positions two layers of the material 1 were sequentially appended to make symmetrical layer arrangement. Finally, material 5 as shown in figure 5.5(b) was added before a metal plate treated with the releasing agent was placed on the top.

Similarly for G-SIMS manufacturing, material 3 was laid on a flat metal surface treated with the releasing agent followed by another material 3. On the second layer of material 3, material 4 was added. The two 'material 3' layers were laid one after the other with the upside-down position on material 4 and lastly, material 5 as shown in figure 5.5(c) was attached. Then a metal plate treated with the releasing agent was placed on the top of the laminate.

The curing process of each laminate was undertaken in an autoclave set of temperature, time, pressure, and heating ramp [14]. The vacuum bag was vented to the atmosphere after the required pressure was acquired.

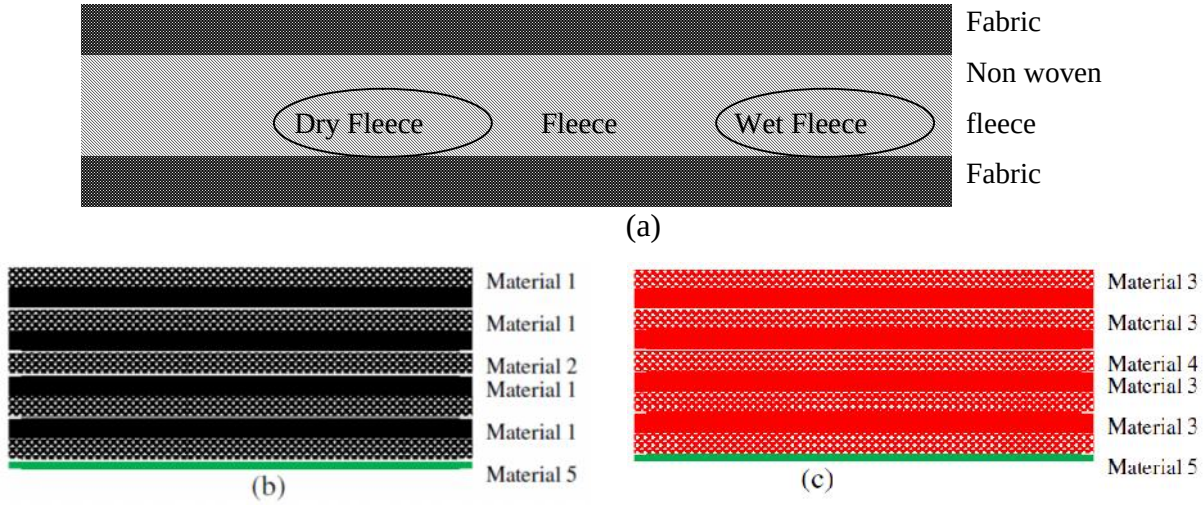

Figure 5.5 SIMS arrangement (a) SIMS (b) C-SIMS Laminate (c) G-SIMS Laminate

where

Material 1: SIMS carbon/epoxy prepreg/Non WovenGG380T(T700)-DT806R-53 NP400N

Material2:Carbonepoxyprepreg, GG380T(T700)-DT806R-53

Material 3: SIMS glass/epoxy prepreg/Non-Woven VV380T-DT806R-52 NP400N

Material 4: Glass epoxy prepreg, VV380T-DT806R-52

Material 5: Surface Film FS 003

5.2.3. Glass matrix reinforced thermoplastic, GMT

Glass matrix reinforced thermoplastics (GMT) become suitable for high-impact, structural applications in the automotive industry [11]. GMTs have usually made as an endless fiberglass mate reinforced plastic with randomly oriented glass fibers. The Quadrant developed a glass mat in various ways based on the glass mat structure. The first one (figure 5.6(a)) is with continuous glass fiber reinforcement that is randomly oriented and therefore results isotropic. It has good surface quality in addition to good mechanical isotropic properties. The other type is a GMTex (figure 5.6(b)), which has reinforcement made with from 25mm to 75mm length glass fibers with a random arrangement and consistent distribution. The third type is the GMT-UD with a chopped fiberglass mat reinforced plastic laminate with randomly oriented glass fibers, additionally reinforced with unidirectionally oriented glass fiber layers(see figure 5.6(c)). GMT-UD is primarily applicable to uniaxially stressed parts [15]. This research deals with GMT and GMT-UD.

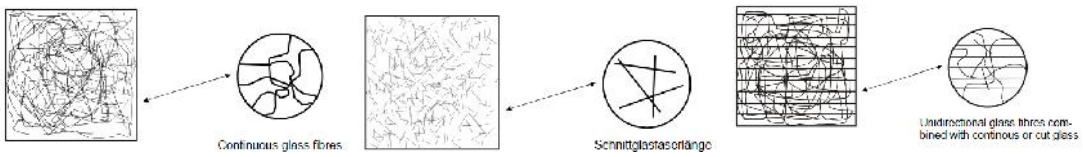

(a) GMT (b) GMTex (c) GMT-UD

Figure 5.6 GMT materials [15]

These GMT family (GMT and GMT-UD) composite materials were extensively characterized. Belingardi et a. [11] conducted the tensile (both longitudinal and transverse direction), compressive (both longitudinal and transverse direction), and drop-dart tests. The same author applied these materials for the vehicle frontal bumper beam. Additionally, Belingardi et al. [9] dealt with the experimental and numerical simulation of the materials. The authors performed experimental tests (quasi-static and impact loading conditions) to observe the force-displacement, and energy displacement diagrams, and other important parameters such as damage index, energy profile, and energy absorption. Furthermore, visual inspection of the

perforated specimens of the material damage mechanisms and support explanation of the different energy absorption performances were dealt with. The intralaminar fracture test helps to have considerable knowledge about the behavior of materials related to damage conditions.

5.2.4. Manufacturing of GMT

As earlier mentioned, the GMT materials were supplied by Quadrant. A classic GMT was manufactured using a double belt press. First glass fiber mats, unidirectional fibers with polymer melt-extruded through wide slot nozzles are impregnated under pressure and temperature. The material was thereafter cooled under pressure. Quadrant usually produces GMT in the manufacturing widths of 1000mm to 1400mm, width is not below 100mm [15].

5.3. Experimental design and data reduction

The fracture toughness and resistance curves have to be determined by combining the force-displacement responses and external visual recording during the test. To obtain the final values, the appropriate reduction methods have to be considered. The experimental conditions and the calculation methods are explained below.

5.3.1. Experimental design

The specimens were cut with the 2CTC shape from the panel according to the dimensions shown in figure 5.7 with GMT-UD-3.9mm, GMT-3.8mm, C-SIMS 6mm, G-SIMS 5mm thickness. Specimen crack was cut with 1mm thickness saw for 25mm length from load point line, then 5mm length with 0.2mm thickness saw and finally 0.1mm thickness razor blade was used for sharp crack initiation. The final initial crack length is a (see figure 5.7(a)). Millimeter lines useful to identify the crack growth conditions during the test execution were glued, next to the crack edges. The specimens were ready for the test as shown in figure 5.7(c).

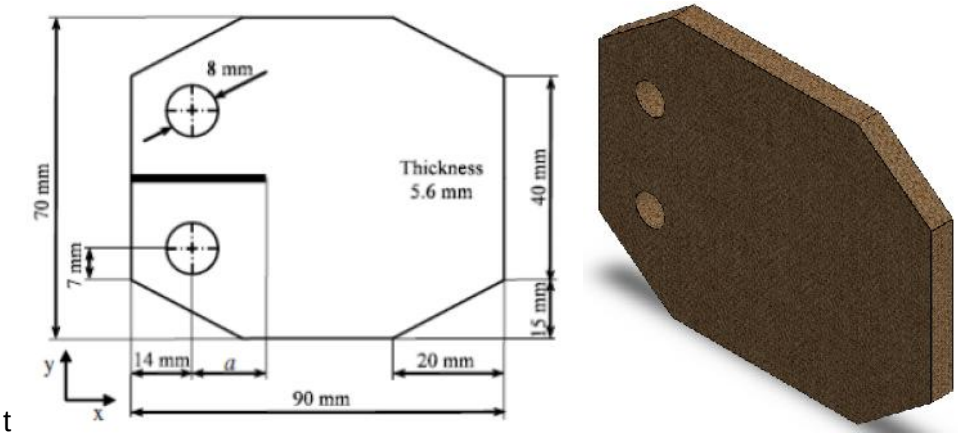

t

(a) (b)

(c)

Figure 5.7 SIMS and GMT family specimens (a) dimensions of the 2CTC specimen, (b) three dimensional model,(c) G-SIMS specimens

Fracture tests were performed with 100 kN capacity servo-hydraulic testing machine INSTRON-8801. The tests were conducted according to ASTM E399-09 standards [3] and the modified intralaminar composite materials specimen model [10]. The intralaminar test apparatus, shown in figure 5.8(c), was used to apply the load on the specimens. Tests were carried out at a room temperature of 19 C^{o} and a constant displacement rate of 1mm/min. The load and displacement were measured the testing machine transducers and acquired by a specific acquisition board. The crack length propagation was recorded using a digital video camera.

(a) (b) (c)

Figure 5.8Experimental test setup for compact tension specimen (a) experimental setup, (b) specimen-fixture setup during testing, (c) fixture-specimen model

5.3.2. Data reduction

The reduction methods for mode I intralaminar fracture toughness of composite materials has not been standardized yet. The energy release rate of mode I, G_{IC} can be calculated using area method, compliance calibration method, modified compliance calibration with optically measured crack length method, modified compliance calibration with effective crack length method, ASTM E399 and J-integral methods [16, 17].

In this research, ASTM and J-integral methods have been considered to calculate the fracture toughness and behaviors. Despite the ASTM methods are usually applicable for isotropic materials and contested by literature due to inflated values for heterogeneous materials, this study included the ASTM method in order to compare the results with the recommended reduction method and to calculate the fracture toughness of GMT material. Energy release rates of the material are calculated from stress intensity factors, K_{IC} as indicated in equation (5.1) [3].

$$G_{I} = \frac{K_I^2}{\sqrt{2E_1E_2}}\sqrt{\sqrt{\frac{E_1}{E_2}} + \frac{E_1}{E_2} - \vartheta_1} \qquad (5.1)$$

where $K_{I} = \frac{P_C}{t\sqrt{w}} f\left(\frac{a}{w}\right)$ (5.1a)

and

$$f(a/w) = \frac{2+a/w}{(1-a/w)^{1.5}}[0.886 + 4.64(a/w) - 13.32(a/w)^2 + 14.72(a/w)^3 - 5.6(a/w)^4] \qquad (5.1b)$$

a = crack size

P_c = the measured critical load that causes fracture,

t = the thickness of the specimen,

w = the effective length of the specimen/ dimension

E_1 and E_2 = the Young's moduli in the 1 and 2 directions respectively

G_{12} = the shear modulus

v_{12} = the Poisson's ratio

The other preferable reduction method is the J-integral/VCCT, which have been developed for composite materials. Based on Balnco et al. [10], and Laffan et al. [16], the J- integral method was used to calculate the critical energy release rate/fracture toughness and resistance curves using equation (5.2).

$$G_{I} = f(a)\left(\frac{P_C}{t}\right)^2 \qquad (5.2)$$

where $f(a) = c_3a^3+c_2a^2+c_1a + c_O$ (5.2a)

Values for C_i constants were calculated from experimental modified compliance calibration.

The area method, which may not be universal, compliance calibration methods, and modified compliance calibrations are not considered here. The C_i constants were determined from compliance and crack lengths. The measurements of crack lengths were taken from the crack growth observation: during the first 5mm crack growth it was captured for each 1 mm increment while the rest was captured for each 5 mm increments. The compliance was determined from experimental results and the finite element methods (see figure 5.9).

Table 5.1 Material properties [11, 13]

Materials	Young Modulus, GPa		Shear elastic Modulus, GPa	T. Poisson's ratio
	E_1	E_2	G_{12}	
C-SIMS	28.7	24.3	6,09	0.105
G-SIMS	11.08	9.7	5.4	0.21
GMT	5.81		5.81	0.284
GMT-UD	11.07	6.48	4.21	0.307

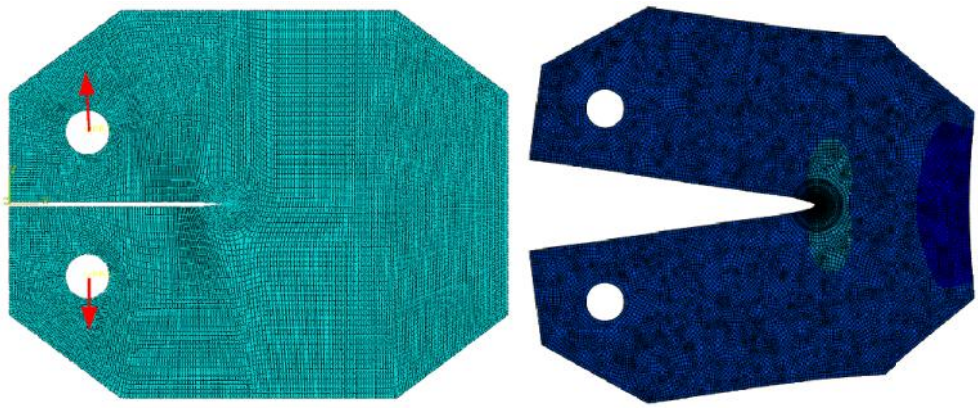

Figure 5.9 Finite element models

5.4. Result and discussion

The results that are displayed under these discussions are the force-displacement, intralaminar fracture toughness, and resistance curves. For each group of materials and specific material types, the crack growth behaviors are discussed.

5.4.1. Result and discussion of SIMS

The force-displacement diagram describes the stiffness trend and it is needed to calculate the

compliances. As earlier described, the compliances help to calculate the sensitive part of the reduction behavior that, in turn, helps to calculate the fracture toughness and the resistance curves. The C-SIMS and G-SIMS have different load-displacement curves, which depend on the nature of the materials themselves and specimen thicknesses.

5.4.1.1. Force displacement response

The load-displacement responses depend on the stiffness of the materials, the damage initiation, and propagation behaviors. The force-displacement diagram usually contains four stages. However, the zones depend on the material types: SIMS materials show at first a linear loading zone (I), then a damage development and process zone (II), then a crack propagation zone and crack zone expansion (III) followed by the final failure zone [14]. As shown in figure 5.10 the experiment gave good repeatability of force-displacement diagrams. The initial linear parts of the diagrams have good repeatability (nearly superimposed and with nearly identical slopes) while scattered profiles are shown during crack propagation. The average stiffness, in the region I for C-SIMS and G-SIMS resulted in 1177.16N/mm and 914.36N/mm respectively.

Damage usually starts to develop [3, 18] when the stiffness loses the linearity (see figure 5.10). As the crack continues propagation, stable and unstable crack growths have been obtained. The up and down of the curve shows the stability and instability ranges. The down and the unstable crack growth shows where the matrix is damaged while the curve moves up due to the rupture of tows/fibers. Since the woven part was arranged from the outside part of the plate, this influences the regularity of the sequence of saw-toothed that is not uniform.

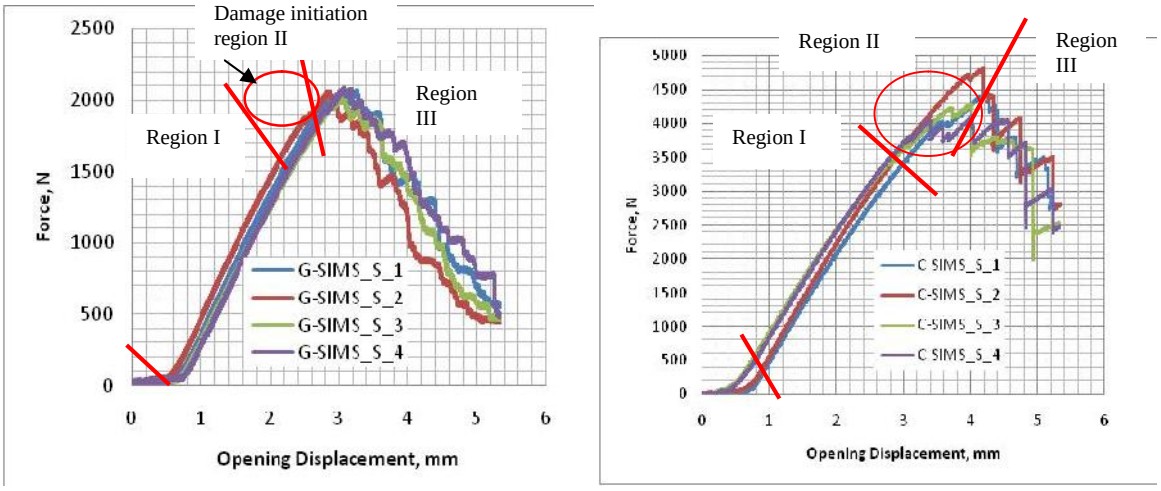

(a) (b)

Figure 5.10 Force displacement responses (a) G-SIMS, (b) C-SIMS

5.4.1.2. Fracture toughness and resistance curves of SIMS

The fracture toughness of the materials for the compact tension test is proportional to the failure load. The mode I fracture toughness is directly proportional to the load P_c, see eq (5.1a), where P_c is a critical load, which, in the present case, is equal to P_Q (see figure 5.11 type I). The critical load is determined by constructing a secant line (with a 95% slope of the initial straight characteristic) and the critical load is considered the first point where the nonlinearity of the materials starts (see figure 5.11) [3]. For absolute linear materials (type III in figure 5.11), the maximum load can be taken as a maximum ultimate load to calculate the fracture toughness. SIMS and GMT family materials show linearity deviation before the maximum failure load is obtained (type I in figure 5.11). Thus, all four types of materials were calculated according to this basic principle.

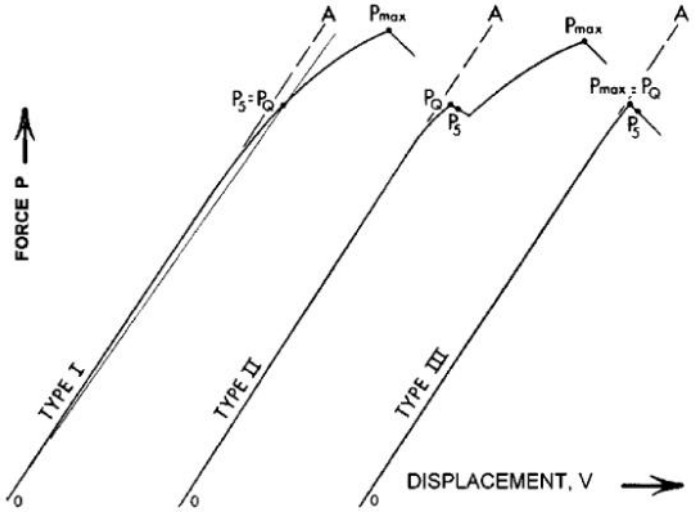

Figure 5.11Critical load determinations according to ASTM 399 standard [3]

According to the ASTM 399-99 (with the properties of table 5.1), the critical fracture toughness of the C-SIMS and G-SIMS were calculated 18.01kJ/m^2 and 12.97kJ/m^2 (eq. (5.1)) respectively while using the modified compliance calibration methods they resulted in 15.85kJ/m^2 and 12.22kJ/m^2 (eq. (5.2)) respectively. The purpose of R-curves is to describe the relationship between the resistance to fracture and the propagation of crack lengths [8] and as the crack growth resistance to fracture increases. From the tensile test, the stress-strain curve shows the property of high brittleness [13]. The property of brittleness could be due to the semi impregnated (dry region) process meanwhile the fracture toughness of the SIMS material could be lowered. The resistance curve of C-SIMS shows a relevant increment of the energy release

rate for 6mm crack length propagation and, after the crack length, a reaches 40mm, a nearly horizontal curve with large dispersion is observed (see figure 5.12(a)). As it resulted for C-SIMS, the G-SIMS shows large dispersion after about 10mm crack length propagation (see figure 5.12(b)).

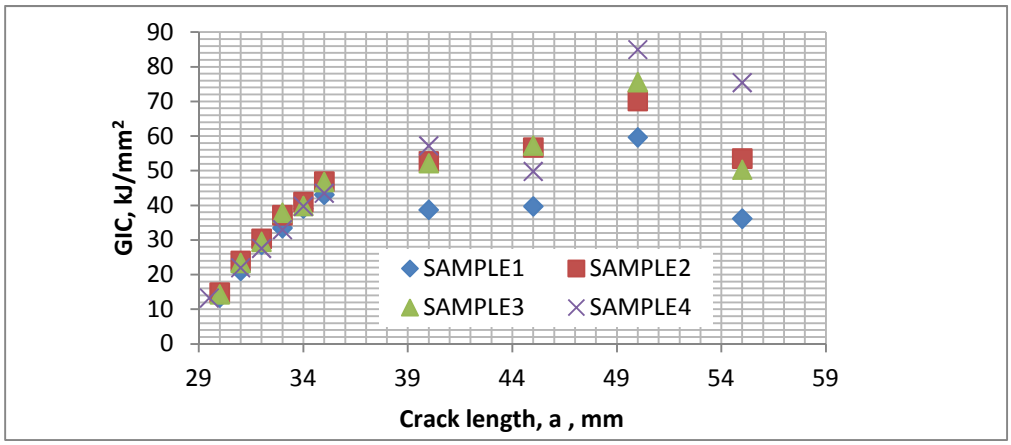

(a)

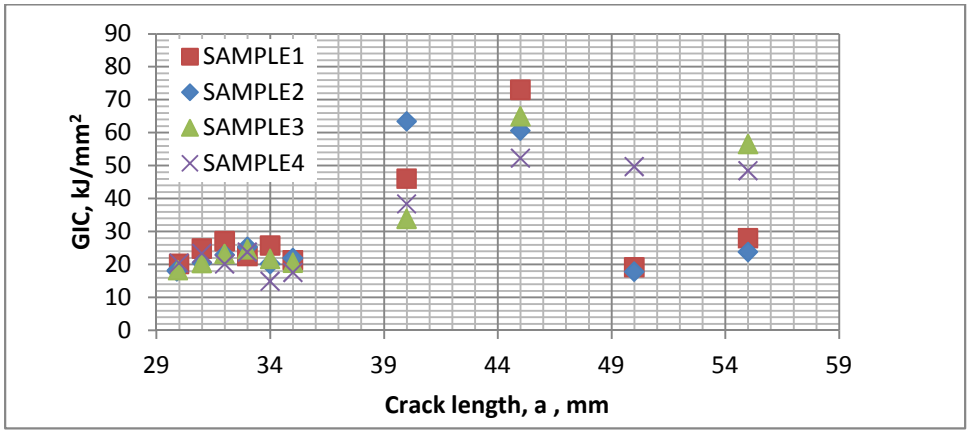

(b)

Figure 5.1 2Resistance curves of (a) G-SIMS, (b) C-SIMS

5.4.2. Result and discussion of GMT

The conventional GMT materials can be described as semi isotropic materials while modifying GMT, by addition of UD fibers, changes the semi isotropic behaviors. Unlike the SIMS materials, GMT materials do not show clear valleys and hills in the crack propagation region of force-displacement curves (see figure 5.13). The main reason is the formation of fiber bridging and the materials' semi isotropic property.

5.4.2.1. Force displacement response

The stiffness of GMT and GMT-UD specimen obtained 619.05 N/mm and 578.67 N/mm respectively. The force-displacement responses of GMT and GMT-UD show good repeatability and linearity of stiffness in the region I, however relatively large dispersion is obtained in region III after the damage starting points. The responses of both types of materials dispersed after the damage starts and the crack propagation continues. The diagrams show more dispersion as the crack grows. The force-displacement diagram shows smooth curves, unlike unidirectional composite materials where crack grows perpendicular to the fiber directions and SIMS materials. Generally, GMT shows relatively smooth damage growth like isotropic materials. GMT-UD was expected to the up and downs if the crack growth would be perpendicular to the axis of the unidirectional fiber.

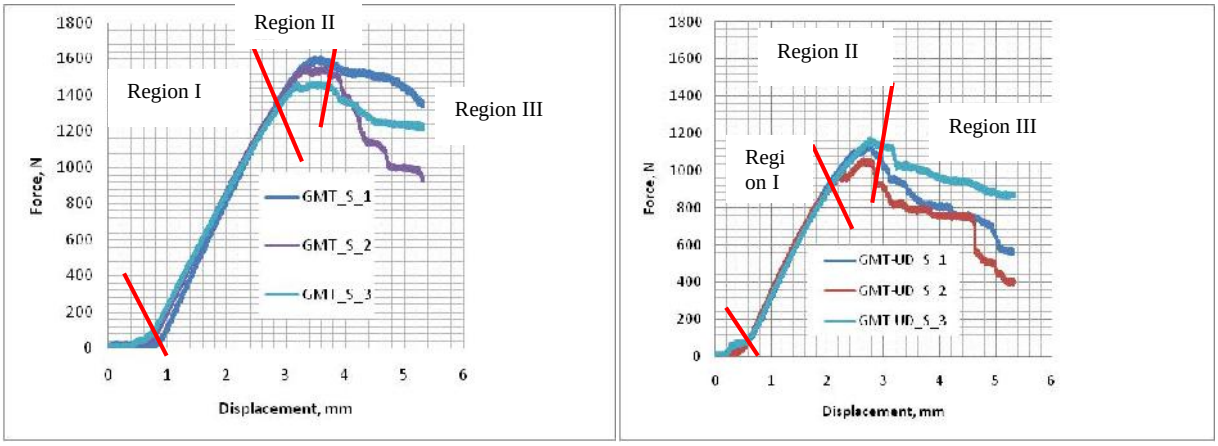

Figure 5.13 Force displacement responses (a)GMT, (b) GMT-UD

5.4.2.2. *Fracture toughness and resistance curves of GMT-UD*

As the detailed images, shown under the section of fractography (figure 5.17), will illustrate the directions of crack propagation for GMT and GMT-UD are not in the same line of action. Thus, the fracture toughness of GMT was calculated based on ASTM399-09 (based on table 5.1) while for the GMT-UD the same procedure as SIMS materials was followed. The values of fracture initiation of GMT-UD using modified compliance calibration and ASTM method are 1.60kJ/m^2 and 2.69kJ/m^2 respectively. The fracture toughness of GMT was calculated using ASTM method and the result was computed 21.05kJ/m^2. The experiment shows dispersed crack propagation of the material GMT and the crack directions largely varied. The resistance curve of GMT-UD as shown in figure 5.14 demonstrates the crack propagation behavior of composite materials.

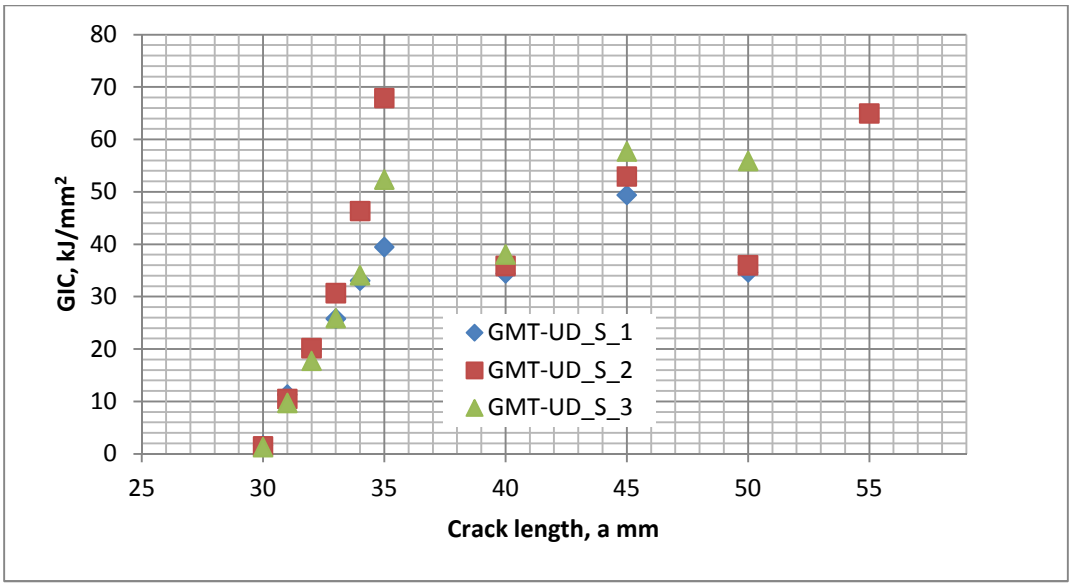

Figure 5.14 Resistance curves of GMT-UD

5.5. Intralaminar fractography of SIMS and GMT

The damage progress of the materials during the test can be studied by means of the pictures that show the practical materials' damage during operation. The discussion focuses on the materials loaded to mode I and in a tension test. When the applied load changes in direction or it cannot be classified as mode I but as a combination of mode I and II, the practical damage may be changed and to examine the special behaviors, it may include the combination of all loads.

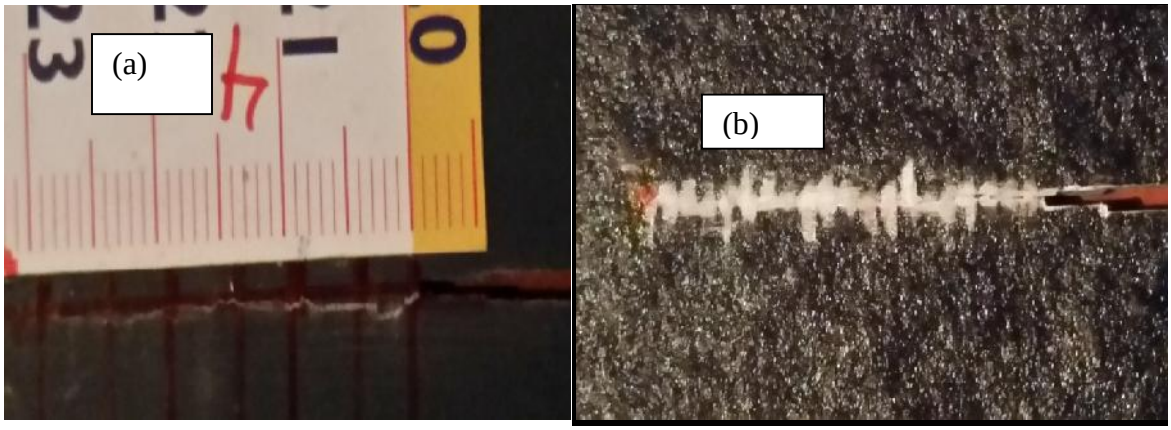

Figure 15 The damage behavior of G-SIMS (a) cosmetic face, (b) the crack propagation at the back face

The G-SIMS material is very brittle and the crack growth propagates along a straight line. During crack propagation, very short delamination obtained. The towed fiber delaminated until it ruptures when it reaches to the perpendicular twill position (see figure 15(a and b)). In the case

of GMT-UD, damage progress similar to C-SIMS was observed however, straight-line propagation could not be obtained (see figure 17(a)).

C-SIMS cracking process is similar to the G-SIMS however, the woven part of the C-SIMS shows relatively larger delamination as it is shown by the red line (see figure 16(a)) whereas the fleece show short pullout but delamination, figure 16(b and c). The separation of the woven part delaminates from the outside position.

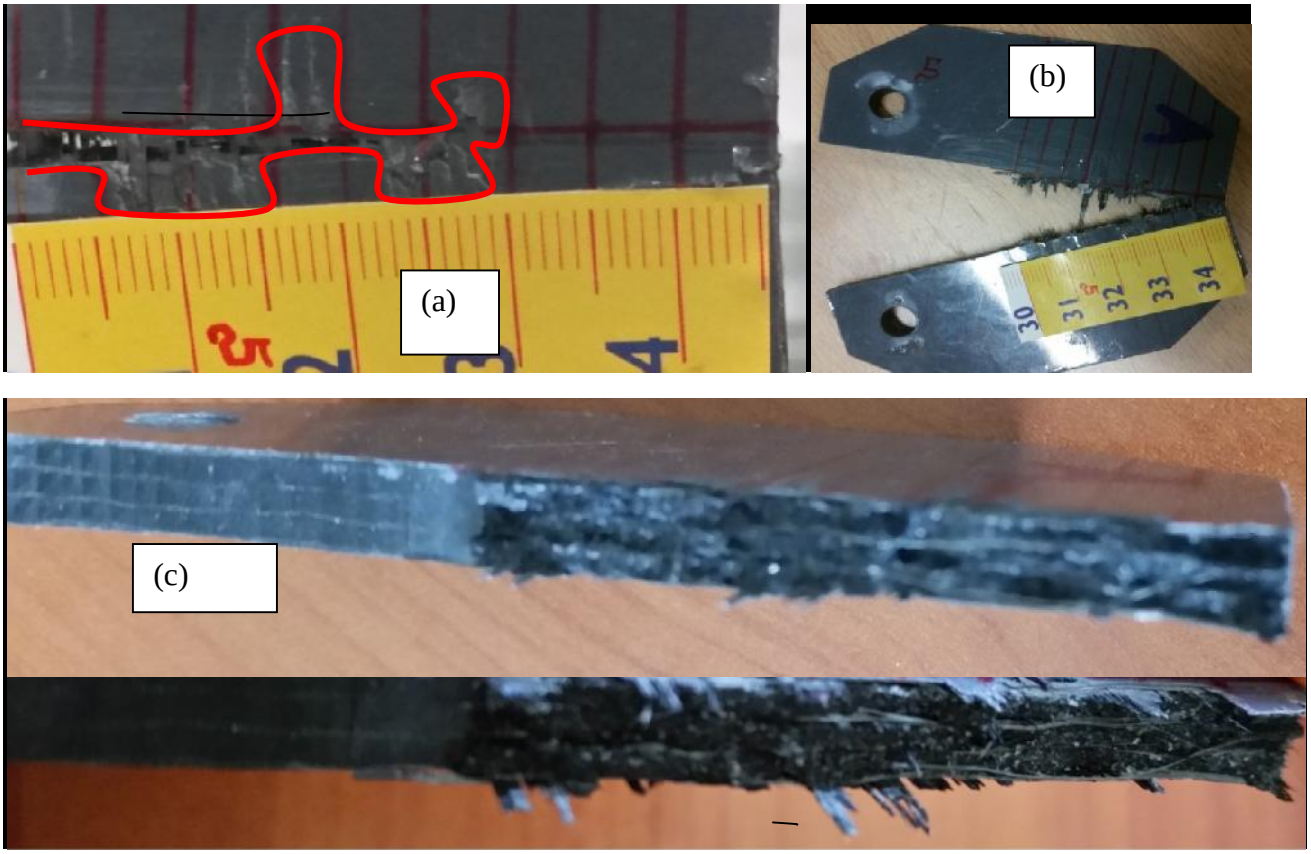

Figure 5.16 Fractography of (a) C- SIMS cosmetic surface, (b) C-SIMS at extra load, (c) cracked surface of C-SIMS

For GMT materials, the directions of the cracks are unpredictable. However, the nature of composite materials overtakes the crack behavior and direction by forming fiber bridging. The two types of GMT family materials show different crack propagation directions.

The crack propagation for the GMT-UD material followed wave formation with the axis of the straight line as shown in figure 5. 17(c) that is collinear to the initial crack but the fiber bridging is obtained as the crack propagates. Since the specimens were prepared and the initial cracks were introduced in the direction parallel to the fiber axis, the crack propagation follows the same direction due to the reflection of cracks. The zigzag type of crack propagation for GMT-UD

shows how the crack prefers to rupture the randomly distributed fibers rather than the unidirectional fibers (see figure 5.17(c)) and the weak constituents. Figure 5.17(a and b) shows the shifting of the crack growth directions. In addition to altering crack direction, un-cracked damage formations are shown (see figure 5.17(a)) while another specimen (see figure 5.17(b)) forms a kink crack with a direction above 60^{O} from the initial crack axis.

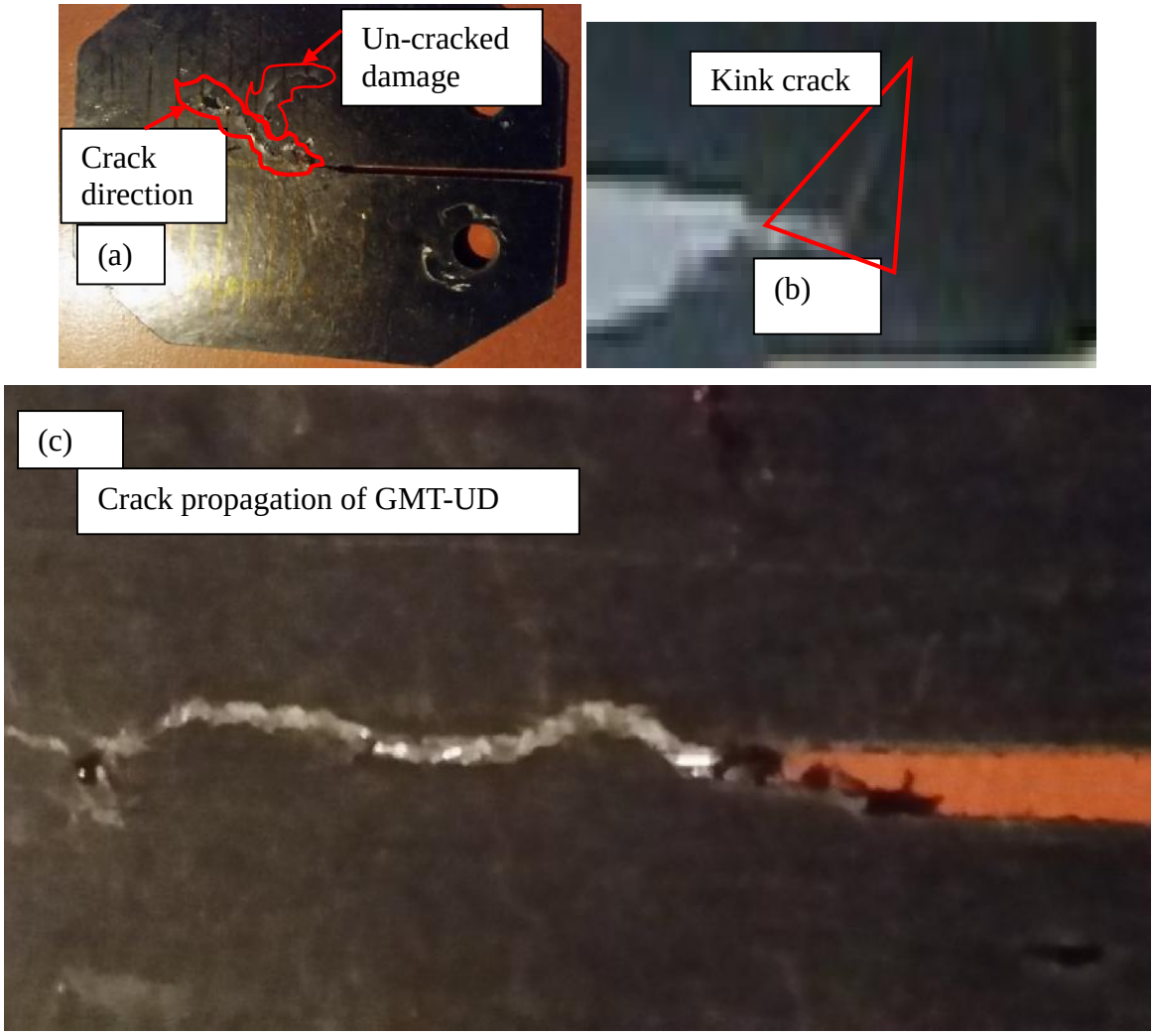

Figure 5.17 Fractography of (a) cracked specimen of GMT, (b) crack growth and direction of GMT, (c) cracked specimen of GMT-UD

The directions of the crack growths for the traditional GMT materials are unpredictable and it could prefer to follow the randomly distributed fiber directions. From the tested GMT specimens, all crack propagation preferred different directions like metallic materials. Based on the general theory of metallic materials, the paths of the cracks could follow the direction of the weak constituents and defects such as vacant atomic sites, weak elements of impurities, due to

self-interstitials/ improper atomic positions, etc. Thus, the random direction of the crack and kink crack propagation could be due to the weak, the uneven distribution and directions of the fibers. Its semi isotropic nature makes the direction of the cracks unpredictable and inconsistent. From the crack growth behavior of GMT, it is difficult to calculate the resistance curve. During the experimental test, the lateral bending of the GMT specimen was observed. Therefore, for GMT materials two double-tapered specimens may not completely avoid lateral bending.

5.6. Conclusion

5.6.1. Fracture toughness and crack behaviors of C-SIMS and G-SMIS

Good mechanical performance and low cost make SIMS a very attractive option for industrial applications such as in transportation and personal protection [14]. Besides, in case of repeated impact test, the G-SIMS and C-SIMS have a perforation at the 4^{th} number of impacts and serious damage at the 8^{th} number of impacts respectively for 34.11 J drop-dart impact energy [13] that is a rather good performance.

Likewise, the results of this research demonstrated the damage initiating and damage development processes. The resulting values for the initial fracture toughness were rather high, in particular for the C-SIMS that resulted to be nearly 40% better than the G-SIMS. The damage development processes of C-SIMS demonstrated more scattering profiles while the G-SIMS showed less dispersion. For both materials, the pullouts of tows of the twills occurred, however more delamination happened on the C-SIMS. Therefore, it is possible to state that the direction of the crack propagation was straight-line except for the woven prepreg or external layer.

The fracture initiation followed the damage development for the two types of materials however scattering obtained as the curve became stable. Following large dispersions of damages in region III, the energy release rate became similar.

5.6.2. Fracture toughness and crack behaviors of GMT and GMT-UD

In general, the fracture toughness for GMT and GMT-UD was calculated using the ASTM method. The intralaminar fracture toughness of GMT offered better values than GMT-UD however, the GMT-UD has better impact resistance and damage tolerance relative to GMT. GMT-UD has a progressive failure mode with cracks that develop along the fiber direction resulting in higher energy absorption values with respect to GMT [11]. The direction of crack propagation for GMT material changed during the test evolution and it became unpredictable, unlike GMT-UD. Furthermore, GMT material showed short crack propagation. Furthermore,

more fiber bridge was obtained for GMT material. The crack propagation of GMT-UD was followed by lower fiber bridging relative to the GMT. GMT and GMT-UD tested to the application of a vehicle frontal bumper beam with lightweight (the weight saving is of the order of magnitude of 55%) and GMT-UD revealed better performance [19]. Therefore, the GMT-UD can be applied for structures where the axis of the GMT-UD fiber should be perpendicular to the longer side of the panel to minimize the crack propagation.

5.7. References of chapter five

1. Laffan MJ, Pinho ST, Robinson P, McMillan AJ, Translaminar fracture toughness testing of composites: A review, Polymer Testing 31 (2012) 481–489
2. Sato N, Hojo M, Nishikawa M, Intralaminar fatigue crack growth properties of conventional and interlayer toughened CFRP laminate under mode I loading, Composites: Part A 68 (2015) 202–211
3. ASTM E399-09. Standard test method for plain-strain fracture toughness of metallic materials. Annual Book of ASTM Standards; Philadelphia (USA): American Society for Testing and Materials; 2009
4. Liu H, Wang G, Mai Y, Zeng Y, On fracture toughness of nano-particle modified epoxy, Composites: Part B 42 (2011) 2170–2175
5. Pinho ST, Robinson P, Iannucci L, Fracture toughness of the tensile and compressive fibre failure modes in laminated composites, Composites Science and Technology 66 (2006) 2069–2079
6. Li X, Hallett SR, Wisnom MR, Zobeiry N, Vaziri R, Poursartip A, Experimental study of damage propagation in Over-height Compact Tension tests, Composites: Part A 40 (2009) 1891–1899
7. Blanco N, Trias D, Pinho ST, Robinson P, Intralaminar fracture toughness characterization of woven composite laminates. Part I: Design and analysis of a compact tension (CT) specimen, Engineering Fracture Mechanics 131 (2014) 349–360
8. Xu X, Wisnom MR, Mahadik Y, Hallett SR, Scaling of fracture response in Over-height Compact Tension tests, Composites: Part A 69 (2015) 40‑48
9. Czabaj MW, Ratcliffe JG, Comparison of intralaminar and interlaminar mode I fracture toughnesses of a unidirectional IM7/8552 carbon/epoxy composite, Composites Science and Technology 89 (2013) 15–23
10. Blanco N, Trias D, Pinho ST, Robinson P, Intralaminar fracture toughness characterization of woven composite laminates. Part II: Experimental characterization, Engineering Fracture Mechanics 131 (2014) 361–370
11. Belingardi G, Beyene AT, Jichuan D, Energy absorbing capability of GMT, GMTex and GMT-UD composite panels for static and dynamic loading – Experimental and numerical study, Composite Structures 143 (2016) 371–387

12. Birman V, Kardomateas GA, Review of current trends in research and applications of sandwich structures, Composites Part B 142 (2018) 221–240
13. Belingardi G,Beyene AT, Ji J, Materialcharacterizationandimpact performanceof SemiImpregnatedMicro-Sandwichstructures,SIMS, politectico di Torino- Dipartimento di Ing. Meccanica e Aerospaziale,corso Duca degli Abruzzi, 24-10129 Torino Italia url: www.dimeas.polito.it
14. Nieri P, Montanari I, Terenzi A, Torre L, Kenny JM, Semi impregnated micro-sandwich structures, A novel composite configuration for low-cost panels with improved toughness, Presented at the SAMPE Europe 29th International Conference and Forum - SEICO 08 (Hotel MERCURE Paris Porte de Versailles - March 31st - April 02nd)
15. Quadrant Plastic Composite AG, Glass fiber mat reinforced thermoplastics : processing guidelines , 6th edition/ url: www.quadrantcomposites.com
16. Laffan MJ, Pinho ST, Robinson P, Iannucci L, Measurement of the in situ ply fracturetoughness associated with mode I fibre tensile failure in FRP. Part II: Size and lay-up effects, Composites Science and Technology 70 (2010) 614–621
17. Laffan MJ, Pinho ST, Robinson P, McMillan AJ, Translaminar fracture toughness: The critical notch tip radius of 0^o plies in CFRP, Composites Science and Technology 72 (2011) 97–102
18. Li X, Hallett SR, Wisnom MR, Numerical investigation of progressive damage and the effect of layup in over height compact tension tests, Composites: Part A 43 (2012) 2137–2150
19. Belingardi G, Beyene AT, Koricho EG, Martorana B, Alternative lightweight materials and component manufacturing technologies for vehicle frontal bumper beam, Composite Structures 120 (2015) 483–495

Chapter 6 Conclusions and Future Work

6.1. Conclusion

Each chapter has its own summarized and articulated conclusions, the important ideas are finally compiled within this section. The compiled points help the readers to grasp quickly.

6.1.1. Literature and part I: Glass fiber reinforced plastic

6.1.1.1. Literature

The various natures and levels of damages of composite materials such as micro, messo and macro revision guide the mechanisms of improving and customizations in the development of the composite materials. Specifically, the enhancing natures of nanomaterials for specific applications have to be accessible and the loadings of different nanomaterials need summarization. Effects of sizes, loadings, nature, morphological aspect, etc. for strength and fracture approaches require ease accessibility. The review fills the gaps of the lack of detailed research results for specific bulk materials and specific nanomaterials with a report of all the relevant parameters. It also tries to establish a general conclusion about the influence of nanoparticles on the mechanical properties of composite materials.

So that the particular conclusions are drawn from the review:

- Customization, specific properties, and lightness can overtake the need for the upcoming structural, semi-structural, and non-structural materials in the emergent stage.
- The material, structure, and the history of technology registered about the advancement while catastrophe increases accordingly. Thus, the reviews concerned about the damages of composite materials lie in large percentages by poor adhesion or manufacturing imperfections. This implies that the sophistication of composite material needs research in the composite materials' damage of constituents, interfacial behavior between the constituents, failure conditions of the structure, intralaminar damage, interlaminar failure, and enhancement in every aspect of the properties.
- Damages out of degradation can be prolonged by applying new technological advancement. The intralaminar/translaminar, interlaminar, and interfacial damage resistance can be enhanced using nanomaterials. However, the number of nanomaterials can improve the positive behavior of the material-specific nanomaterials are used for particular applications.

- Composite strength and toughness are strongly affected by loadings (wt.% and vol.%), particle size, particle/matrix adhesion, morphology.
- Strength depends on effective stress transfer between filler and matrix, and toughness/brittleness is controlled by adhesion.
- Addition of nanoclay for the enhancement of the mechanical properties and fracture toughness become effective at the same time for low percentage in weight (i.e. lower than 5 wt.%) of particle loadings, especially when particle dispersions are fine and, sometimes, modification helps to enhance the adhesion property with the bulk materials.
- Nanomaterials may affect the bulk negatively unless they are treated properly. It includes avoiding agglomeration, appropriate determination of aggregation, suitable thermal condition, curing the combined materials, loadings, etc. the large size, poor compatibility, and poor adhesions enhances the damage progress of the composite materials.

Generally, the future market governs the development of lightweight materials and minimization of pre-degradation. Thus, multidimensional failure study and new approach will keep the globe safe. Furthermore, the addition of nanomaterials in composite materials enhance the mechanical properties, fracture toughness if the application type, suitable process, loadings, size, type of nanomaterials are implemented appropriately. If not it could be the cause of damage and it may influence the bulk material's behavior in an unsatisfactory way or even detrimentally. On the other hand, the review helps the researchers to some extent giving a guide on how the nanomaterials can be selected for the fracture toughness and main mechanical properties of heterogeneous materials.

6.1.1.2. Fundamental material characterizations and Interlaminar fracture behavior

The fundamental material characterization and interlaminar fracture study provide the effect of the presence of layered nanoclay, Cloisite 20B, on the tensile, compression and interlaminar fracture characteristics of GFRP. The observed results can be summarized as follow:

- Inclusion of Cloisite 20B nanoclay into epoxy alters the tensile strength, compressive strength, modules of elasticity of GFRP.
- Moreover, it is possible to conclude that the inclusion of a small amount of Cloisite 20B nanoclay has beneficial, even if limited, effects on the mechanical properties of the considered S-glass fabric/epoxy composite. Slightly smaller/comparable improvement

effect obtained if compared with others Cloisites nanoclay family. However, Cloisite 20B can be preferred because of its non-toxicity and flame-retardant behavior.

- Inclusion of 0.5 wt.%, 1 wt.%, and 2 wt.% Cloisite 20B nanoclay into epoxy improved the interlaminar toughness of GFRP by 12.65%, 21.49%, and 54.07% respectively.
- The resistance curve shows a stable energy release rate distribution starting at from 55mm as crack length increases. The average line becomes horizontal which agrees with the general theory of the resistance curve of the composite materials.
- Generally, the voids, which cause damage initiations decreases as the weight by percentage increases at least until the loading reaches at 2 wt.%.

Overall, it is possible to conclude that the inclusion of a small amount of nanoclay has beneficial, effects on the fracture behavior of the considered S-glass fabric/epoxy composite while a small amount of percentage obtained in strengths and moduli. From literature data, it can be noted that good improvements have been achieved in comparison with other Cloisites family. Furthermore, the adopted Cloisite is highly preferable because of its non-toxicity, better melt flow rate, low elongation at break and flame-retardant behavior when it is combined with SC-15 epoxy and S-glass fiber.

6.1.2. Part II: Intralaminar fracture behavior of SIMS and GMT

The strength approach characterization and energy absorption of GMT and SIMS made approachable. The two types of materials became good candidates for structures and semi structures, which are exposed to impact load. The fact that composite materials have failed internally such as delamination and crack propagation, which is perpendicular to the plane of the structure.

6.1.2.1. Intralminar behavior of SIMS

The intralaminar experimental test showed brittle crack propagation. The property of the brittleness could be the good interfacial adhesion between fiber and matrix. Besides the dry fleece layer could cause to have lower fracture toughness however, the fleece layers showed better energy absorption.

6.1.2.2. Intralminar behavior of GMT

The intralaminar fracture toughness of GMT offered better than GMT-UD however, the GMT-UD has better impact resistance and damage tolerance. Thus, GMT is preferable for through

crack susceptible structures though GMT-UD can be applied for better strength and stiffness in the fiber direction.

6.2. Future work

The GFRP enhanced with Cloisite 20B nanoparticles addition, has a property of fire retardation and advisable to apply for any structures that are exposed to fire and crushes. Besides the enhanced GFRP material could be customizable for structures that need better interlaminar fracture resistance applications. Meanwhile, the investigation of intralaminar fracture characteristics, dynamic fracture behavior, at low and medium speed impact of GFRP composite materials modified with Cloisite nanoparticles addition could be the potential promising research direction in order to complete the analysis and provide a comprehensive picture of advantages and limitations of the proposed materials for vehicles and other engineering applications.

At the same time, the analysis of the effect of the relative angle between the fiber direction and the crack direction in the intralaminar propagation, of the interlaminar fracture toughness and delamination behaviors, of the compressive intralaminar fracture and dynamic behaviors could be the next research investigations for SIMS and GMT.

Finally the study of the fracture mechanics response of real composite pieces, to assess the possibility of transferring what has been pointed out in the coupon test to real parts, will be the medium term research target.

Appendix

A.1. Tensile and compressive test-tips

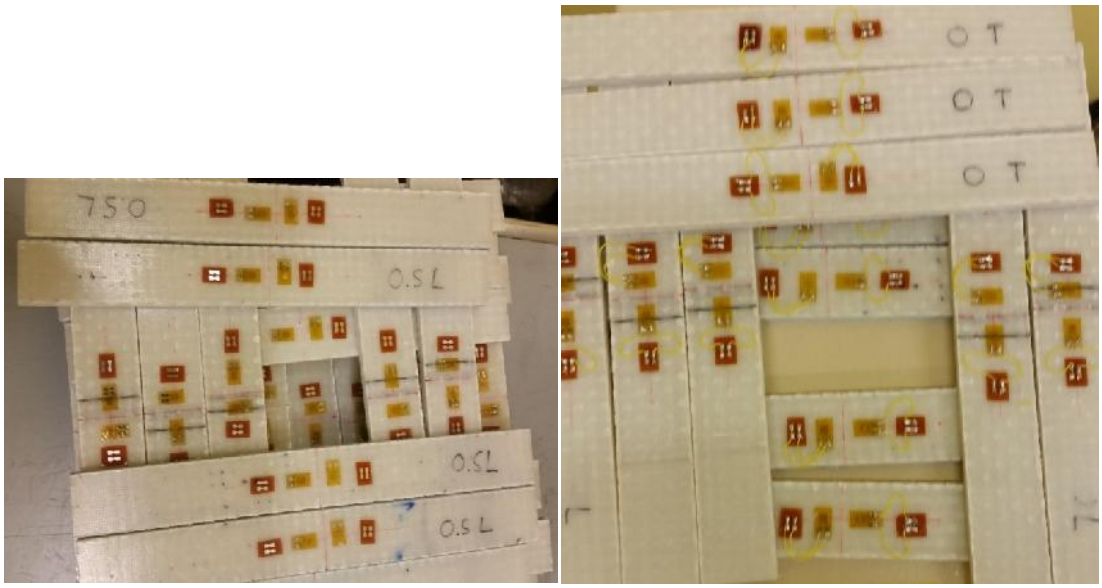

Figure A.1 prepared specimens

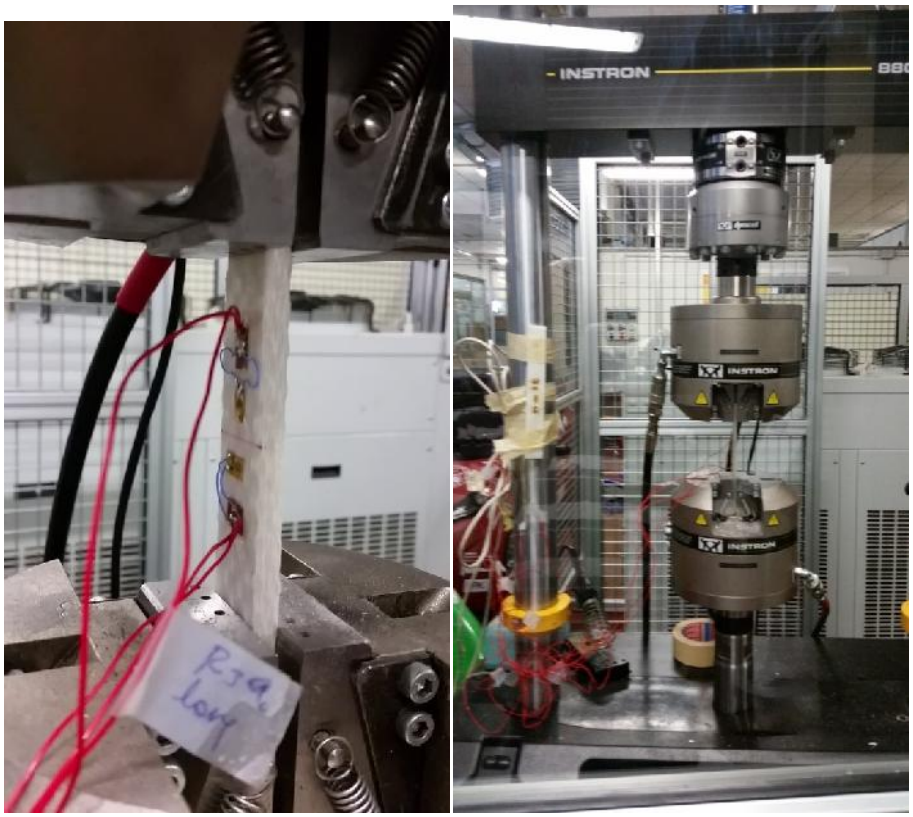

Figure A.1.2 Test setup

Company	Super Duper Multi National Conglomerates R Us
Laboratory Name	Central Laboratories
Ingresso di testo personalizzato 1	Scattina A.
Velocità 1	2,00000 mm/min
Humidity (%)	50,00000
Temperature (deg C)	18,00
Numero di provini nel lotto	10

ABC Ltd.
975 Fraser Drive
Burlington, Ontario Canada

Operator ID	
Laboratory Name	
Company	
Temperature (deg C)	18,00
Humidity (%)	50,00
Velocità 1	1,30000 mm/min
Number of specimens	4

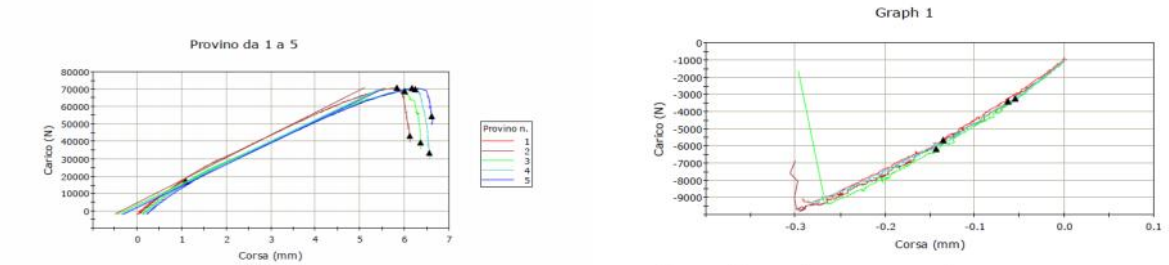

Figure A.1.3 Graphical test outputs of tensile and compressive tests

A.2. Interlaminar test tips

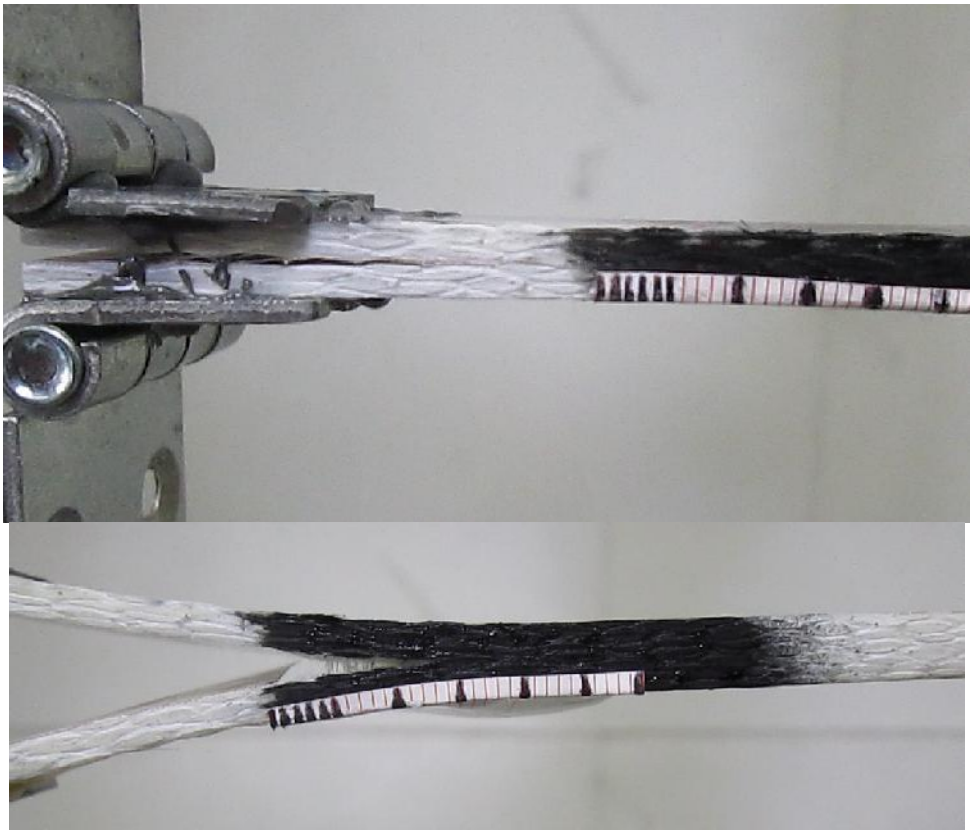

Figure A.2.1 Interlaminar fracture test setup

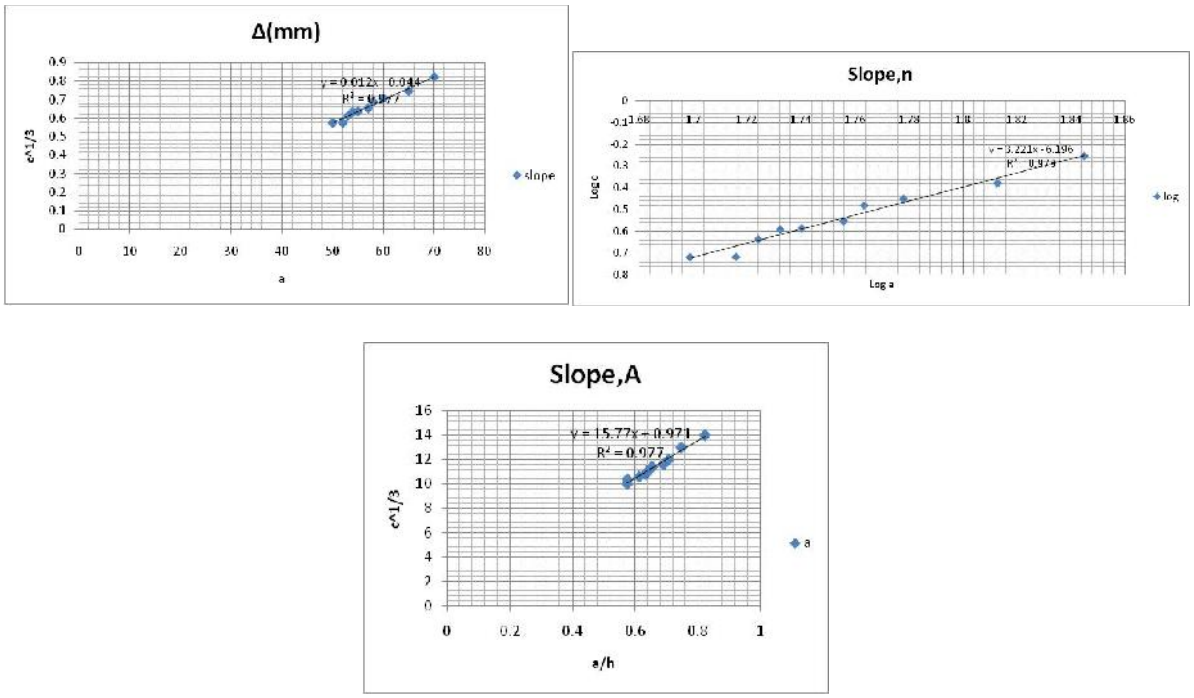

Figure A.2.2 Sample diagrams of the reduction methods for single specimen

Table A.2. data sheet table of a single sample

DCB STANDARD DATA REPORTING SHEET	LAB:	DATE

Material	Procedure		Panel No.	Max Cure T		FAW=	$V_{f=}$
Specimen Number=2	Avg. b (mm)=25	Avg. h(mm) =4.95	Max Δh(mm) =0.05	Insert Material =Teflon		Insert thickness =13μm	
Hinge Type	Hinge size		Block size	Surface prep.		Adhesive	
Test Temp. 18C^{o}	Test RH% 50		Load rate= 3mm/min	a_o=50mm	Δ=3.66667	n=3.221	A_1=15.77

a_o(mm)	δ(mm)	P(N)	δ/a_o	G_{IC}	MBT	CC	MCC	comments
50	7.4	42	0.148	NL	0.339409	0.391136	0.412065	
50	8.996	47.145	0.17992	VIS	0.459965	0.530065	0.54378	
50	8.6	46	0.172	5%	0.429802	0.495305	0.511593	

points	a(mm)	δ(mm)	P(N)	δ/a	$G_{IC[kJ/m^2)}$	MBT1	MBT	CC	MCC	comments
1	50	8.996	47.145	0.17992	Prop	0.493696	0.459965	0.530065	0.54378	
2	52	9.116	47.55	0.175308	Prop	0.486057	0.454041	0.521863	0.55591	
3	53	11.158	48.366	0.210528	Prop	0.58917	0.551048	0.632573	0.645703	
4	54	11.918	46.558	0.220704	Prop	0.593348	0.555621	0.637058	0.639978	
5	55	12.198	46.997	0.221782	Prop	0.601971	0.564348	0.646317	0.65826	
6	57	13.399	47.825	0.23507	Prop	0.647704	0.608557	0.695418	0.715557	
7	58	15.594	47.264	0.268862	Prop	0.726034	0.682865	0.779519	0.772872	
8	60	16.517	46.726	0.275283	Prop	0.73431	0.69202	0.788404	0.790263	
9	65	18.834	45.159	0.289754	Prop	0.745639	0.705823	0.800568	0.822699	
10	70	20.999	37.794	0.299986	Prop	0.645496	0.613367	0.693048	0.697051	

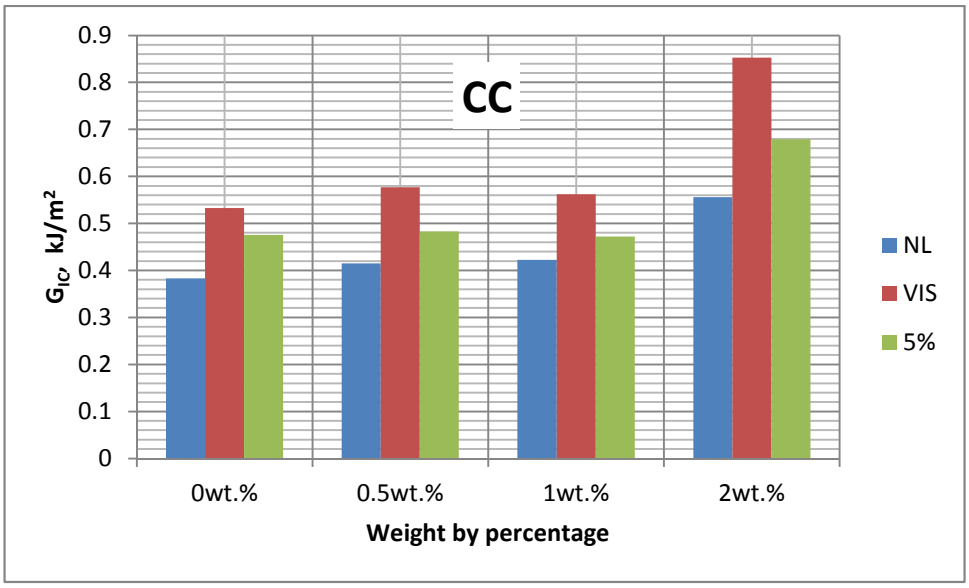
CC
0.9
0.8
0.7
0.6
0.5
0.4
0.3
0.2
0.1
0
G_{IC}, kJ/m²
0wt.%
0.5wt.%
1wt.%
2wt.%
Weight by percentage
NL
VIS
5%

(a)

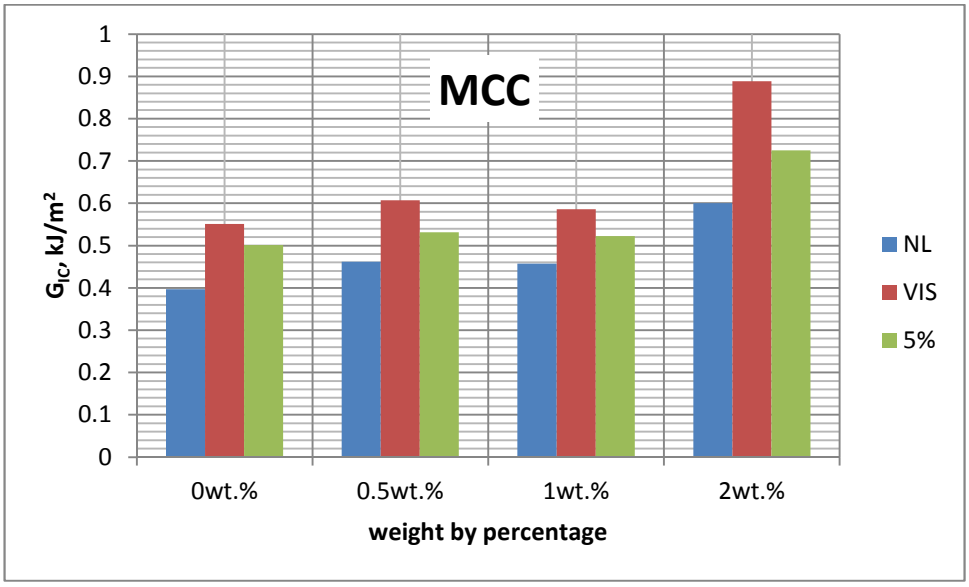
MCC
1
0.9
0.8
0.7
0.6
0.5
0.4
0.3
0.2
0.1
0
G_{IC}, kJ/m²
0wt.%
0.5wt.%
1wt.%
2wt.%
weight by percentage
NL
VIS
5%

(b)

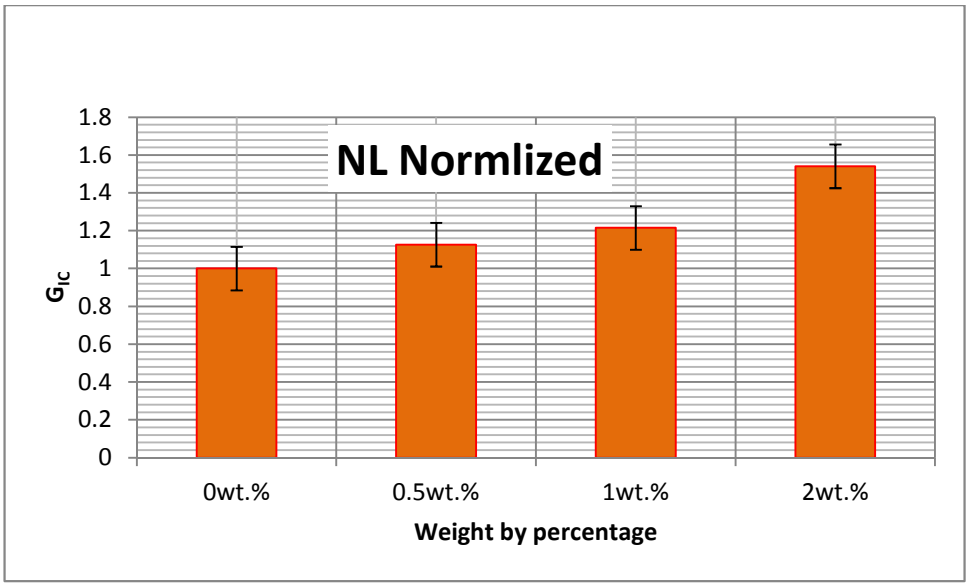

(c)

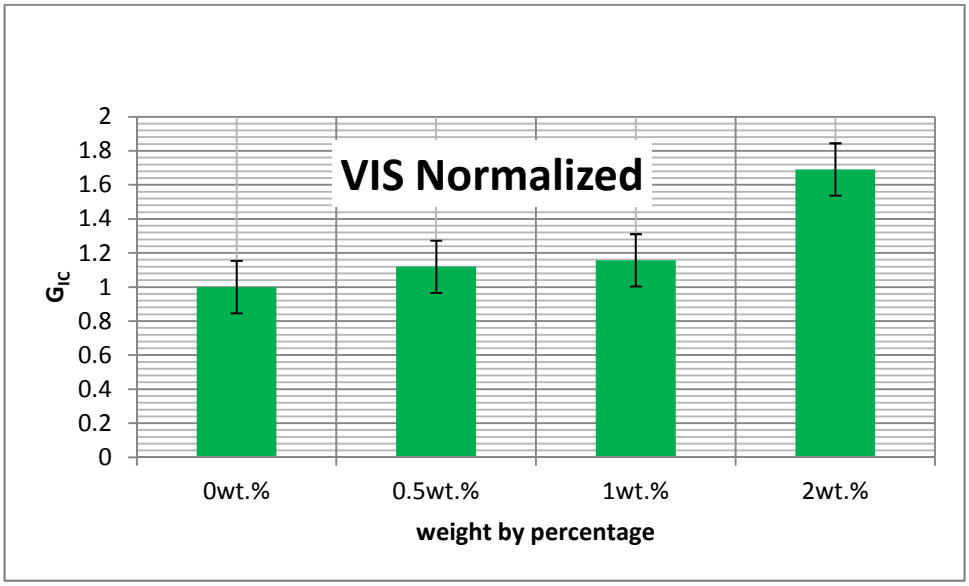

(d)

Figure A.2.3 selected diagrams of interlaminar fracture (a-d)

A.3. Intralminar fracture test tips

Figure A.3.1 finishing equipments of specimen preparation

Figure A.3.2 test set up

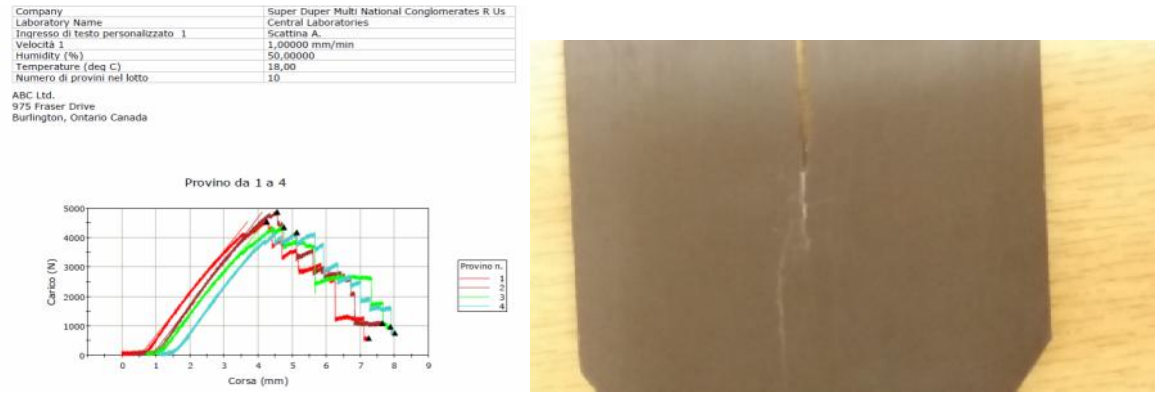

Figure A.3.3 result outputs and representative of specimens after testing